

# **A MICROPROCESSOR BASED RAIL TRACK MONITORING SYSTEM**

**A Thesis Submitted  
In Partial Fulfilment of the Requirements  
for the Degree of  
MASTER OF TECHNOLOGY**

*By*  
**G. N. M. SUDHAKAR**

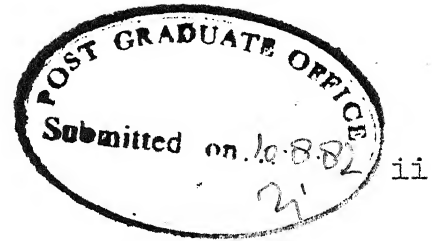
*to the*  
**DEPARTMENT OF ELECTRICAL ENGINEERING  
INDIAN INSTITUTE OF TECHNOLOGY, KANPUR  
SEPTEMBER, 1982**

5 JUN 1984

CENTRAL LIBRARY

Acc. No. A 82781





# CERTIFICATE

Certified that the work entitled 'A MICROPROCESSOR  
BASED RAIL TRACK MONITORING SYSTEM' by G.N.M. Sudhakar has  
been carried out under our supervision and this has not  
been submitted elsewhere for a degree.

A handwritten signature in dark ink, appearing to read "K.R. Sarma".

Dr. K.R. Sarma  
Professor  
Department of Elect. Engg.  
I.I.T. Kanpur

A handwritten signature in dark ink, appearing to read "V.P. Sinha".

Dr. V.P. Sinha  
Professor  
Department of Elect. Engg.  
I.I.T. Kanpur

## ACKNOWLEDGEMENTS

I would like to express my thanks to Dr. K.R. Sarma and Dr. V.P. Sinha for suggesting the topic of this thesis and extending the guidance and encouragement during the course of this work.

I am grateful to Mr. Bh. A.R.B. Raju, Research Engineer, for his timely help, useful discussions and comments during the design, fabrication part of the system hardware.

My special thanks go to Mr. B.V. Ramana, Research Engineer, I.I.T. Kanpur, for his help during the testing and assembling of different hardware modules. A few discussions with him helped me a lot in the software development.

I would also like to express my thanks to my friends Satyanarayana, Phani, Gopi, Sridhar and Satyaprasad for their help in proof reading, sketching etc.

My thanks are also due to Mr. J.D. Varma of Mechanical Engineering Department for his efficient typing of the thesis.

G.N.M. Sudhakar

MY SPECIAL THANKS GO TO SRI. DESH DEEPAK  
JOINT DIRECTOR, RDSU, LUCKNOW AND HIS COLLEAGUES FOR  
SUPPLYING THE NECESSARY INFORMATION AND DATA NEEDED  
FOR THIS WORK

G. N. M. SUDHAKAR

## TABLE OF CONTENTS

	Page
LIST OF FIGURES	
LIST OF TABLES	
ABSTRACT	
CHAPTER 1 : INTRODUCTION	1
1.1 Definition of Track Irregularities	1
1.2 Existing Measurement System	4
1.3 Proposed System	7
1.4 Proposed Signal Processor	9
CHAPTER 2 : FILTERING TECHNIQUES FOR TRACK IRREGULARITY MEASUREMENT	18
2.1 Introduction	18
2.2 Digital Integrators	19
2.3 Digital Filters	20
2.4 Incremental Computation Scheme for Digital Filtering of Low Frequency Signals	24
2.4.1 Difference between Normal and Incremental Computation	24
2.4.2 Using Digital Incremental Com- putation (DIC) for Digital Filtering	25
2.5 Noise Study, Design Procedure	27
2.5.1 Noise Power in Second Order Recursive Filters	28
2.6 High Pass Filtering Using DIC Scheme	33
2.7 High Pass Filter for Track Profile Measurement	34

Chapter 3	: POWER SPECTRAL MEASUREMENT OF TRACK IRREGULARITIES	42
3.1	Introduction	42
3.2	Power Spectral Density	42
3.2.1	Mathematical Analysis	44
3.2.2	Estimates of PSD	46
3.3	Computation of PSD	49
3.4	Fast Fourier Transform Algorithm	50
3.5	Implementation of FFT on 6800 Microprocessor	57
Chapter 4	: MICROPROCESSOR BASED SYSTEM	68
4.1	Introduction	68
4.2	System Specifications	68
4.2.1	Environmental Specifications	69
4.2.2	Signal Processing Requirements and Real Time Nature of the Signal Processor	69
4.3	System Description	71
4.3.1	Microcomputer System Hardware	72
4.3.1.1	CPU Module	72
4.3.1.2	16K ROM Module	75
4.3.1.3	16K Dynamic RAM Module	76
4.3.1.4	RAM Refresher Module	78
4.3.1.5	8K Static RAM Module	79
4.3.1.6	Console Module	80
4.3.1.7	Cassette and RS 232 Interface Module	82
4.3.1.8	Baud Rate Clock and TTY Interface (20MA Loop)	84

4.3.2	Micro Computer System Configuration and Software	85
4.3.3	The Specific Application Dependent Hardware	88
4.3.3.1	A/D Converter Module	88
4.4	System Operation	90
Chapter 5	: RESULTS AND CONCLUSIONS	111
REFERENCES		
APPENDIX		

## LIST OF FIGURES

- Fig. 1.1 Description of Track Irregularities
- Fig. 1.2 Centre Line Unevenness
- Fig. 1.3 Centre Line Alignment of Track
- Fig. 1.4 Midchord Measurements
- Fig. 1.5 Vertical Profile Measurement
- Fig. 1.6 Lateral Profile Measurement
- 
- Fig. 2.1 Simpson Integration
- Fig. 2.2 Filtering Scheme
- Fig. 2.3 Realization of Single Pole High Pass Butterworth Filter
- Fig. 2.4 Illustration of Equivalence Between Conventional and DIC Filters
- Fig. 2.5 Block Diagram for the DIC Structure First Order Filter
- Fig. 2.6 Block Diagram of DIC Filter with Input and Output Inform
- Fig. 2.7 Second Order Conventional Filter
- Fig. 2.8 Second Order DIC Filter
- Fig. 2.9 Fixed Point Quantization Noise Model
- Fig. 2.10 Quantization Noise Probability Density Function for the Rounding Operation
- Fig. 2.11 Quantization Noise Model for Second Order Filter
- Fig. 2.12 Block Diagram of a Second Order DIC Filter
- Fig. 2.13 First Order High Pass Butterworth Filter - DIC Structure

- Fig. 3.1 (a) Complete 8 point Decimation-in-time FFT  
(b) Complete 8 point Decimation-in-Frequency FFT
- Fig. 3.2 Relationship between the numbers in m and m+1 stage
- Fig. 3.3 FFT inplace algorithm flow chart
- Fig. 3.4 FFT program and its loops
- Fig. 4.1 System architecture
- Fig. 4.2 Operator - system operation interface flow diagram
- Fig. 4.3 Circuit diagram of CPU module
- Fig. 4.4 Circuit diagram of 16 K ROM module
- Fig. 4.5 Circuit diagram of 16 K dynamic RAM module
- Fig. 4.6 Timing signals for RAM module
- Fig. 4.7 Jumper termination and associated address for RAM module
- Fig. 4.8 RAM refresher module
- Fig. 4.9 Timing signals of RAM refresher module
- Fig. 4.10 Circuit diagram of 8 K static RAM
- Fig. 4.11 Circuit diagram of console module
- Fig. 4.12 Circuit diagram of cassette and RS232C interface module
- Fig. 4.13 Timing chart for WRITE operation
- Fig. 4.14 Timing chart for READ operation
- Fig. 4.15 Circuit diagram of baud rate clock and TTY interface
- Fig. 4.16 Circuit diagram of A/D converter module
- Fig. 5.1 Test signals of high pass and integrator
- Fig. 5.2 PSD of a typical track profile



## LIST OF TABLES

Table 3.1	Obtaining the BIT Reversed Number Index
Table 4.1	Edge Connector Tongue Designation and Signal Summary
Table 4.2	Memory Mapping on CPU Module
Table 4.3	ACIA Serial Connector Signal Summary

## ABSTRACT

Rail track monitoring is very essential to have a smooth and safe ride on railcars. Standards have been adopted to provide a minimum comfort level for a passenger. Hence it is necessary that a suitable track monitoring system should be available for the measurement of track irregularities.

At present midchord measurement scheme has been adopted by Indian Railways. This has got poor frequency response in the pass band of interest. In this thesis, a better system, which makes use of accelerometers to pick up the track irregularities is proposed. Since the accelerometers give second derivatives of track irregularities, suitable digital filtering techniques using Digital Incremental Computation (DIC) scheme have been developed.

Since track categorization will be done on the basis of power spectral measurement of the track irregularity, Fast Fourier Transform algorithms are used for the spectrum analysis.

A completely independent dedicated signal processor consisting of an input digitizer, a control unit using 6800 microprocessor, memory modules for both program and data storage, cassette, RS 232 C console and teletype interface modules, a small console module consisting of fifteen digit eight segment LEDs and a Hex

key board is developed; the system configuration and hardware details are described in detail.

The filtering and power spectral analysis is done on software basis on 6800.- Assembly language programs are developed for this and are described in detail.

## CHAPTER 1

### INTRODUCTION

To have a smooth and safe ride of railway vehicles, the track tolerances should be within the acceptable limits and hence track monitoring is an essential part of railway operation. With the trend towards high speed transportation, the existing electrical and mechanical track irregularity measuring systems are inadequate and a better track monitoring system is proposed in this thesis.

In this chapter various parameters of the track irregularities are described and the methods of measurement are briefly reviewed. Also an outline of the proposed system is presented.

#### 1.1 DEFINITION OF TRACK IRREGULARITIES

Traditionally the track irregularities have been described by the following parameters.

- a) Unevenness of left rail
- b) Unevenness of right rail
- c) Alignment of left rail
- d) Alignment of right rail
- e) Cross level
- f) Gauge
- g) Twist

However, the track geometry can be equivalently described by the following four parameters (see Fig. 1.1)

- a) Absolute centre line unevenness of the track - Z
- b) Absolute centre line alignment of the track - Y
- c) Cross level - XL
- d) Gauge - G

Since the cross section of both rails change significantly during the service, it is necessary to define these parameters unambiguously. A typical track geometry is shown in Fig. 1.1. The various parameters are described below.

a) Centre Line Unevenness of Track (Z)

The centre line unevenness of track is defined as the variation of midpoint of track in vertical plane from an arbitrary datum. This datum will be a horizontal plane for tangent track and standard changing horizontal plane (taking into account super elevations) in case of curved tracks (Fig. 1.2)

b) Centre line Alignment of Track (Y)

The centre line alignment of track is defined as variation of midpoint of track in horizontal plane from an arbitrary datum. This datum is a straight line for tangent track and true circular or spiral shape in case of curved track (Fig. 1.3).

c) Cross Level (XL)

If the tangent of two rail head crowns make a slope with horizontal, the cross level is defined as  $2L \cdot \theta$  where  $2L$  is normal spacing between the centre line of two rail heads, and  $\theta$  is the angle the tangent makes with horizontal datum as shown in Fig. 1.1.

d) Gauge (G)

Gauge is measured as the distance between the two rail heads some distance 'h' below the rail crown ( $h = 14 \text{ mm}$ ).

e) Midpoint of the Track (M)

The midpoint of the track is defined by first finding out midpoint of gauge line and then constructing a line perpendicular to the tangent of crowns of two rail head profiles.

The traditional parameters can be derived from these basic parameters as follows:

a) Unevenness of left rail will be  $Z + \theta \cdot L$

b) Unevenness of right rail will be  $Z - \theta \cdot L$

c) Alignment of left rail will be  $Y + G/2$

d) Alignment of right rail will be  $Y - G/2$

e) Twist will be  $XL (1) - XL (2) / B$  where

$B = \text{base}; \quad XL (1), \quad XL (2)$  are the cross levels at the two end points of the base.

In the track irregularity measurements, the loaded or unloaded conditions play a very important role and these irregularities should be measured only under loaded conditions. Considering the present day speeds, the deflections of the track due to its own dynamics will be very small when compared to the loaded profile of the track geometry, hence are ignored. Also the deflections due to track springing are also ignored.

Since the moving railway vehicles will get the inputs from the track geometry irregularities and depending upon the speed of the vehicle these inputs correspondingly excite the vehicle which results in vibration of the vehicle components. The railway vehicles are strong resonant systems hence this interaction is best understood in frequency domain. Each track geometry parameter is modelled as a random process and by finding out the direct and cross spectras of the random processes a more useful information can be obtained in the design of track and Railway vehicles.

## 1.2 EXISTING MEASUREMENT SYSTEM

The Indian Railways at present monitor the routes using the Amsler track recording cars which mainly monitor the track geometry parameters like vertical unevenness, gauge and twist. Such cars measure these parameters through 'mid-chord versine measurement' using a 3.6 metre chord. The length is chosen to be compatible with the existing

bogie length. From the track geometry parameters obtained through the 3.6 metre chord, the tracks are classified into the categories A, B, C, D, depending upon the tolerances. However, the wavelength of the track defects was completely ignored in this analysis as shown below.

Let 'd' be the distance along the track and  $f(d)$  be the track irregularity. Let 'L' be the chord length used for the midchord measurement scheme. Let AB be the chord and C is the midpoint of the chord. Considering the irregularity to be a pure sine wave form, different cases are illustrated in Fig.1.4. From this it can be observed that the transfer function of the midchord at the 'peak inputs' can be approximated by

$$|H(\lambda)|^2 = \left| 1 - \cos \frac{\pi L}{\lambda} \right|^2 \quad (1.1)$$

where  $\lambda$  is the wavelength of the irregularity. However, as the chord moves away from the peak (Fig.1.4 case d), this approximation is not valid and the performance further deteriorates. Thus not only the value of  $\lambda$  but also the position of the chord affects the measurement of irregularity. Hence various frequencies present in the track irregularity are distorted by various amounts.

For a dynamic system like a railway vehicle, the response is completely dependent upon the input frequency. Since the midchord measurement vitiates the track geometry



by attenuating the longer wavelengths (since for large  $\lambda$  and for a given L,  $L \ll \lambda$ , the change in the irregularity is very small where as the irregularity with respect to a datum is not so), Amsler cars cannot measure the amplitudes of longer wavelengths.

It is a necessary condition that the wavelengths where the vehicles have substantial response should be least affected for the track irregularity measurements to have a relevance in estimating the vehicle response. Choosing such a chord which satisfies the above requirement for all vehicles at all speeds is a very difficult task. The speed variations come into picture because the vehicle frequencies in Hertz are related to the track irregularities through the speed of the vehicle, given by

$$f = \frac{v}{\lambda} \quad (1.2)$$

where

$v$  = speed of the vehicle in metres/sec.

$\lambda$  = track irregularity wavelength in metres

$f$  = frequency in Hz.

For higher speeds the larger wavelengths become more important and the chord length for midchord measurements has to be longer to ensure that track irregularities for long wavelengths are not attenuated.

A better system is proposed for the track irregularity measurement which makes use of accelerometers mounted on axle boxes for picking up the irregularity waveform. Since the accelerometers have good response in the wavelength range of interest a better estimation of the irregularities is possible.

### 1.3 PROPOSED SYSTEM

In the proposed system accelerometers are placed on axle boxes (Fig.1.5). Since the axle box is in contact with the rail wheels, the accelerometers pick the random vibration of the wheel caused by the track irregularity. These signals are suitably processed to obtain the actual irregularity through the use of suitable signal processing methods. The power spectra of these signals are evaluated for the purpose of track categorization and in the design of tracks and railway vehicles. The measurement of rail vertical profile and lateral profile is given below.

#### a) Absolute Vertical Profile

To measure the absolute vertical profile, an accelerometer is mounted on each of the 2 axle boxes of one wheel axle set of the vehicle. Assuming that the wheels will always remain in contact with the rail in vertical plane, the output of the accelerometer will be double integrated and suitably filtered in the wavelength band of 2 m to 40 m to acquire correct vertical profile. The central

line absolute vertical profile of the track, then, can be calculated by taking the average of the absolute vertical profile of left and right rail and the dynamic cross level will be evaluated by taking the difference of the absolute vertical profiles of left and right rails (Fig. 1.5).

b) Absolute Lateral Profile

This measurement is also similar to the above. But because of the standard play between the track gauge and wheel gauge, the assumption of wheel remaining in contact with the rail is no more valid in this case. Hence to measure absolute lateral profile, an accelerometer can be mounted on the axle box thus monitoring the lateral movement of the axle and distance of the inside rail face can be measured with respect to the axle with the help of two contact sensors, one each, looking into the rail face. Then the output of the two contact sensors and the lateral motions of the wheel set which will be obtained by double integrating will be manipulated to obtain the absolute lateral profile of left and right rail (Fig. 1.6). Then the profiles are suitably filtered so that the correct information is available in the wavelength band of 2 m to 40 m and then by taking the average of lateral profile of left and right rail will give the central line alignment of the track and the difference gives the gauge of the track. Thus all the four basic parameters needed for the track geometry irregularity can be completely identified.

## Data Processing

After acquiring all the four track geometry parameters namely central line unevenness, central line alignment, cross level and gauge, are to be suitably processed for using the same for track maintenance. For this processing, digital signal processing schemes will be much more useful, hence the data for every length of 512 points at an interval of 2 m is proposed for analysing purpose. The power spectral density of each of the track parameter will be evaluated for this 512 points length and the value of roughness constant will be calculated by fitting the following model of Power Spectral Density (PSD) for the track irregularities.

$$\text{PSD} = A \lambda^2 ; \quad \text{PSD is in mm}^2/\text{cycle/M} ;$$

$\lambda$  is wavelength in M

A is roughness constant.

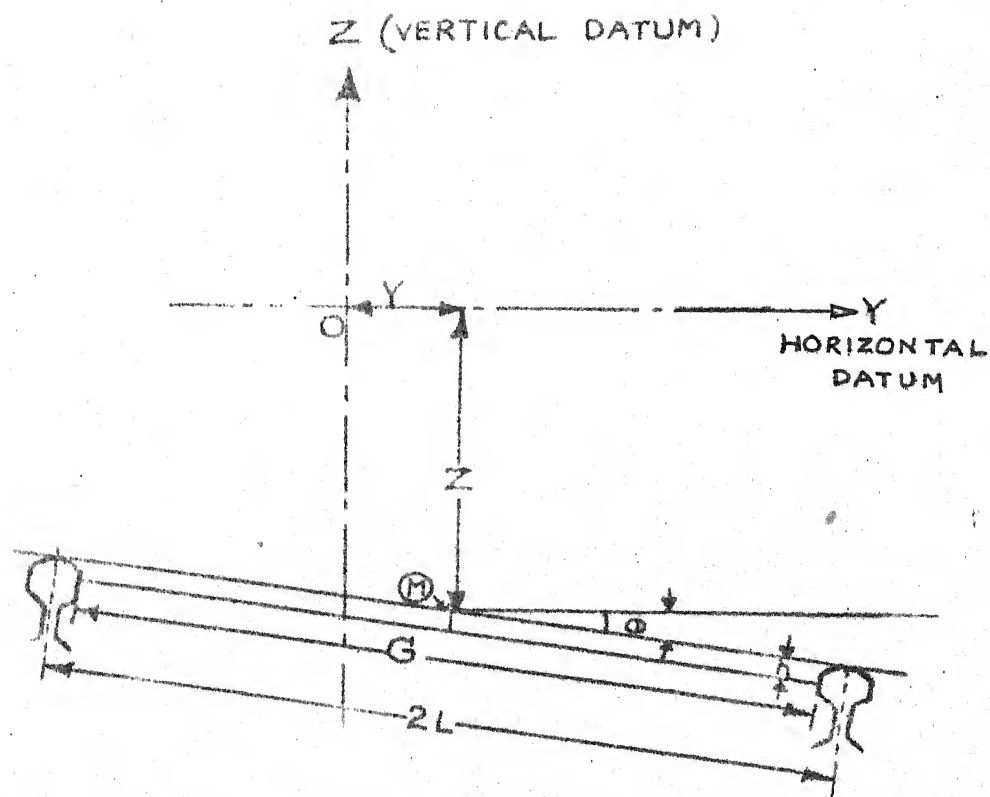
The value of A for each of the 4 track parameters can then be printed out.

### 1.4 PROPOSED SIGNAL PROCESSOR

As digital techniques offer various advantages over the analog schemes at these low frequencies, digital schemes are proposed in this system. For this, the data from the accelerometer is properly conditioned, digitized and then stored using appropriate signal conditioners and

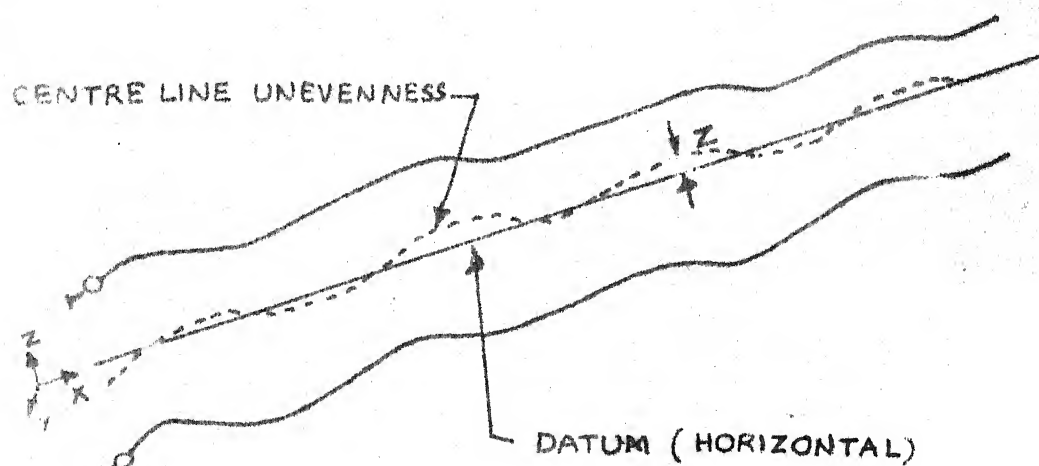
Analog to Digital converters. The different operations are performed on the data to obtain the actual track irregularity. Although hardware digital filters can be used, as the power spectral measurement of the track irregularities is also involved, instead of building different dedicated hardware supports the whole system is configured using a completely independent dedicated microcomputer with one of the easily available microprocessors and its family support. In this way, all the digital filter schemes, and power spectral measurement of the track irregularities can be obtained through the software developed for the microcomputer.

6800 microprocessor and its family support is used in this system and a complete block diagram of the proposed system is shown in Fig. 4.1. The system consists of a central processing unit (CPU) module, memory modules for program and data storage, analog multiplexer and A/D converter modules for the sampling of input data and various interface modules to interact with the system. All these modules are assembled, tested and details are discussed in Chapter 4.

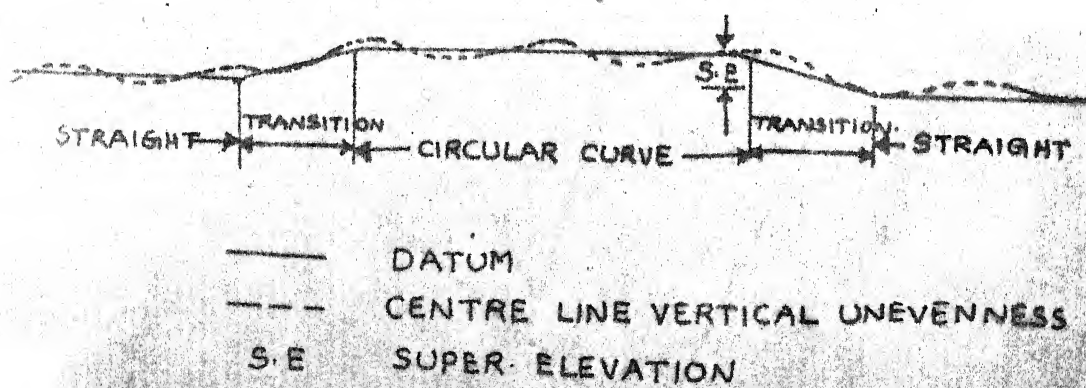


- |           |   |                        |
|-----------|---|------------------------|
| M         | - | MID. POINT OF TRACK    |
| $2L.\phi$ | - | CROSS LEVEL            |
| G         | - | GAUGE                  |
| Z         | - | CENTRE LINE UNEVENNESS |
| Y         | - | CENTRE LINE ALIGNMENT  |

FIG. 1.1. DESCRIPTION OF TRACK IRREGULARITIES

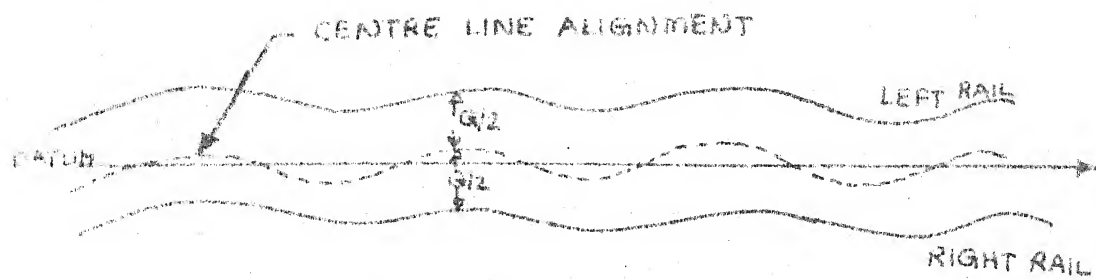


a) STRAIGHT TRACK

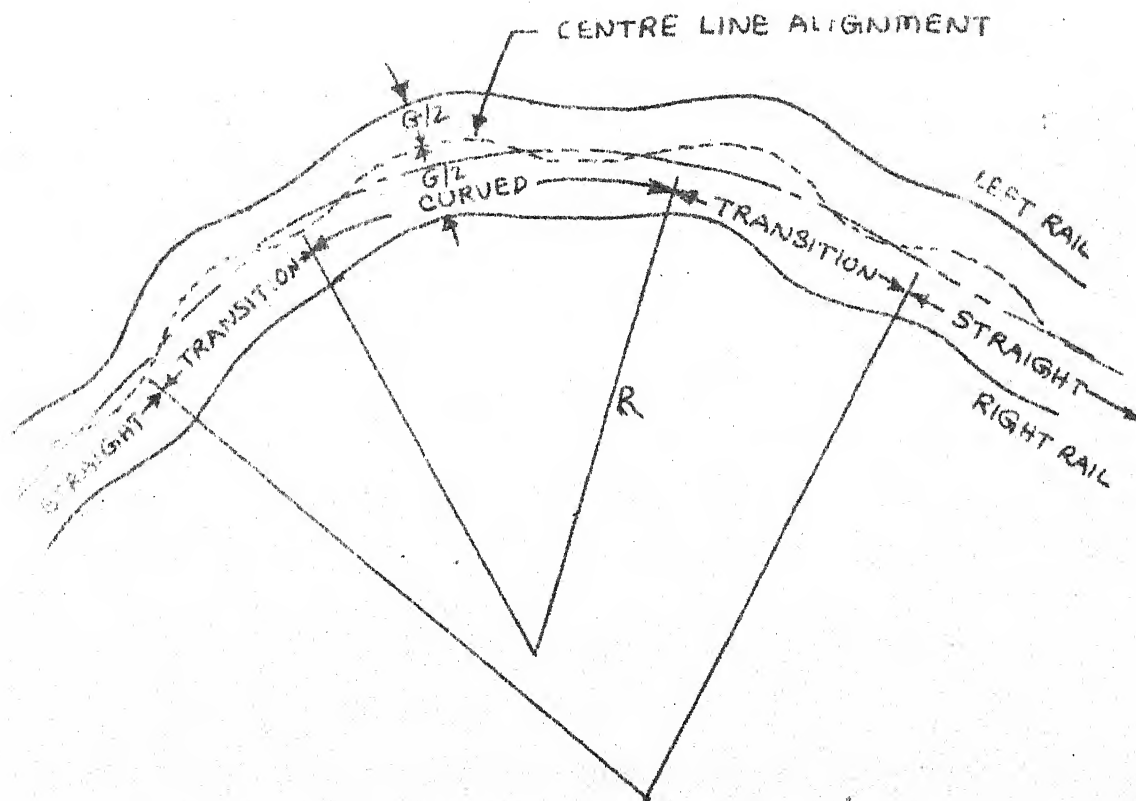


b) CURVED TRACK

FIG. 1.2. CENTRE LINE UNEVENNESS OF TRACK



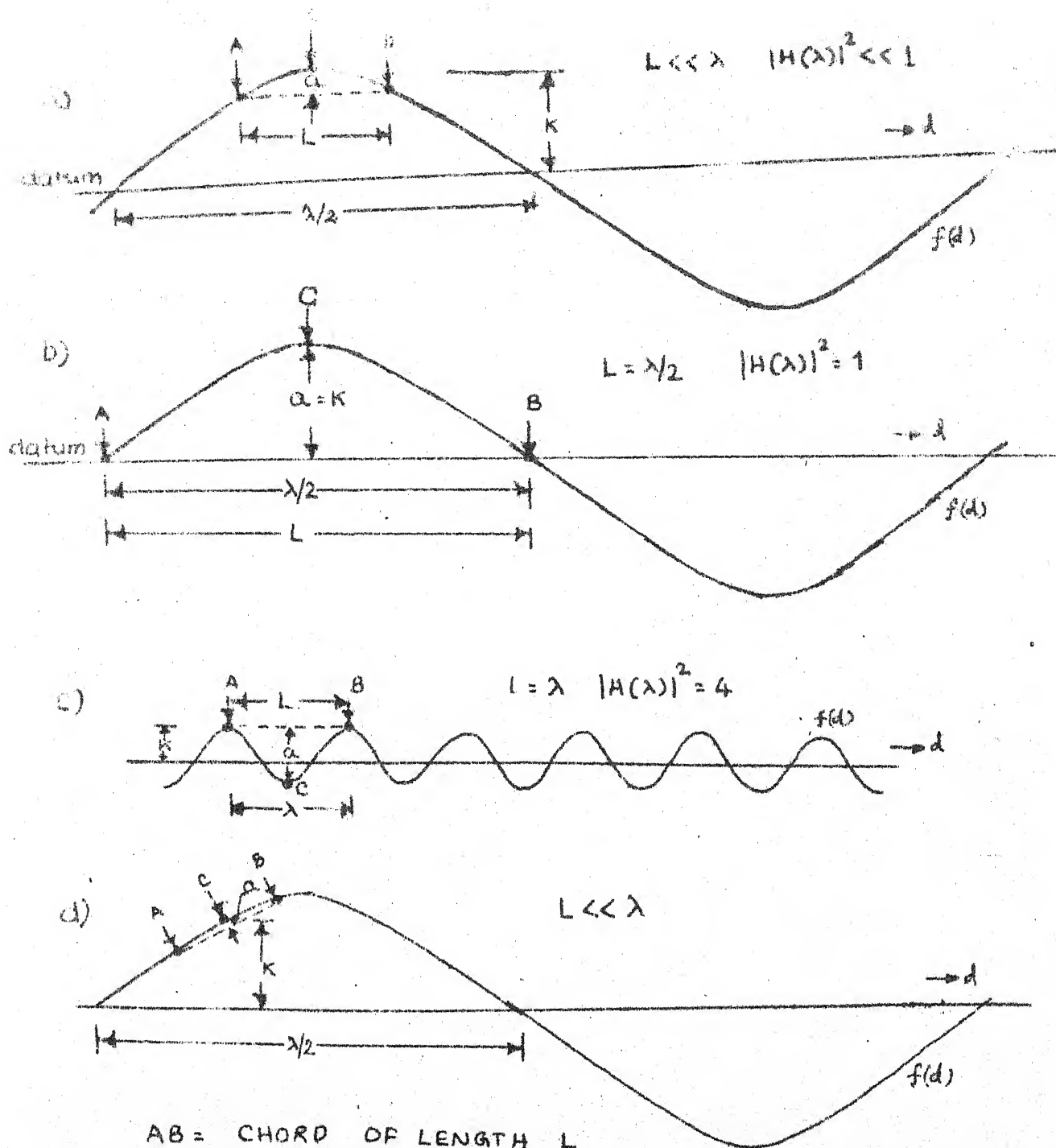
a) STRAIGHT TRACK



b) CURVED TRACK

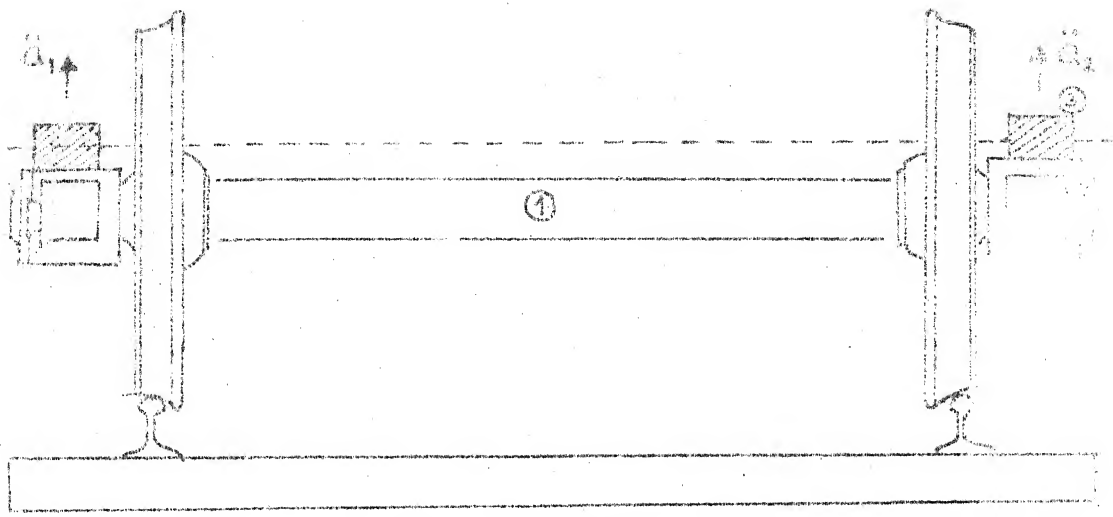
FIG. 13. CENTRE LINE ALIGNMENT OF TRACK





- AB = CHORD OF LENGTH  $L$   
 C = MID POINT OF THE CHORD  
 $f(d)$  = track irregularity  
 $d$  = distance along the track  
 $a$  = measured irregularity  
 $K$  = True irregularity  
 $\lambda$  = wave length of the irregularity

FIG. 1.4. MIDCHORD MEASUREMENTS



- ① WHEEL AXLE SET
- ② AXLE BOX
- ③ ACCELOROMETER

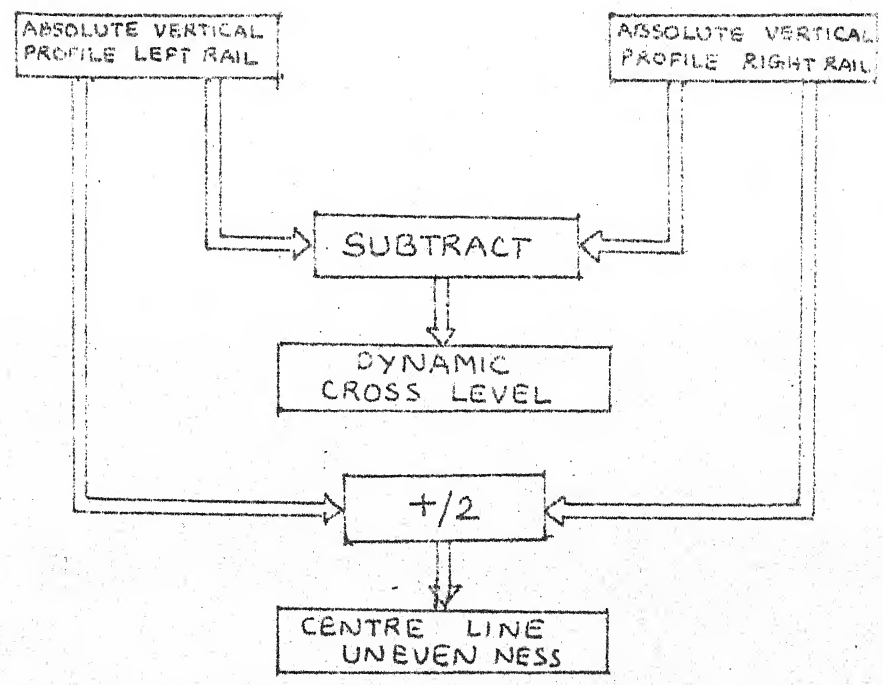
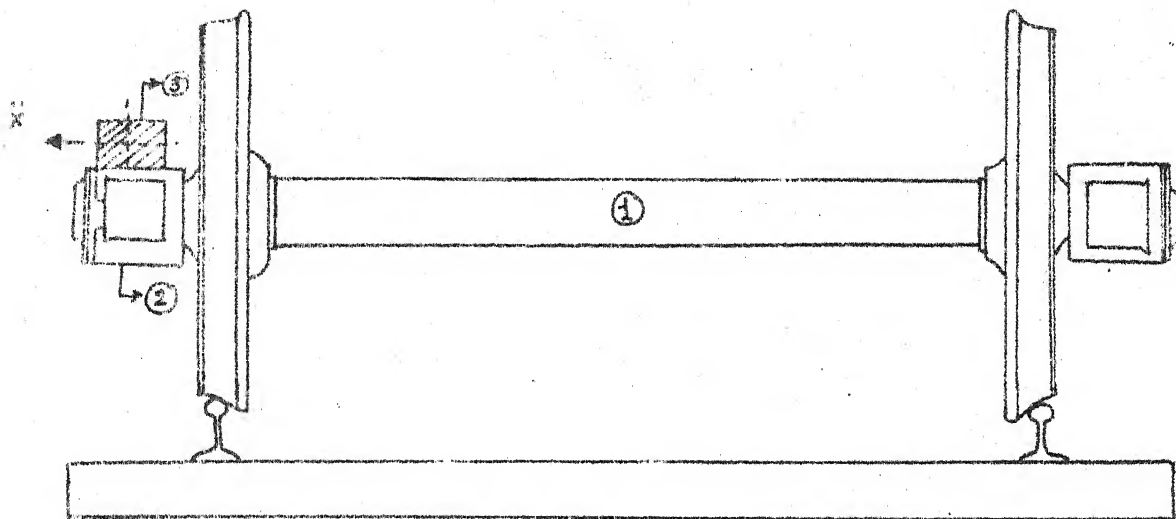


FIG. 1-5 ABSOLUTE VERTICAL PROFILE



1. WHEEL AXLE SET
2. AXLE BOX
3. ACCELEROMETER

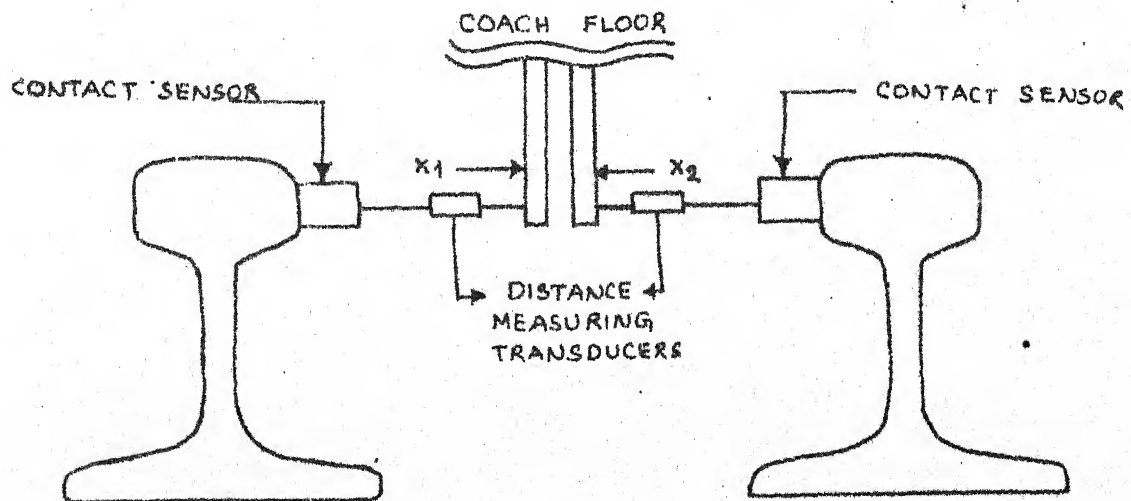
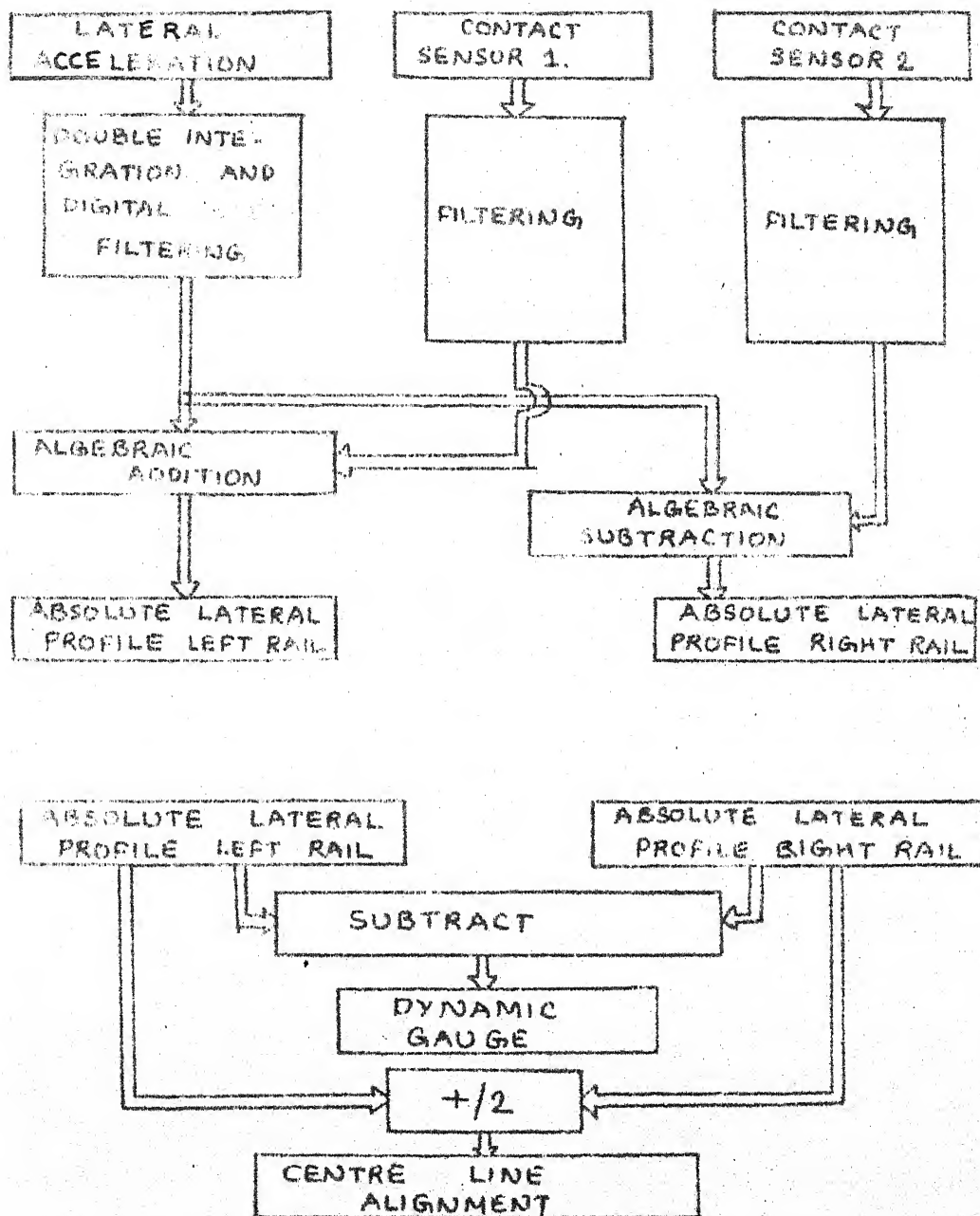


FIG. 1.6. LATERAL PROFILE MEASUREMENT



LATERAL PROFILE MEASUREMENT

## CHAPTER 2

### FILTERING TECHNIQUES FOR TRACK IRREGULARITY MEASUREMENT

#### 2.1 INTRODUCTION

The proposed system for track monitoring measures the track irregularities using accelerometers mounted on axle boxes of the rail carriage. The accelerometers pick up the second derivatives of the track irregularities i.e., if  $a(d)$  is the irregularity, the output of the accelerometer is  $\ddot{a}(d)$  where  $d$  is the distance along the track. There is thus a need for suitable filtering techniques to obtain the actual track irregularity from the accelerometer output signal.

Whether it is the measurement of vertical profile or lateral profile, an accelerometer is associated with each and therefore the method of obtaining the different irregularities will be the same viz., the output of the accelerometer is to be suitably conditioned and then double integrated, to obtain the actual irregularity  $a(d)$ . Since the frequency of interest for the track irregularities is very low the design and stability of analog integrators at these frequencies pose various problems hence are not feasible for this application. A better approach will be to process by digital techniques in which the various inputs after sampling and storage are filtered using digital filters. These filters can be implemented either in hardware or software.

In the hardware scheme, the filters are implemented using arithmetic logic units, control and registers which are used for algebraic manipulation. In the software scheme, programs for various filters should be written which will then be processed using dedicated computers.

In this chapter, digital filter schemes are described which can be used for this application. Assembly language programs for 6800 microprocessor applications have been developed and are listed in Appendix.

## 2.2 DIGITAL INTEGRATORS

As mentioned, to obtain the track irregularity, the accelerometer output signal should be double integrated. For adopting the digital schemes, these signals should be sampled and quantized using a proper Analog-to-Digital (A/D) converter. Since the variation in the track irregularity cannot be very large with respect to distance, the frequencies of interest are very small. Hence a simple Simpson Integration for this application can be adopted. This is shown in Fig. 2.1.

Let  $f(x)$  be the accelerometer output; if  $f(x)$  is sampled at a constant spatial interval of  $\Delta x$ , then

$$\int_{x=0}^k f(x) dx \simeq \sum_{i=0}^k f(x_i) \Delta x = \Delta x \sum_{i=0}^k f(x_i) \quad (2.1)$$

where  $\Delta x$  is the sampling distance and  $f(x_i)$  is the

sampled and quantized value of the signal at distance  $x_i$ . Since  $\Delta x$ , the sampling distance is constant, the integrator merely consists of an adder as given by Eq. (2.1), and a scaling factor.

If this scheme is directly applied to the digital computer applications, Integrator may overflow due to the limited precision of the computers. Especially when a DC component is overriding on the signal, this DC level will be adding up causing the computer to overflow. Similarly, depending upon the input signal, the output of the Integrator may consist a DC level thus causing overflow for the second integrator to be followed which is used for the double integration purpose. Similarly very low frequencies also cause the overflow of integrators. Hence a high pass prefilter, which filters out all the DC and very low frequencies should be used before an integrator. A complete scheme for obtaining a track irregularity from the accelerometer is as shown in Fig. 2.2. In the following sections, the digital filtering schemes are described.

### 2.3 DIGITAL FILTERS [1], [2]

Analogous to Analog filters, there are many types of digital filters like Butterworth, Tschebycheff, Elliptical etc. [2]. The digital filters can also be represented using zero-pole plots as in the case of Analog filters. Considering the real time application of track

profile measurement, the computation time for the digital filter should not be very high. And also the magnitude of the signal in the pass band of interest should not be affected by the filter response. Hence a single pole high pass Butterworth filter is chosen for this application although higher order filters give much sharper cut-off frequency. Since the processing time for Non-Recursive filters [2] is high, the recursive filter implementation is the best possible solution for this application.

The transfer function of one-pole high-pass Butterworth filter in Z - domain is given by

$$\frac{Y(Z)}{X(Z)} = H(Z) = \frac{1 - Z^{-1}}{(w - 1) Z^{-1} + w + 1} \quad (2.2)$$

where

$$Z = \exp(2\pi i f/N)$$

$$w = \tan(\pi f_c/N)$$

$$N = \text{Number of samples per second}$$

$$f_c = \text{Cut off frequency of the filter in cycles/sec.}$$

$$f = \text{any frequency for which transfer function is to be calculated.}$$



From this equation, the recursive relation for the filter is

$$Y_i = \left( \frac{1}{1+w} \right) \left[ (1-w) Y_{i-1} + X_i - X_{i-1} \right] \quad (2.3)$$

where  $f_i$  represents the present value,  $f_{i-1}$  is one state earlier value.  $X_i$  represents the present input and  $Y_i$  is the present output. The above recursive equation can be realized as given in Fig. (2.3).

As it can be seen from this realization, since the present input is subtracted from the previous input, the DC component is removed at the output of the filter. Since  $w$  is a function of cut off frequency, by properly choosing a value for  $w$ , the cut off frequency can be fixed. Since all the computer operations will be in binary arithmetic, it is better to choose a ' $w$ ' which is in multiples of 2 so that divisions and multiplications can be performed very easily. In the practical track monitoring routines, it was observed that a cut off frequency of 0.125 Hz is suitable. Considering the present speed range of interest (120 KMPH) and sampling rate of 512 samples per every Km, a value of  $2^{-5}$  for  $w$  is chosen.

For the integration, the trapezoidal integration scheme also works out to be better, for which the transfer function is given by

$$I(Z) = \frac{h}{2} \left( \frac{1+Z^{-1}}{1-Z^{-1}} \right) \quad (2.4)$$

from which the recursive relation works out to be

$$Y_i = Y_{i-1} + \left( \frac{X_i + X_{i-1}}{2} \right) h \quad (2.5)$$

where  $f_i$  is the present value,  $f_{i-1}$  is one state earlier value,  $h$  is the sampling interval. The recursive relation for high pass filter and a trapezoid integrator combined together will be

$$Y_i = \left( \frac{1}{1+w} \right) \left[ (1-w) Y_{i-1} + \left( \frac{X_i + X_{i-1}}{2} \right) h \right] \quad (2.6)$$

The composite filter is simulated on DEC 1090 computer. Whether it is the Simpson or trapezoidal integration, the following observations are made for the composite filter

- a) Settling time of the composite filter is high.
- b) When the complete double integration scheme is implemented, due to the settling time error, there is a fluctuating DC component observed at the output.

As this settling time is large, the filtered output doesn't correspond to the actual profile for this period. Hence, during this time the data is to be ignored. A better alternative in which settling time can be reduced is the 'incremental computation scheme' which works on the principle of differential input - output scheme in which increments in the data are used for processing.

## 2.4 INCREMENTAL COMPUTATION SCHEME FOR DIGITAL FILTERING OF LOW FREQUENCY SIGNALS [4]

Normally, for the digital filters which operate at low frequencies, the ratio of cut off to sampling frequency is very small. In other words, for the filters which have low ratios of cut-off to sampling frequency, the poles are located close to the unit circle in the  $Z$  - plane. The recursive filters which operate with the poles very close to  $Z = 1$  and use finite word lengths are prone to the effects of sensitivity and round off errors. A great deal of work has been done to reduce these errors and also different schemes have been presented in using the incremental computation for the low frequency signals. Detailed discussions can be found in the reference [4].

### 2.4.1 Difference Between Normal and Incremental Computation [4]

Definition:

- a) Normal Computation : A computation procedure that evaluates each value the dependent variable assumes independent of its previous values is referred to as the normal computation scheme. The value of the dependent variable computed in this manner is termed 'normal value'.

- b) Incremental Computation: Normally many physical system are slowly varying. In other words, for a given change in the independent variable, the amount by which the dependent variable changes from its previous value is very small. The succeeding value that the dependent variable assumes can be computed by adding an increment or decrement to the one previously computed. A scheme that employs this principle in evaluating values that the dependent variable assumes is referred to as an incremental computation.

#### 2.4.2 Using Digital Incremental Computation (DIC) for Digital Filtering

Let the required transfer function be  $H(Z) = Y(Z) / X(Z)$ . In the conventional filters where the normal scheme of computation is adopted, the input and output are not in incremental form. In the DIC scheme the input is followed by a differencer, a transfer function  $H'(Z)$  for which the input and output are in incremental form and an output integrator as shown in Fig. 2.4. As from this illustration, for the two structures to be identical the transfer functions  $H(Z)$  and  $H'(Z)$  should be identical. A simple DIC structure of first order filter is shown in Fig. 2.5.  $e_1(n)$  and  $e_2(n)$  are the noise sources arising from the quantization operations for multiplication and integration. The transfer function  $H'(Z)$  of the DIC structure is

$$H'(Z) = \frac{Y(Z)}{X(Z)} = \frac{(B_0 + B_1 G_1) - B_0 Z^{-1}}{1 - (1 - A_1 G_1) Z^{-1}} \quad (2.7)$$

The transfer function of the first order conventional filter is

$$H(Z) = \frac{Y(Z)}{X(Z)} = \frac{c - d Z^{-1}}{1 - a Z^{-1}} \quad (2.8)$$

In order to the transfer functions to be equivalent corresponding coefficients in transfer functions are to be equated. From this, the DIC filter coefficients are given by

$$\begin{aligned} B_0 &= d \\ B_1 &= (c - d) / G_1 \\ A_1 &= (1 - a) / G_1 \end{aligned} \quad (2.9)$$

where  $G_1$  is the gain of the integrator.

A block diagram of the DIC filter with inputs and outputs in normal form is shown in Fig. 2.6. The coefficients  $A_i$ ,  $B_i$  will be chosen such that  $H'(Z) = G_0 H(Z)$  where  $G_0$  is a scale factor and is imposed by the structure since it operates upon the increments of the input. And also  $G_0$  can be used for controlling the dynamic range of the filter. Normally  $G_0$  should be chosen such that  $|\Delta Y|_{\max} = |\Delta X|_{\max}$ . In the above DIC structured filter, the input and output are in incremental form. In order to specify the complete structure of the DIC, the scheme in Fig. 2.6 will be adopted where input and output are in normal form.

## Second Order Filter

A second order filter can also be derived using DIC schemes on similar lines. Consider the second order transfer function

$$H(Z) = \frac{c - d Z^{-1} + Z^{-2}}{1 - a Z^{-1} + b Z^{-2}} \quad (2.10)$$

The structures of second order conventional and DIC filters are given in Fig. 2.7 and Fig. 2.8. From Fig. 2.8 the transfer function of DIC filter is given by

$$H'(Z) = \frac{(B_0 - B_1 G_2 + B_2 G_1 G_2) - (2 B_0 + B_1 G_2) Z^{-1} + B_0 Z^{-2}}{1 - (2 - A_1 G_2 - A_2 G_1 G_2) Z^{-1} + (1 - A_1 G_2) Z^{-2}} \quad (2.11)$$

The corresponding coefficients are

$$B_0 = 1$$

$$B_1 = (d - 2) / G_2$$

$$B_2 = (1 + c - d) / G_1 G_2$$

$$A_1 = (1 - b) / G_2$$

$$A_2 = (1 - a + b) / G_1 G_2$$

where  $G_i = 2^{-b_i}$  is the gain of the integrator.

$e_1(n)$ ,  $e_2(n)$ ,  $e_3(n)$  are the noise sources arising from the quantization operation of multiplication and integration.

## 2.5 NOISE STUDY, DESIGN PROCEDURE [4]

The roundoff errors that occur in recursive digital filters employing fixed point arithmetic are mainly due to the finite word length of the digital computers.

The first error is caused by the addition of two fixed-point numbers resulting in overflow. By restricting the dynamic range of the signal level, the overflow can be controlled not only at the input and output but also at other intermediate points. The second error is due to the multiplication of the signal with the filter coefficients. When two numbers are multiplied, the resulting product word length is not equal to the sum of the lengths of the two words being multiplied. In a recursive filter, this product is again multiplied with a sample of the input signal in the next recursion. But the length of the product should be quantized to limit the register length. This quantization of the product word gives rise to an error that accumulates as succeeding multiplications are made. The model for fixed point round off noise following a multiplication is shown in Fig. 2.9.

#### 2.5.1 Noise Power in Second Order Recursive Filters

Consider a transfer function for second order recursive filter

$$H(Z) = \frac{c}{1 - aZ^{-1} + bZ^{-2}} \quad (2.13)$$

For obtaining the model of recursive filter the following assumptions are made. The operation of quantization used is rounding.

- a) Any two different samples from the same noise sources are uncorrelated.
- b) Any two noise sources associated with different multipliers are uncorrelated.
- c) Each noise source is uncorrelated with the input sequence.

Let the variable be represented by  $(b' + 1)$  bits in the fixed point arithmetic which includes the sign bit also. Then each noise source can be modelled as a discrete stationary white random process with uniform power spectral density as shown in Fig. 2.10.

With the above assumptions the filter can be modelled as shown in Fig. 2.11. When the input signal is completely absent or becomes constant, the three assumptions of uncorrelatedness fail and the filter exhibits an oscillatory behaviour at the output which is termed LIMIT CYCLE OSCILLATION. The round off noise power at the output is given by [4]

$$\sigma_c^2 = \frac{1 + b}{6 (1 - b) (1 + b - a) (1 + b + a)} \quad (2.14)$$

for the conventional filter.

A similar expression can be derived for the DIC filter given by

$$\sigma_d^2 = \frac{G_1^2 G_2^2 (1 + b) + [3 G_2^2 + 2 (3 - a - b)] (1 - a + b)}{6 (1 - b) (1 - a + b) (1 + a + b)} \quad (2.15)$$



where  $G_1 = 2^{-b_1}$  and  $G_2 = 2^{-b_2}$  are the gains of the integrator. Normally  $G_2$  is of the order of  $2^{-7}$  hence  $G_2^2$  can be neglected in the above equation.

$$\therefore \sigma_d^2 \simeq \frac{3 - a - b}{3(1 - b)(1 + a + b)}$$

or

$$\sigma_d^2 \simeq \frac{2A_1 + A_2 G_1}{3A_1(4 - 2A_1 G_2 + A_2 G_1 G_2)} \quad (2.16)$$

From this it can be seen that  $G_1$  and  $G_2$  affect the round off errors. The expressions for  $A_1$  and  $A_2$  are (from 2.12)

$$A_1 = (1 - b) / G_2 = (1 - b) 2^{b_2} \quad (2.17)$$

$$A_2 = (1 - a + b) / G_1 G_2 = (1 - a + b) 2^{b_1} \cdot 2^{b_2} \quad (2.18)$$

Choice of  $b_2$  :

From the above it can be seen that  $A_1$  depends only on  $G_2$  while  $A_2$  depends upon both  $G_1$  and  $G_2$ . Therefore depending upon the values assigned for  $G_1$  and  $G_2$  in the numerator of (2.16), the following situations will arise

$$a) \quad 2A_1 \ll A_2 G_1 \quad (2.19)$$

$$b) \quad 2A_1 \gg A_2 G_1 \quad (2.20)$$

and in the denominator, normally,

$$c) \quad 2A_1 G_2, A_2 G_2 G_1 \ll 4 \quad (2.21)$$

Using (2.19), (2.21) in (2.16)

$$\sigma_d^2 \simeq A_2 G_1 / 12 A_1 \quad (2.22)$$

From this, small values of  $A_1$  should be avoided, otherwise round off error increases. It was shown [4], from experimental studies, that values of  $A_1 < 1$  should be avoided. Therefore  $A_1 \geq 1$  is preferred to minimize the round off error. Using this condition in (2.17),

$$(1 - b) 2^{b^2} \geq 1$$

or

$$b_2 \geq \log_2 \left( \frac{1}{1 - b} \right) \quad (2.23)$$

and the value of  $G_2$  can be obtained by choosing a value for  $b_2$  using the above equation.

Choice of  $b_1$  :

A choice for  $b_1$  can be obtained by setting

$|y_1|_{\max} \simeq |y_2|_{\max}$  in Fig. 2.8 . Let  $h'_1(n)$  and  $h'_2(n)$  be the impulse responses from the input nodes to those at which  $y_1(n)$  and  $y_2(n)$  present [4].

Then

$$|y_1|_{\max} \simeq |\Delta x|_{\max} \sum_n |h'_1(n)| \quad (2.24)$$

$$|y_2|_{\max} \simeq |\Delta x|_{\max} \sum_n h'_2(n) \quad (2.25)$$

where

$$\begin{aligned}
 H_1'(Z) &= \frac{(1 + c - d) + (ad - a - d - bc + 1) Z^{-1} + (1 - a + b) Z^{-2}}{G_1 G_2 D(Z)} \\
 &= \sum_n h_1'(n) Z^{-n} \quad (2.26)
 \end{aligned}$$

$$\begin{aligned}
 H_2'(Z) &= \frac{(c - 1) + (a - d) Z^{-1} + (1 - b) Z^{-2}}{G_2 D(Z)} \\
 &= \sum_n h_2'(n) Z^{-n} \quad (2.27)
 \end{aligned}$$

$$D(Z) = 1 - a Z^{-1} + b Z^{-2} \quad (2.28)$$

Using these equations,

$$\begin{aligned}
 G_1 G_2 \sum_n |h_1'(n)| &\simeq G_2 \sum_n |h_2'(n)| \\
 \text{or} \\
 2^{-b_1} \sum_n |h_1'(n)| &\simeq \sum_n |h_2'(n)| \\
 \text{or} \\
 b_1 &\simeq \log_2 \frac{\sum_n |h_1'(n)|}{\sum_n |h_2'(n)|} \quad (2.29)
 \end{aligned}$$

Choice for dynamic range scaling factor  $G_0$ :

From the Fig. (2.6), where the implementation of DIC filter using the input and output are in normal form is presented, the scaling factor  $G_0$  can be obtained by choosing  $|\Delta y|_{\max} = |\Delta x|_{\max}$  or from the figure it is the same as

$$|Y_3|_{\max} = |x|_{\max} \quad (2.30)$$

Using this  $G_0$  can be evaluated as

$$G_0 \geq \frac{Y_3 \max}{x \max} \frac{1}{\sum_n |h(n)|} \quad (2.31)$$

where  $h(n)$  is the impulse response of the filter.

In this  $\sum_n |h(n)|$  is the infinite summation and a reasonable value of  $n$  should be chosen such that the error in the summation is small. In the extreme case

$$G_0 \simeq \frac{Y_3 \max}{x \max} \frac{1}{\sum_n |h(n)|} \quad (2.32)$$

The value of  $G_0$  obtained from this equation can be adjusted to the nearest binary number in order to eliminate the multiplier. FORTRAN programs for calculation of these parameters are given in [4].

## 2.6 HIGH PASS FILTERING USING DIC SCHEME

The transfer function for a second order high pass filter is of the form

$$H(Z) = \frac{(1 - Z^{-1})^2}{1 - a Z^{-1} + b Z^{-2}} \quad (2.33)$$

Comparing this with the transfer function of the second order filter

$$H(Z) = \frac{c - d Z^{-1} + Z^{-2}}{1 - a Z^{-1} + b Z^{-2}} \quad (2.34)$$

we get  $c = 1$ ;  $d = 2$ ; using this the coefficients for DIC structure can be obtained as

$$\begin{aligned} B_0 &= 1; & B_1 &= 0; & B_2 &= 0 \\ A_1 &= (1 - b) / G_2; & A_2 &= (1 - a + b) / G_1 G_2 \end{aligned} \quad (2.35)$$

The block diagram is shown in Fig. 2.12.

## 2.7 HIGH PASS FILTER FOR TRACK PROFILE MEASUREMENT

As described earlier, a one pole Butterworth high pass filter is first implemented for the real time application of track profile measurement. For this the high pass function considered will be

$$H(Z) = \frac{1 - Z^{-1}}{(w - 1) Z^{-1} + w + 1} \quad (2.36)$$

For this filter, the working programs in 4, are implemented on DEC-1090 computer and the following coefficients for the DIC scheme are obtained.

$$B_0 = 1 \quad A_1 = 1 \quad b_2 = 5 \quad G_0 = 1$$

and the DIC high pass filter will be as shown in Fig. 2.13.

The proposed system thus would consist of a first order Butterworth high pass filter using DIC structure and a simpson integrator. An assembly language program for 6800 microprocessor has been developed and is given in Appendix A. This program is for the composite filter consisting of a high pass filter and integrator. The programme is tested on 6800 microprocessor development system and the results and discussions are presented in Chapter (5).

After obtaining the different track irregularity parameters namely verticle profile of left and right

rails, through simple algebraic manipulation described in Chapter 1, one can derive all the other irregularities like unevenness, gauge etc.

In the following Chapter, the power spectral measurement of these irregularities through Fast Fourier Transform (FFT) technique is described.

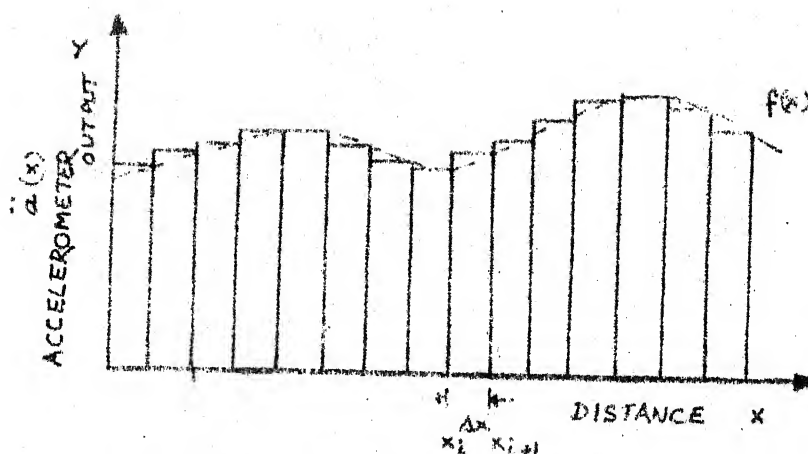


FIG. 2.1. SIMPSON INTEGRATION

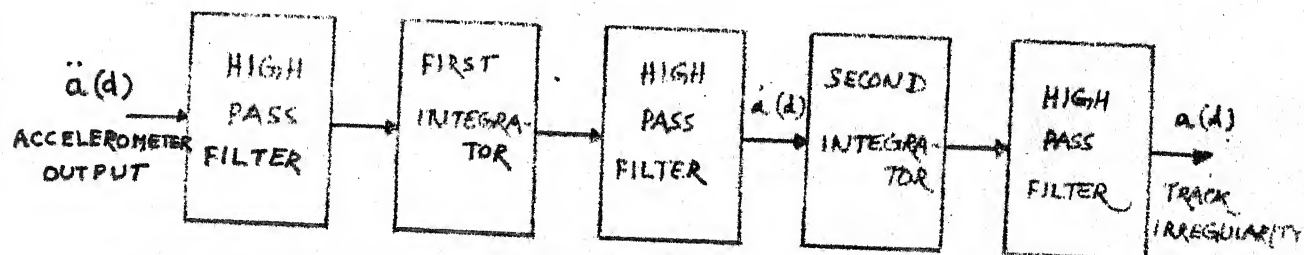


FIG. 2.2. FILTERING SCHEME

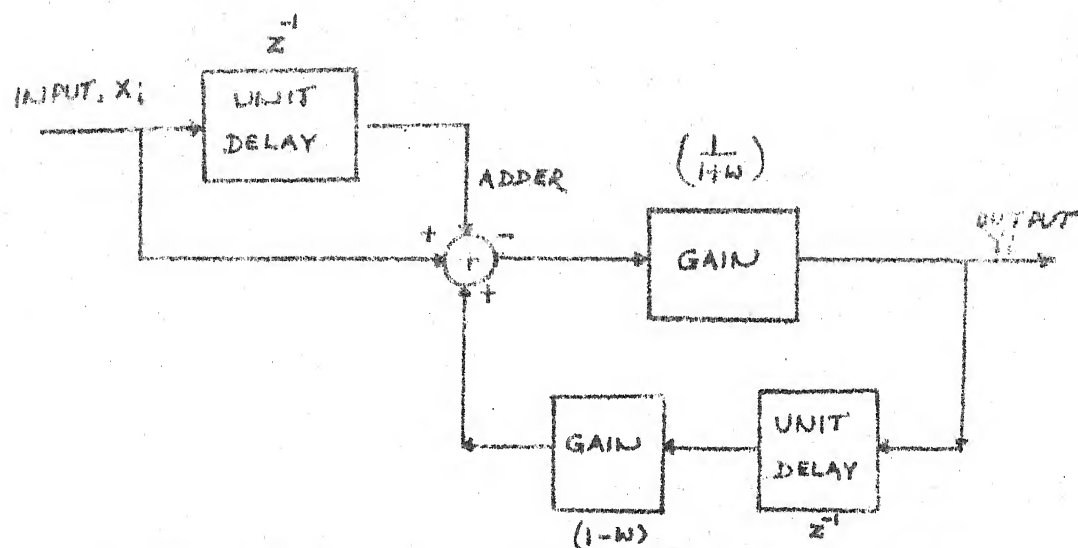


FIG. 2.3. REALIZATION OF SINGLE POLE HIGH PASS BUTTERWORTH DIGITAL FILTER.

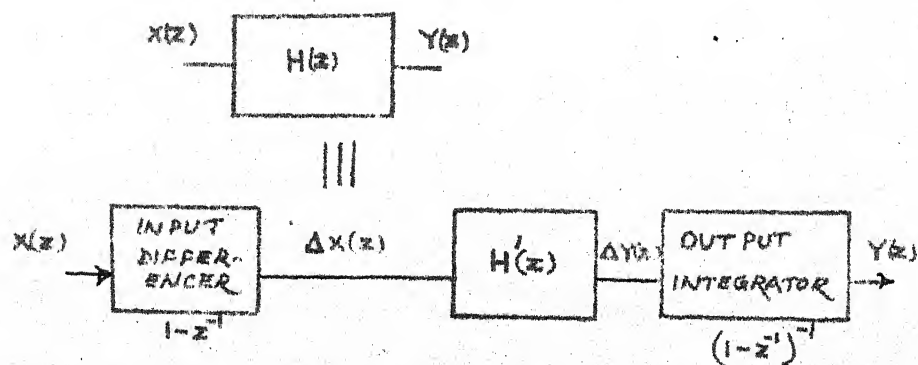


FIG. 2.4. ILLUSTRATION OF THE EQUIVALENCE BETWEEN CONVENTIONAL AND DIC FILTERS.



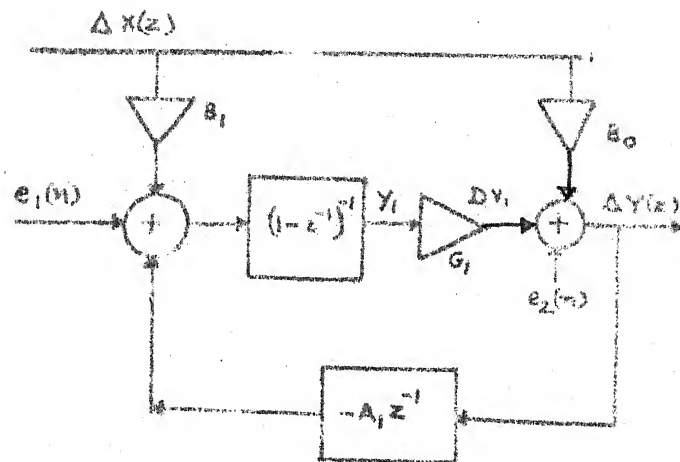


FIG. 2.5 BLOCK DIAGRAM FOR THE DIS STRUCTURE OF FIRST ORDER FILTER.

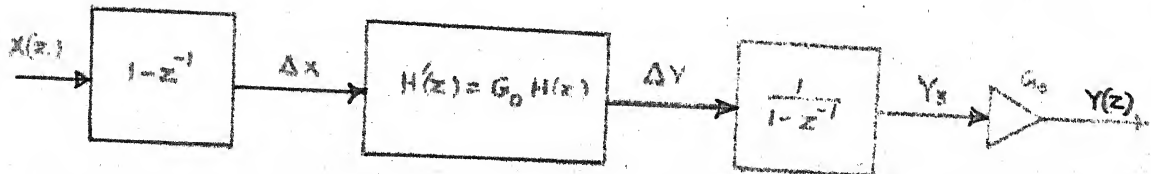


FIG. 2.6. BLOCK DIAGRAM OF DIC FILTER WITH INPUT AND OUTPUT IN NORMAL FORM.

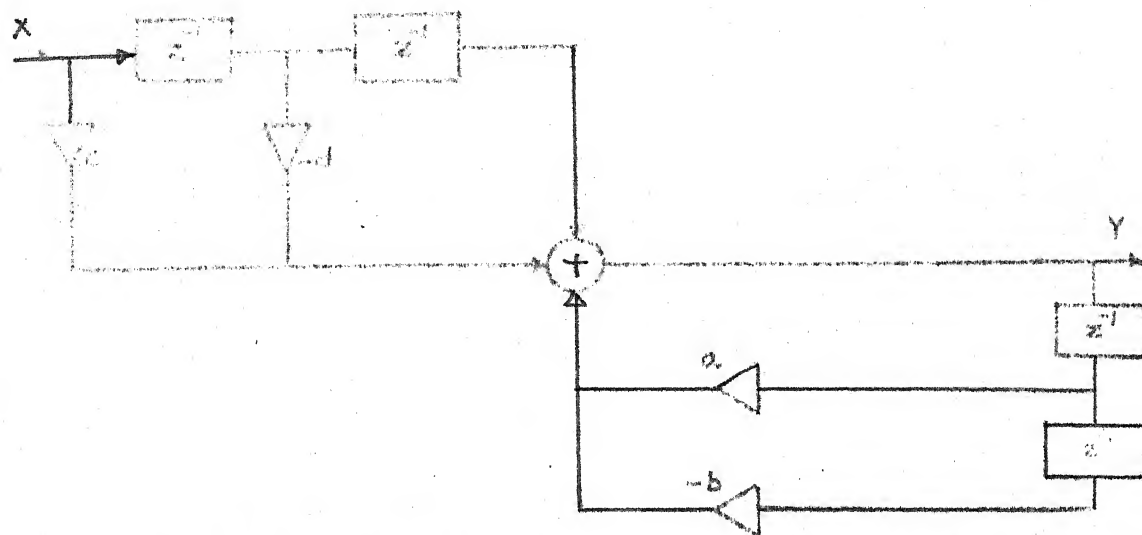


FIG. 2.7. SECOND ORDER CONVENTIONAL FILTER.

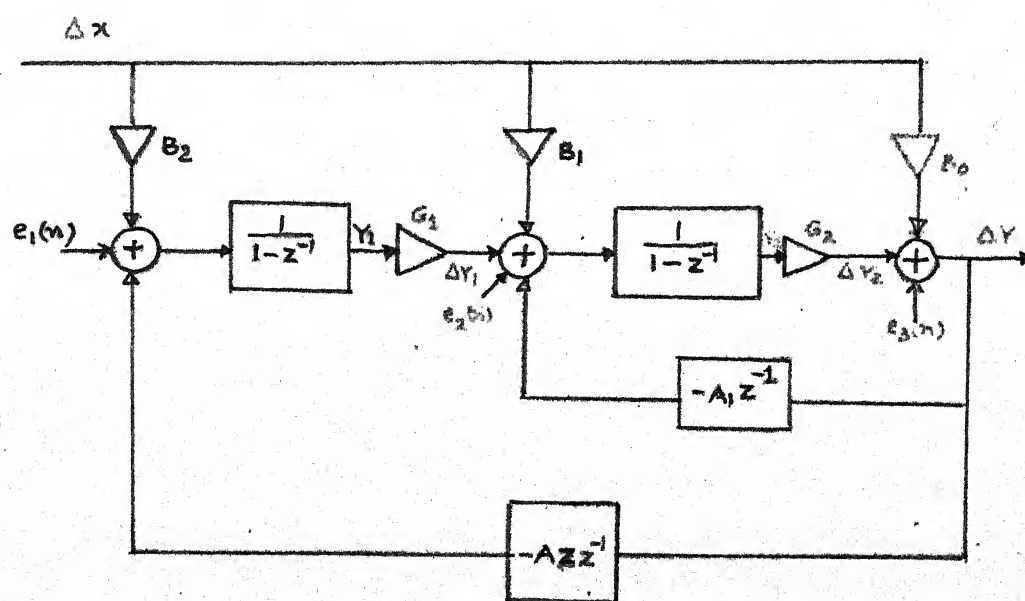


FIG. 2.8. SECOND ORDER DIC FILTER.

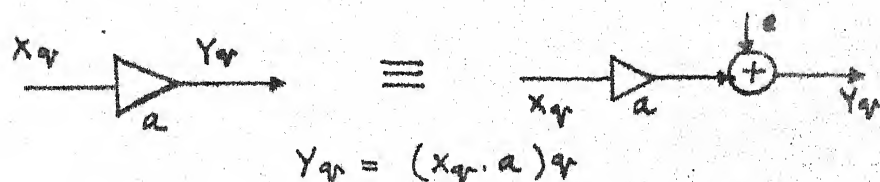


FIG. 2.9. FIXED POINT QUANTIZATION NOISE MODEL.

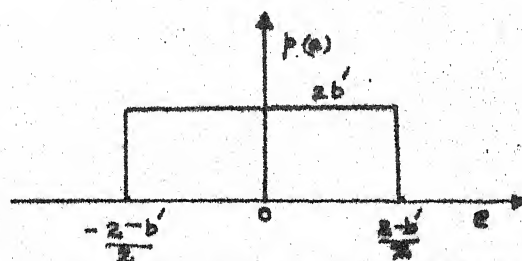
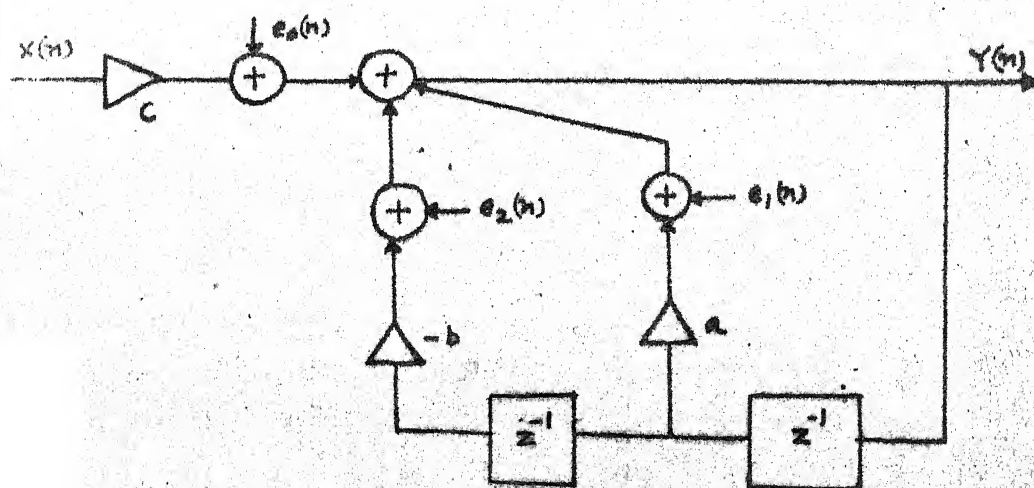


FIG. 2.10. QUANTIZATION NOISE PROBABILITY DENSITY FUNCTION FOR THE ROUNDING OPERATION.

FIG. 2.11. QUANTIZATION NOISE MODEL FOR SECOND ORDER FILTER  $H(z) = \frac{c}{1 - az^{-1} + bz^{-2}}$

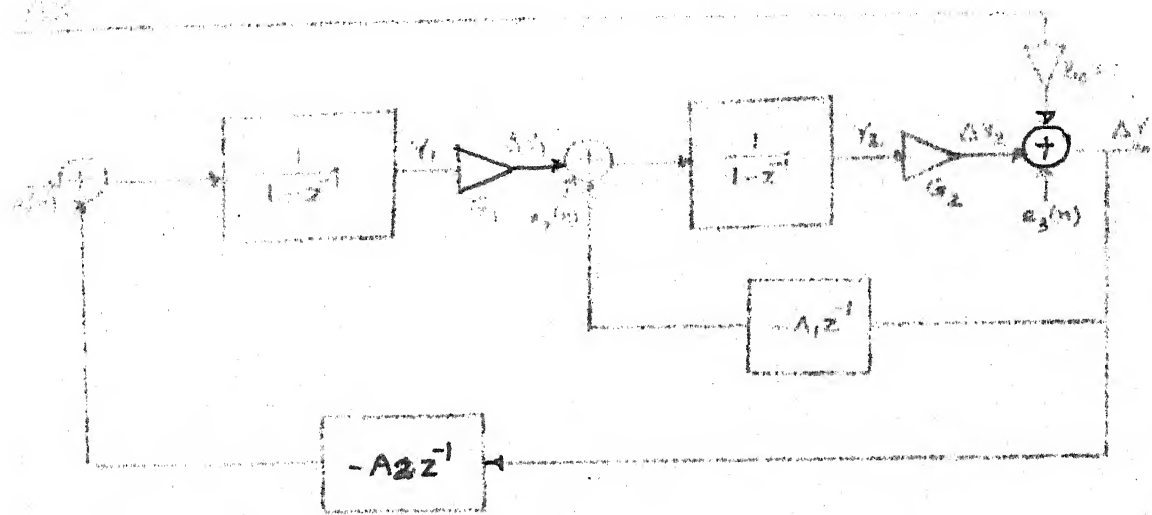


FIG. 2.12. BLOCK DIAGRAM OF A SECOND ORDER DDC FILTER.

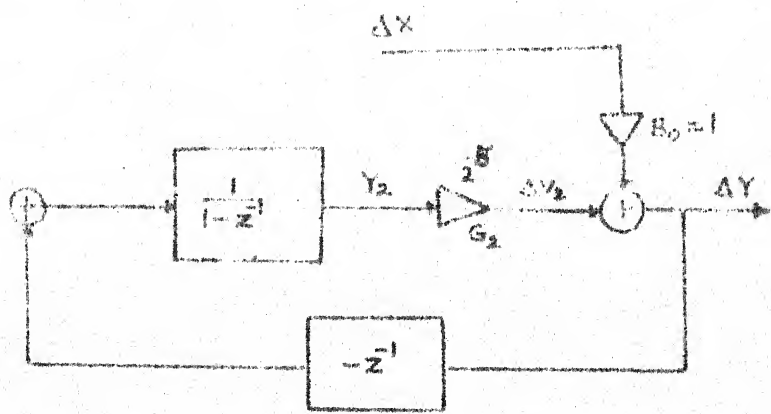


FIG. 2.13. FIRST ORDER HIGH PASS BUTTERWORTH FILTER - DDC STRUCTURE.

## CHAPTER 3

### POWER SPECTRAL MEASUREMENT OF TRACK IRREGULARITIES

#### 3.1 INTRODUCTION

As the trains move on irregular tracks the comfort of the passenger is affected. Standards have been established for minimum comfort to be provided. Equivalently standards are also laid down for categorization of rail tracks through roughness factors. These factors are intimately connected to the Power Spectral Density (PSD) of the random process correspondent to track irregularities.

In Chapter 2 the methods of obtaining the waveforms corresponding to the track irregularities are discussed. Using this the power spectral density associated with the irregularity is to be obtained. A set of  $N$  samples associated with the track irregularity is available to estimate the power spectral density. In the following sections, the estimation of PSD through the use of Fast Fourier Transform (FFT) is discussed. The implementation of FFT on 6800 microprocessor is also described.

#### 3.2 POWER SPECTRAL DENSITY (PSD)

The random process is said to be 'strongly stationary' when all the possible moments of the process

are time invariant. The process is said to be 'weakly stationary' in wide sense if the first two moments namely mean and autocorrelation of the process are time invariant. Practically it was observed that track irregularity parameters constitute a weakly stationary random process.

The PSD of a process is defined by

$$S_X(\omega) = \int_{-\infty}^{\infty} R_X(\tau) e^{-j\omega\tau} d\tau \quad (3.1)$$

where  $X$  is the random process,  $S_X(\omega)$  is the PSD and  $R_X(\tau)$  is the autocorrelation of  $X$ . The PSD is non negative for all  $\omega$  and even function. Because of this the PSD is defined only over the positive frequencies from Zero to  $+\infty$  and is referred to as 'one sided spectrum'. The ordinates of one sided spectrum will be double the right half of mathematically generated two sided spectral density, and is used here. The important constraint underlying the definition of PSD is that the sample function (or realization) of the process should be a record from a stationary random process of infinity. However, the concept of PSD is also equally applicable to weak stationary process. Since it is not possible to take a record length of infinity, a realizable length  $L$  will be chosen to make the definition of PSD physically realizable and to obtain a consistent estimate of PSD.

### 3.2.1 Mathematical Analysis [5]

Although the concept of random process has been developed for continuous-time random signals, the same can be easily applied to the case of discrete-time random signals. The mean and autocorrelation of a discrete process  $X(nT)$  can be expressed as

$$E [X(nT)] = \int_{-\infty}^{\infty} x p(x; nT) dx = \mu_x \quad (3.2)$$

$$R_X(kT) = E [X(nT) X(nT + kT)] \quad (3.3)$$

$$\text{or } R_X(k) = E [X_n X_{n+k}] \quad (3.4)$$

where  $k$  is the time separation or lag.

In the discrete case, the  $N$  samples from a realization of a zero-mean stationary random process will be used to 'estimate' its autocorrelation function, which is defined as

$$R(k) = E [x_n x_{n+k}] \quad (3.5)$$

First the estimation  $R(0) = \sigma^2$  will be considered. Let the estimate be

$$\hat{\sigma}^2 = R_N(0) = \frac{1}{N} \sum_{i=0}^{N-1} x_i^2 = \frac{x_0^2 + x_1^2 + \dots + x_{N-1}^2}{N} \quad (3.6)$$

In this, if  $k$  is large  $x_i$  and  $x_{i+k}$  will be effectively independent even though the realizations  $x_0^2$ ,  $x_1^2$ , ... need not be independent.

The estimate  $\hat{\sigma}^2$  is eq. (3.6) is unbiased (for large  $N$ ) since  $E[\hat{\sigma}^2] = \sigma^2$  and also consistent since  $\lim_{N \rightarrow \infty} E[(\hat{\sigma}^2 - \sigma^2)^2] = 0$  i.e. variance is zero. Hence for large  $N$ , the  $\hat{\sigma}^2$  from a single realization has a high probability of nearing the true value  $\sigma^2$ .

In the similar lines, the estimate for  $R_N(k)$ , the autocorrelation function at other lags can be proposed as

$$R_N(k) = \frac{x_0 x_{|k|} + x_1 x_{|k|+1} + \dots + x_{N-1-|k|} x_{N-1}}{N} \quad (3.7)$$

$$= \frac{1}{N} \sum_{i=0}^{N-|k|-1} x_i x_{i+|k|} \quad k = 0, \pm 1, \pm 2, \dots, \pm N-1 \quad (3.8)$$

which averages all possible products of samples separated by a lag of  $k$  and for large  $k$  there are very few possible products. For  $k \geq N$ , there are no possible pairs with this lag available, hence it will be assumed that the estimate of  $R_N(k)$  is zero.

$$\therefore R_N(k) = \begin{cases} \frac{1}{N} \sum_{i=0}^{N-|k|-1} x_i x_{i+|k|} & k = 0, \pm 1, \pm 2 \dots \pm N-1 \\ 0 & k \geq N \end{cases} \quad (3.9)$$

$R_N(k)$  is an evenfunction of  $k$ , as is true in the case of  $R(k)$ . Here  $N$  denotes that the realization is of  $N$  samples in length.



The mean value of the above estimate is

$$\begin{aligned} E [R_N(k)] &= \frac{1}{N} \sum_{j=0}^{N-1-|k|} E [x_j x_{j+|k|}] \\ &= \left(1 - \frac{|k|}{N}\right) R(k) \end{aligned} \quad (3.10)$$

Thus the sample autocorrelation function in (3.9) is biased since the mean of the estimate is not the true autocorrelation function  $R(k)$  at lag  $k$ . However, as  $N \rightarrow \infty$ , the term  $|k|/N$  vanishes. Hence  $R_N(k)$  is asymptotically unbiased. An unbiased estimate can be easily obtained by dividing the sum in (3.10) by  $(N - |k|)$  rather than  $N$ . Then

$$E [R_N(k)] = \frac{1}{N - |k|} \sum_{j=0}^{N-1-|k|} E [x_j x_{j+|k|}] \quad (3.11)$$

However it was shown [5] that for the estimate of (3.10) variance is small for  $N \gg |k|$  for which bias is also small. Therefore, unless a large number of lag products is available for an estimate at a  $k$ , the resulting estimate  $R_N(k)$  will not be reliable.

### 3.2.2 Estimates of PSD

The power spectral density and autocorrelation function of a realization are related through the Discrete Fourier Transform (DFT), given by

$$S(\omega) = \sum_{k=-\infty}^{\infty} R(k) e^{-jk\omega T_s} \quad (3.12)$$

Considering the estimate of  $R(k)$  as  $R_N(k)$ , given by (3.9), the spectral estimate  $S_N(\omega)$  will be,

$$S_N(\omega) = \sum_{k=-\infty}^{\infty} R_N(k) e^{-jk\omega T_s} \quad (3.13)$$

The spectral estimate  $S_N(\omega)$  is also related to the data samples  $X_N(\omega)$  through the DFT,

$$S_N(\omega) = \frac{1}{N} \left| \sum_{n=0}^{N-1} x_n e^{-jn\omega T_s} \right|^2 = \frac{1}{N} |X_N(\omega)|^2 \quad (3.14)$$

This can be proved as follows. Consider the truncated signal

$$x_n^N = \begin{cases} x_n & n = 0, 1, \dots, N-1 \\ 0 & \text{otherwise} \end{cases} \quad (3.15)$$

Then

$$R_N(k) = \frac{1}{N} \sum_{n=-\infty}^{\infty} x_n^N x_{n+k}^N \quad (3.16)$$

From (3.13)  $S_N(\omega)$  is given by

$$\begin{aligned} S_N(\omega) &= \frac{1}{N} \sum_{k=-\infty}^{\infty} \sum_{n=-\infty}^{\infty} x_n^N x_{n+k}^N e^{-jk\omega T_s} \quad (3.17) \\ &= \frac{1}{N} \sum_{n=-\infty}^{\infty} x_n^N e^{jn\omega T_s} \sum_{k=-\infty}^{\infty} x_{n+k}^N e^{-j\omega(n+k)T_s} \end{aligned} \quad (3.18)$$

$$= \frac{1}{N} X_N(\omega) X_N^*(\omega) = \frac{1}{N} |X_N(\omega)|^2 \quad (3.19)$$

$$\text{in which } X_N(\omega) = \sum_{n=-\infty}^{\infty} x_n^N e^{-jn\omega T_s} = \sum_{n=0}^{N-1} x_n e^{-jn\omega T_s}$$

Considering the estimate  $S_N(\omega)$ , the mean of  $S_N(\omega)$  is,

$$E[S_N(\omega)] = \sum_{k=-\infty}^{\infty} E[R_N(k)] e^{-jk\omega T_s} \quad (3.20)$$

From (3.10),

$$E[S_N(\omega)] = \sum_{k=-N}^N R(k) \left(1 - \frac{|k|}{N}\right) e^{-jk\omega T_s} \quad (3.21)$$

Thus the spectral estimate is the biased estimate of  $S(\omega)$ , which differs from  $S(\omega)$  by the term

$$v_k^N = \begin{cases} \left(1 - \frac{|k|}{N}\right) & |k| \leq N \\ 0 & |k| > N \end{cases} \quad (3.22)$$

However the  $S_N(\omega)$  is asymptotically unbiased since the term  $|k|/N$  vanishes for large  $N$ . The term  $v_k^N$  is called the 'window function'. The presence of this term in spectral estimate causes the power that presents in a particular frequency range to be smeared out over a wider range. This spreading of the power is also called as 'LEAKAGE'. For having an accurate estimate of PSD, suppression of sidelobes or reduction of leakage is essential. This can be achieved by using spectral windows on raw power spectral density. There are many window functions available [5] and the following are the most popular windows that are practically used.

- a) Rectangular
- b) Hann
- c) Hamming

- d) Blackman
- e) Kaiser

Out of which Hann and Hamming windows are mostly used in many applications.

### 3.3 COMPUTATION OF PSD

There are three methods available to evaluate the PSD

- a) To compute the autocorrelation function and then finding the Fourier transform.
- b) Direct spectra using Fast Fourier Transform Technique.
- c) Filtering the signal through a large number of band filters and dividing the output through each band by the Bandwidth.

Out of these the second method which finds the PSD using Fast Fourier Transform Technique is found to be the fastest. Hence the same will be used in this application. For smoothing out the raw power spectral density, Hann window function will be used as it is easier to implement on a micro computer. The Hann window function in the frequency domain is given by

$$U_T(f) = \frac{1}{2} \hat{U}_T(f) + \frac{1}{4} \hat{U}_T\left(f - \frac{1}{2T}\right) + \frac{1}{4} \hat{U}_T\left(f + \frac{1}{2T}\right) \quad (3.23)$$

where  $U_T(f)$  is the modified function

$\hat{U}_T(f)$  is the raw function

$2T$  is the record length (from  $-T$  to  $T$ )

The computation procedure for PSD is then will be as follows:

- a) Obtain a data sequence of  $N$  samples.
- b) Detrend the data using appropriate filter (removal of Mean)
- c) Compute the Discrete Fourier Transform of the sequence and find out the real and imaginary Fourier coefficients.

$$F(k) = \sum_{i=0}^{N-1} X_i e^{-j2\pi ki/N} = A(k) + j B(k)$$

- d) Compute the one sided raw power spectral density using the following equation

$$S_X(k) = \frac{2}{N} [A^2(k) + B^2(k)]$$

- e) Using appropriate spectral window on raw estimates, compute the smoothened Power Spectral Density.
- f) Calculate smoothened PSD for each realization of the ensemble and take an average to get the PSD of track irregularity.

### 3.4 FAST FOURIER TRANSFORM (FFT) Algorithm [1], [2]

The power spectral measurement involves the computation of Discrete Fourier Transform of the data sequence. The direct evaluation of the DFT involves  $N$

Acc. No. A 82784

complex multiplications and  $(N - 1)$  complex additions for each value of  $X(k)$  and since there are  $N$  such values to be determined,  $N^2$  multiplications and  $N(N - 1)$  additions are necessary. For larger  $N$ , direct evaluation of DFT involves considerable amount of computation. Fast Fourier Transform (FFT) algorithm evaluates the DFT of a sequence in an efficient way by reducing the total number of computations. The FFT algorithm does this by splitting the  $N$  point sequence into two  $N/2$  point sequences.

Let the  $N$  point sequence be  $x(n)$   $n = 0, 1, \dots, N-1$  where  $N$  is a power of two. Defining the two  $N/2$  point sequences  $x_1(n)$ ,  $x_2(n)$  as the even and odd members of  $x(n)$  respectively

$$\begin{aligned} x_1(n) &= x(2n) \quad n = 0, 1, \dots, \frac{N}{2} - 1 \\ x_2(n) &= x(2n + 1) \quad n = 0, 1, \dots, \frac{N}{2} - 1 \end{aligned} \quad (3.24)$$

Then the  $N$ -point DFT of  $\{x(n)\}$  can be expressed as [1],

$$X(k) = X_1(k) + W_N^k X_2(k) \quad (3.25)$$

where  $X_1(k)$  and  $X_2(k)$  are the  $N/2$  point DFT's of  $x_1(n)$  and  $x_2(n)$  respectively. Since  $X(k)$  is defined for  $0 \leq k \leq N - 1$  and  $X_1(k)$ ,  $X_2(k)$  are defined for  $0 \leq k \leq \frac{N}{2} - 1$ . To interpret for the values of  $k \geq \frac{N}{2}$ , the following equation can be used

$$X(k) = \begin{cases} X_1(k) + W_N^k X_2(k) & 0 \leq k \leq \frac{N}{2} - 1 \\ X_1(k - \frac{N}{2}) + W_N^k X_2(k - \frac{N}{2}) & \frac{N}{2} \leq k \leq N - 1 \end{cases} \quad (3.26)$$

This can be obtained using the periodicity property of DFT i.e.  $W_N^{k+N/2} = -W_N^k$ . In a similar manner the  $N/2$  point DFT can be expressed as a combination of  $N/4$  point DFT, i.e.,

$$\begin{aligned} X_1(k) &= A(k) + W_{N/2}^k B(k) \\ X_2(k) &= A(k) + W_N^{2k} B(k) \end{aligned} \quad (3.27)$$

where  $A(k)$  and  $B(k)$  are the  $N/4$  point DFT's of the even and odd members of  $x_1(n)$  respectively. The above process can be continued until a two point DFT arrives. A two point DFT,  $F(k)$ ,  $k = 0, 1$  may be evaluated using no multiplications as

$$\begin{aligned} F(0) &= f(0) + f(1) W_8^0 \\ F(1) &= f(0) + f(1) W_8^4 \end{aligned} \quad (3.28)$$

where  $f(n)$ ,  $n = 0, 1$  is the two point transform being transformed.

Since  $W_8^0 = 1$  and  $W_8^4 = -1$  there are no multiplications involved in computing the above equation. The total number of operations using this scheme is of the order of  $N \log_2 N$ . Thus it can be seen that when  $N$  is large, there is a great reduction in terms of computation.

The above described algorithm is also called as Decimation-in-Time (DIT) algorithm. Since at each stage of the process the input sequence is splitted into

smaller sequences for processing. Another popular form of the FFT algorithm is Decimation-in-Frequency (DIF) algorithm. For this version, the input sequence  $x(n)$  is partitioned into two sequences each of length  $N/2$ . The first sequence  $x_1(n)$  consists of the first two  $N/2$  points of  $x(n)$  where as the second sequence  $x_2(n)$  consists of the last  $N/2$  points of  $x(n)$ . The same mathematical analysis can also be done for DIT algorithm [1]. The diagram in Fig. 3.1 shows the DIT and DIF algorithms for  $N = 8$ .

From these illustrations, it can be observed that, for DIT scheme, for the output to be in natural order the input should be shuffled where as reverse is the case for DIF scheme. Hence whether it is a DIT or DIF shuffling of the data is necessary. Although shuffled, the order of the shuffled sequence can be determined in a simple manner. When  $N$  is a power of 2, the shuffled sequence will be the bit reversed number of the index when it is represented in Binary. For example the following Table shows the shuffled sequence for  $N = 8$ .

Table 3.1

Index	Binary Representation	Bit Reversed Binary	Bit Reversed Index
0	000	000	0
1	001	100	4
2	010	010	2
3	011	110	6
4	100	001	1
5	101	101	5
6	110	011	3
7	111	111	7



The same procedure can be adopted to any index when  $N$  is a power of 2. To calculate the FFT coefficients  $\{W_N^k\}$ , either the coefficients can be formed as a table and then be referenced at various stages during the computation or these coefficients can be computed using

$$W_N^k = \cos \left[ \left( \frac{2\pi}{N} \right) k \right] - j \sin \left[ \left( \frac{2\pi}{N} \right) k \right]$$

where in the first method the extra storage is needed while in the second case computation time is involved.

The FFT algorithms can be further categorized into

- a) Inplace Algorithm
- b) Natural Input-Output Algorithm

a) Inplace Algorithm: In place Algorithm is the one in which a given component of any intermediate vector may be stored in the same location occupied by the corresponding component of the preceding vector. This requires less storage but computational time is higher than the Natural Input Output algorithm. Other characteristic is that either the output spectrum appears in an unnatural order or that the input data should be arranged before entering the computational array, as mentioned earlier. This shuffling process is also called as scrambling operation.

- b) Natural Input-Output Algorithm: This is the one in which a given component of any intermediate vector may not be

stored in the same location occupied by the corresponding component of the preceding vector, thus requiring the extra memory for storing the Intermediate Results. An N-point FFT (N real and N imaginary) will require  $4N$  words of memory as compared to  $2N$  words required for Inplace algorithm. These algorithms maintain a natural input-output order and do not require scrambling operation and as such are faster when compared to the inplace algorithm.

Considering the present application, inplace algorithm is adopted to reduce the memory constraints of the system.

#### Basic Properties of Inplace Algorithm:

From the signal flowgraph the following points can be observed.

- a) There are  $r = \log_2 N$  number of computational arrays.
- b) In each array every node has two incoming paths and two outgoing paths.
- c) In each array, there are two input nodes whose input paths originate from the same pair of nodes in the previous array. Two such nodes are grouped as 'a dual node pair'. In any array there are  $N/2$  pairs of dual nodes.

d) Each array requires  $N/2$  complex multiplications and  $N$  complex additions. Therefore the total number of multiplications and additions required are  $(N/2) \log_2 N$  and  $N \log_2 N$  respectively.

e) Computation of dual node pair requires only one multiplication and two additions. If the weighting factor at one of the nodes in a dual pair is  $W^p$ , then the weighting factor at the other node of the pair is  $W^{p+N/2}$ . Then

$$\begin{aligned} X_1(k) &= X_{1-1}(k) + W^p X_{1-1}(k + N/2^1) \\ X_1(k + N/2^1) &= X_{1-1}(k) - W^p X_{1-1}(k + N/2^1) \quad (3.29) \\ \therefore W^{p+N/2} &= -W^p \end{aligned}$$

where  $X_1(k)$  indicates  $k$  component in the  $1^{\text{th}}$  array.

f) The spacing between dual node pair differs from array to array. In the  $1^{\text{th}}$  array ( $l = 1, 2, \dots, r$ ) the spacing is  $N/2^l$  means  $X(k)$  and  $X(k + N/2^l)$  constitute a dual node pair.

g) To evaluate the value of  $p$  which is the exponent of  $W$  for any index in a given array, represent  $k$ , the node index in the  $1^{\text{th}}$  array in binary form with  $r$  bits, retain the most significant  $l$  bits and add  $(r - l)$  leading zeros to form a  $r$  bit binary number. Reverse the bit order of the resulting number and the decimal equivalent of

the final binary number gives the index  $p$ . The weighting factor for the  $k^{\text{th}}$  node of the  $l^{\text{th}}$  array is  $W^p$ .

- h) The output after  $r$  arrays is in scrambled form. To unscramble the output  $X(k)$  represent the index  $k$  in binary form with  $r$  bits and reverse the bit order. The resulting decimal number is the index  $n$  of  $X(n)$ .

### 3.4 IMPLEMENTATION OF FFT ON 6800 MICROPROCESSOR

As it was found [3], considering the accuracy point of view, a 16 bit word length should be chosen to represent each data word. For a real time application, though less accurate, fixed point arithmetic will be faster than floating point arithmetic. Hence fixed point arithmetic is chosen for this application where the data is represented in Two's complement form, and the binary point is assumed to lie to the left of leftmost magnitude bit. As the execution of the program moves from stage to stage, the magnitudes of the numbers in the sequence generally increase hence there is a possibility of overflow during different stages of computation. To prevent this appropriate techniques of scaling should be adopted in fixed point arithmetic.

Scaling [3]: The power of 2 algorithm, as mentioned earlier, operates on two complex numbers. It takes

these two numbers and produces two new complex numbers which replace the original ones in the sequence.

Let  $X_m(i)$  and  $X_m(j)$  be the original complex number.

The new complex pair is given by

$$\begin{aligned} X_{m+1}(i) &= X_m(i) + W X_m(j) \\ X_{m+1}(j) &= X_m(i) - W X_m(j) \end{aligned} \quad (3.30)$$

The algorithm goes through the entire sequence of  $N$  numbers, taking two at a time. When  $N = 2^M$ , total number of computational stages is  $M$ . With the assumption of binary point lying towards extreme left, the relation between the numbers in  $m$  and  $m + 1$  stage is as shown in Fig. 3.2. The outside square gives the possible values of  $\text{Re}[X_m(i)] < 1$  and  $\text{Im}[X_m(i)] < 1$  and the circle inscribed in the square gives the region  $|X_m(i)| < 1$ . Similarly the inside circle gives the region  $|X_m(i)| < 1/2$ . If the numbers  $X_m(i)$ ,  $X_m(j)$  lie in the region  $|X_m(i)| < 1/2$ , then  $X_{m+1}(i)$ ,  $X_{m+1}(j)$  will be in the larger circle hence overflow condition doesn't arise. However, if  $X_m(i)$  and  $X_m(j)$  are inside the smaller square, it is possible that  $X_{m+1}(i)$ ,  $X_{m+1}(j)$  to be outside the larger square hence overflow arises. So the input sequence should be controlled such that  $|X_m(i)| < 1/2$  to prevent overflow. There are three techniques of scaling, which can be used for this, namely

- a) Shifting right one bit at every iteration

- b) Controlling the sequence so that  $|X_m(i)| < 1/2$
- c) Testing for an overflow.

Out of these, the first method is the simplest and easy to adopt for microprocessor applications and hence it will be used in this implementation.

A flow chart, and the corresponding loops in the FFT in place program is given in Fig. 3.3. As stated earlier in the FFT routine, the  $k$  component in the  $l$  array is given by

$$X_l(k) = X_{l-1}(k) + W^p X_{l-1}(k + N/2^l) \quad (3.31)$$

$$X_l(k + N/2^l) = X_{l-1}(k) - W^p X_{l-1}(k + N/2^l)$$

where  $W^p$  is the multiplier and is a complex number, given by

$$W^p = e^{\frac{-j 2\pi}{N} p} = \cos\left(\frac{2\pi}{N} p\right) - j \sin\left(\frac{2\pi}{N} p\right)$$

As it can be seen, for generating the weights of  $W$ , sine and cosine values are required, and since calculation of sine and cosine functions is time consuming, these values can be generated and stored in the system memory before entering into the FFT program, for reducing the execution time. For this  $N/2$  values of SINE and  $N/2$  values of COSINE are required from 0 to  $\frac{2\pi}{N} \times (\frac{N}{2} - 1)$  in a stepsize of  $\frac{2\pi}{N}$ , which corresponds to  $N/2$  weights of  $W$  from  $W^0, W^1, \dots$  to  $W^{N/2-1}$ . This requires extra  $N$  words for storing the values of SINE and COSINE.

However, values of sine and cosine can be derived by storing only  $N/4+1$  values of sine from 0 to  $\pi/2$  in a stepsize of  $2\pi/N$  i.e. from  $W^0, W^1, \dots$  to  $W^{N/4}$ , as described below. For  $N = 1024$ , this needs the values of sine to be stored from 0 to  $\pi/2$  in a stepsize of  $2\pi/1024$  which corresponds to  $W^0, W^1, \dots$ , to  $W^{256}$ .

#### Calculation of Sine Values ( $N = 1024$ )

- a) First whether the index  $\leq 256$  or  $> 256$  is to be checked.
- b) If index is  $\leq 256$ , then use the index as it is to fetch the appropriate sine value from the array.
- c) If index is  $> 256$ , the index is subtracted from 514 (in general from  $2(N/4+1)$ ) and this value is used as index to fetch the appropriate sine value.

#### Calculation of Cosine Value ( $N = 1024$ )

- a) The program should check whether index  $\leq 256$  or  $> 256$  (in general index  $\frac{N}{4}$  or  $\frac{N}{4}$  ).
- b) If index is  $\leq 256$ , subtract the index from 256 (generally from  $N/4$ ) and this value will be used as index to fetch the value from Sine array.
- c) If the index is  $> 256$ , subtract 256 (generally  $N/4$ ) from the index and this value will be used as the index to fetch the value from Sine array which gives appropriate Cosine values.

By this method, the memory required will be  $N/4+1$  words for storing Sine values to generate the weights which will cut down the memory from  $N$  words to  $N/4+1$  words.

#### Organization of the FFT Program

The FFT subroutine assembly language program mainly calls the following subroutines:

a) COMPLEMENT ROUTINE (COMPL)

This routine finds the Two's complement of 16 bit number when called.

b) OVERFLOW ROUTINE (OFL)

This routine shifts the 16 bit number to right by one bit, equivalently it divides the number by 2.

c) POWER OF TWO ROUTINE (LOG<sub>2</sub>N)

This finds the  $\log_2 N$  where  $N$  is the number of samples and is a power of Two.

d) DOUBLE PRECISION MULTIPLY ROUTINE (DPMUL)

This multiplies the two 16 bit numbers and produces a 16 bit product using Booth's algorithm. Negative numbers are represented in Two's complement form.

e) BIT REVERSAL ROUTINE (BITR)

This finds the Bit reversed number of a 16 bit number.

f) UNSCRAMBLING ROUTINE (UNSCM)

For inplace algorithm, since the output is in scrambled form, this routine orders the output sequence.



A complete assembly listing of FFT for 6800 micro-processor applications which can be used upto  $N = 1024$  is given at appendix. The listing to find the power spectral density which calls the FFT routine is also included in the Appendix. The memory requirements and the results are presented, details are discussed in Chapter 5.

## COMPUTATIONAL ARRAYS

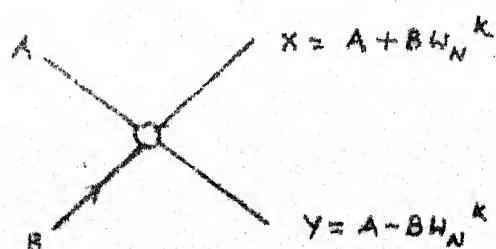
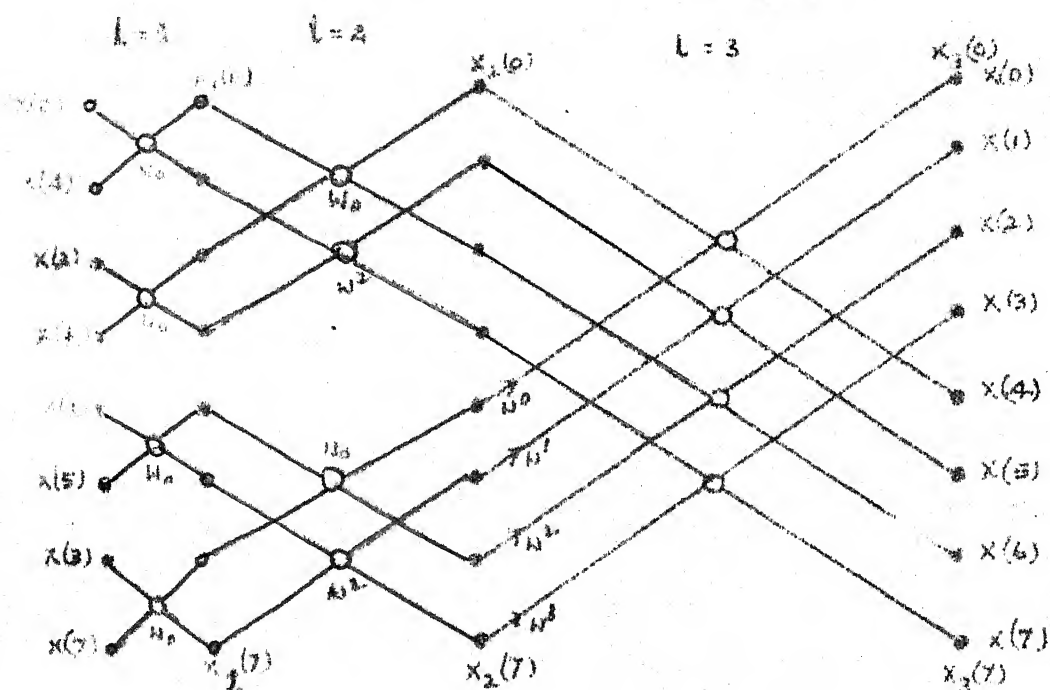


FIG. 3.1 (a) BUTTERFLY FOR DIT:  
COMPLETE 8 POINT DECIMATION-IN-TIME FFT

## COMPUTATIONAL ARRAYS

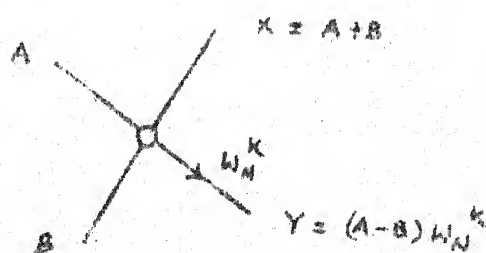
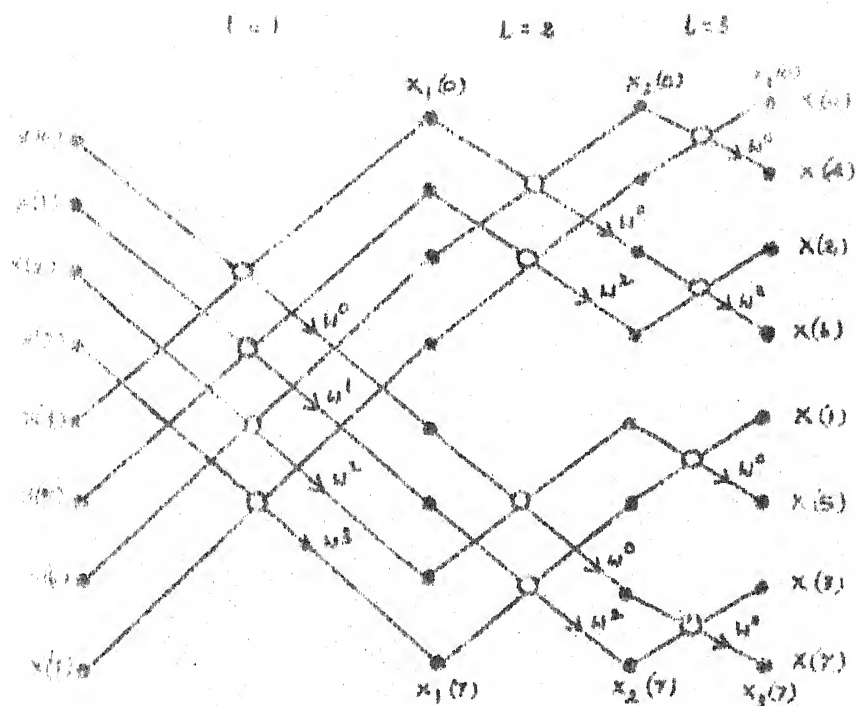


FIG. 3.1 (b) BUTTERFLY FOR DIF  
COMPLETE 8 POINT DECIMATION-IN-FREQUENCY FFT.

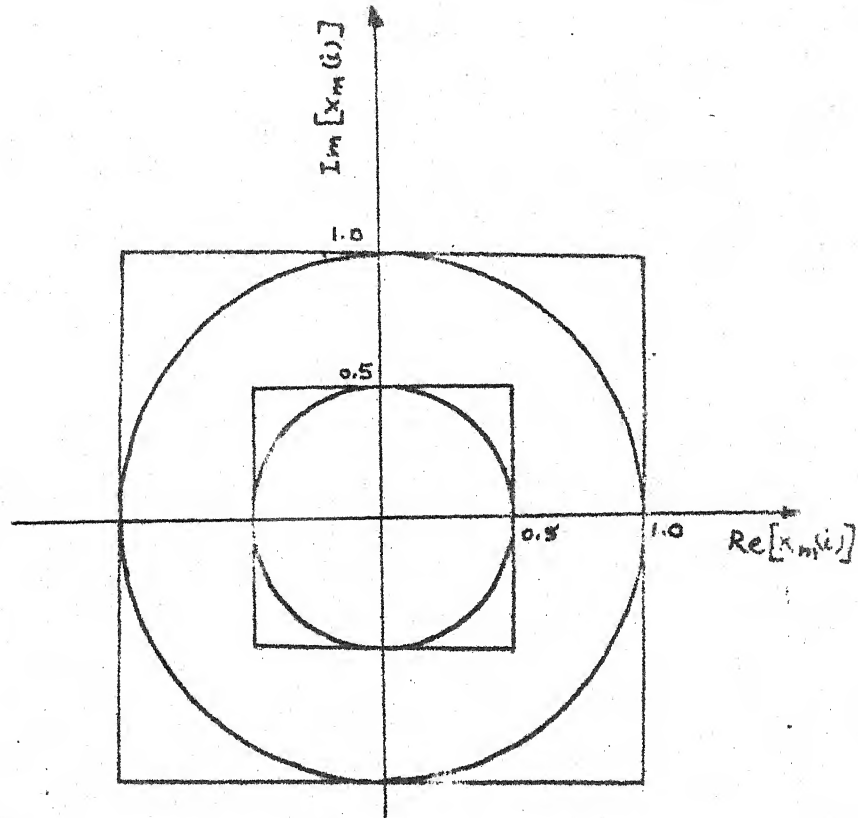


FIG. 3.2. RELATIONSHIP BETWEEN THE NUMBERS IN  $M$  AND  $M+1$  STAGE.

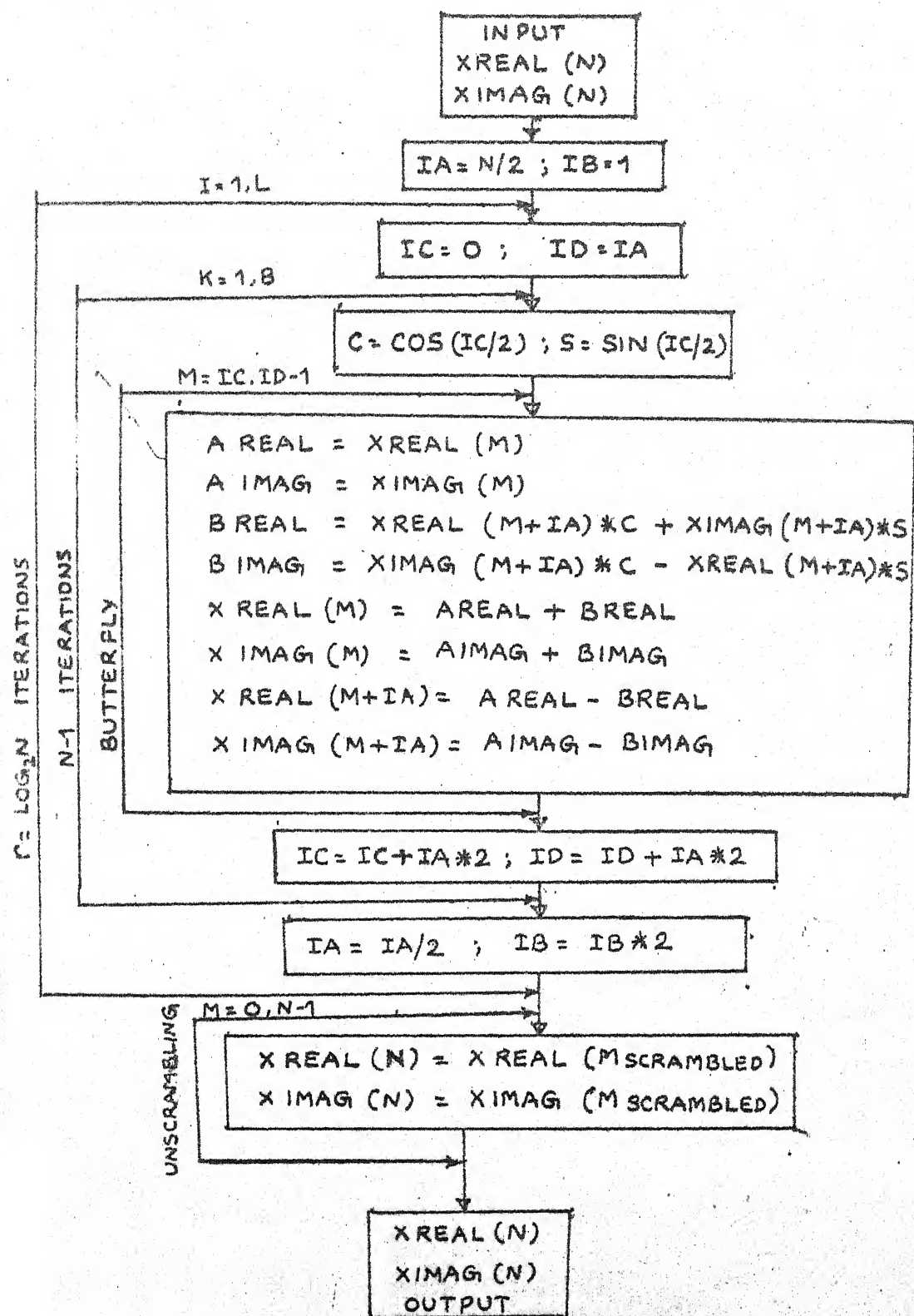


FIG. 3.3 FFT INPLACE ALGORITHM FLOWCHART.

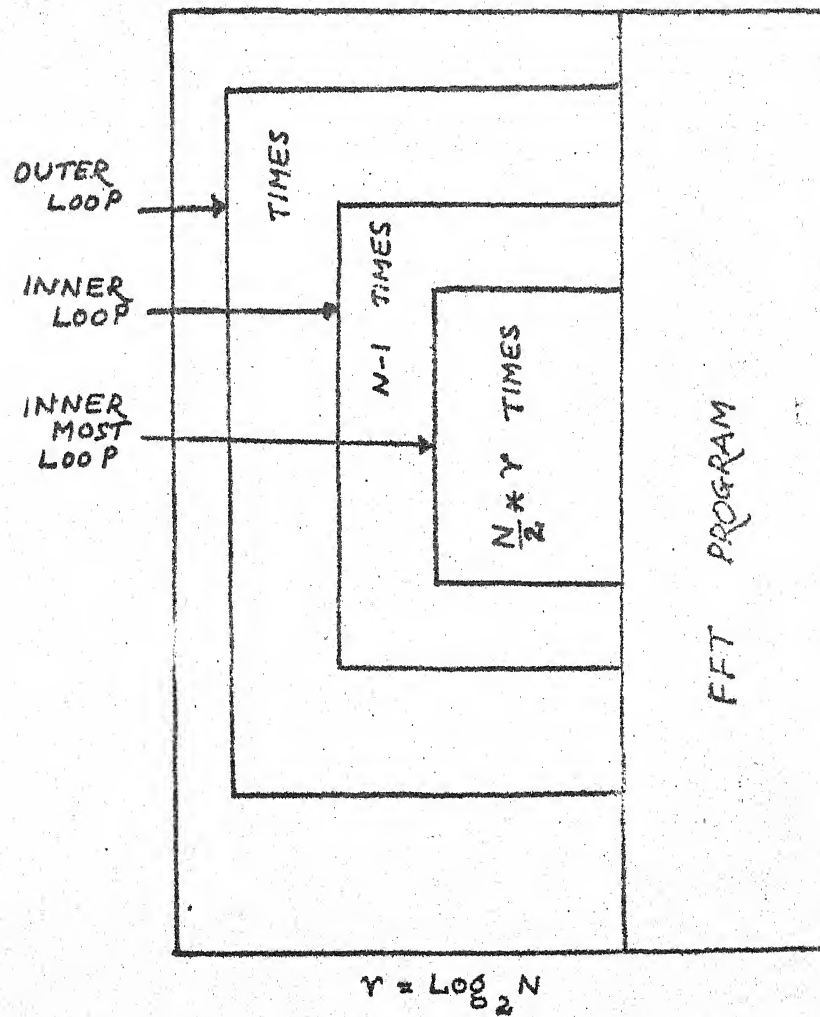


FIG. 3.4 FFT PROGRAM AND ITS LOOPS.

## CHAPTER 4

### MICROCOMPUTER BASED SYSTEM

#### 4.1 INTRODUCTION

The technological revolution, spearheaded by the MICROPROCESSOR, a single chip central processing unit has rendered cost effective real time signal processing practical. A typical real time signal processing scheme like the track profiles measurement using large main frame computers or minicomputers would have been an expensive proposition and therefore impractical for routine track evaluation. With today's microprocessors, a low cost, completely independent on line dedicated signal processing system can be built for such applications.

The 6800 microprocessor and its family support is chosen for the instrumentation proposed for the real time evaluation of railway track profiles. In this Chapter, the track profile measurement system's specifications, system architecture, and hardware details of the system which also include, system packaging have been described in detail.

#### 4.2 SYSTEM SPECIFICATIONS

To make the system upward compatible and to have a proper system-to-user interface and also for having electrical compatability with the existing rail cars, the following specifications for the rail track monitoring system have been laid down.

#### 4.2.1 Environmental Specifications

- a. The system should be able to operate on + 24V DC battery system normally available on railway carriages.
- b. It should be portable and should not require any air-conditioning.
- c. It should be able to survive in the vibration environment normally obtainable on a coach floor.

#### 4.2.2 Signal Processing Requirements and Real Time Nature of the Signal Processor

- a) Track Parameters to be extracted: For every kilometer span of track length, absolute vertical profiles of left and right rails, absolute lateral profiles of left and right rails, dynamic cross level, centre line unevenness, dynamic gauge, centre line alignment and power spectral measurement of each of the track profile is to be evaluated by the system in real time (i.e. max. 30 seconds : the time taken for the rail car to traverse 1 Km at the envisaged maximum speed of 120 Km per hour).
- b) Analog Signal Channels: The system is to process the outputs of four accelerometers mounted on the axle boxes for both horizontal and lateral profiles of the left and right rails. Hence the system should be able to sample, digitize and store them simultaneously from these four transducers for subsequent signal processing.



- c) Conditioning of the Input Signals: The outputs of the accelerometer should be suitably conditioned to the compatible levels of the system input digitizer.
- d) Number of Points Per Channel: The number of sample points for each channel is fixed to be 512 for every kilometre section of the track which corresponds to an approximate spatial sampling of 2 metres. These sampling instant pulses are generated by the wheel and its associated electronics.
- e) Processing Time: Considering the maximum speed of rail car to be 120 Kilometres per hour, there is 30 seconds of time available for each Kilometre traverse. Hence for each Kilometre of track span, all the four channel signal processing and track categorization should be carried out within 30 seconds.
- f) Machine to Operator Interface: The system should be capable of accepting the initial kilometre entry at the time of starting of the run and automatic updating of the kilometre should be done on command at the start of each kilometre of track. Automatic recording or printing of the results at the end of the run, as may be required, is also necessary.
- g) Track to System Interface: Suitable accelerometers will be mounted on axle boxes to get the acceleration signals from the track and these signals will be properly

conditioned before feeding to the signal processor.

#### 4.3 SYSTEM DESCRIPTION

The system architecture is shown in Fig. 4.1. It comprises of a general microcomputer system and a monitor on a bus and application dependent modules. It consists of the following modules:

- a) 6800 processor based CPU module with monitor ROM, stack memory, serial I/O (ACIA), parallel I/O (PIA).
- b) 16 K ROM module for program storage.
- c) 16 K Dynamic RAM module.
- d) Ram Refresher Module which generates all the timing pulses for Dynamic RAM module and address decoding circuitry.
- e) 8K Static RAM module (optional)
- f) Digital Hardware multiplier module.
- g) Console Module which consists of a fifteen digit eight segment display and a Hex Keyboard.
- h) Cassette and RS 232 C interface module.
- i) 20mA Loop TTY interface and Baud rate clock module.
- j) Floppy disc drive controller module (optional).
- k) DMA controller module (optional).
- l) Analog output device controller module (optional).
- m) A/D converter module.
- n) Analog multiplexer module.

In the above, the modules (a) to (k) are for configuring a general microcomputer system where as the modules (l) to (n) are for the envisaged specific application.

#### 4.3.1 Microcomputer System Hardware

In this section, the modules which comprise the microcomputer system that will be used in the proposed system have been described. To make the system modular, double sided printed circuited boards of size  $6\frac{1}{2}" \times 4\frac{1}{2}"$  have been used for all the modules with a 44 pin edge connector contacts that go on to the system bus. The edge connector tongue designation with associated bus signals are given in Table 4.1 and the same will be followed to all the hardware modules except where mentioned.

##### 4.3.1.1 CPU Module

The complete circuit diagram of the CPU module is shown in Fig. 4.3. This mainly consists of a CPU clock and decode circuitry, on board baud rate clock, processor, memory and I/O provisions.

- a) CPU Clock and Decode Circuitry: Since the system uses M6800 microprocessor which uses a two phase clock ( $\phi_1, \phi_2$ ), it is required to generate a two phase non overlapping clock that should run at  $V_{cc}$  level, according to the requirement of 6800 processor. The M6800 uses a 1MHz clock. To derive this a 4 MHz clock has

been used comprising of a 4 MHz crystal and a part of U1 (7400 IC), the output of which will be further divided by a factor of four using U2 (7473). The output of U2 will be a 1 MHz clock which will be buffered using U3 (7404), part of U1, U5 (7437) and two transistors  $Q_1$ ,  $Q_2$  (2N2222) to derive a nonoverlapping two phase clock. The decoding circuitry consists of U4 (7410) which generates the various timing signals, using Valid Memory Address (VMA) of the CPU, like  $VMA.\phi_2$ ,  $\overline{VMA.\phi_2}$ ,  $\overline{RCS}$ . The  $\overline{RCS}$  is the chip select for the Read Only Memory (ROM) on CPU module where the 'Monitor' of the system actually resides.  $\overline{RCS}$  is 'ANDED' configuration of  $\phi_2$  clock, ROMEN1, ROMEN2 where ROMEN1 is ROM ENABLE1 and ROMEN2 is ROM ENABLE2. These signals are derived from Ram Refresher Module. ROMEN1 is a buffered version of  $R/\overline{W}$  (Read/write) and ROMEN2 will be in active state when the MSB address lines have got an Hex address of 'F'.

- b) On Board Baud Rate Clock: This clock will be used in conjunction with Asynchronous Communication Interface Adapter (ACIA 6850) for serial I/O application. This is a simple astable multivibrator using U15 (555), a timer IC with a precise baud rate (300 baud) adjustment using a trimpot. If higher baud rates are required this on board baud rate clock should be disabled, and external clock should be connected to the system.

- c) Processor, Memory and I/O: This section is the heart of the system consisting of 6800 microprocessor, 1 K R/W memory (a part will be used as stack memory), two Peripheral Interface Adapters (PIA 6820) for parallel I/o communication, an ACIA (6850) for serial I/o applications and a 1 K ROM space where the 'Monitor' ROM resides. The processor address, data and control lines are brought on to the edge connector contacts which go into the system bus. The PIA outputs are available on a 50 pin Eurocard type connector. The ACIA connections are brought on to a 14 pin DIP socket. For serial and Parallel I/O communications proper jumper assemblies should be used for the Eurocard type connector and DIP socket. In the system configuration that is used for this application, the DIP jumper assembly goes to the RS 232 and cassette interface module which in turn can be used for the Asynchronous communications like cassette, RS 232 C, Teletype etc. The memory mapping of the various I/O extensions and the memory on CPU module is shown in Table 4.2. The system reset is hard wired through a pushbutton switch to the reset pin (pin 40) of the processor (or tongue Z of the edge connector). The serial connector (14 pin DIP socket) signal summary is given at Table 4.3. After the power-on condition and the system reset, the monitor that resides in the ROM takes the control of the system. For its use, the monitor mainly uses the stack area on board.

#### 4.3.1.2 16 K ROM Module

This module provides 16 K byte memory accessory for the control module. This module uses 2708 erasable/programmable type ROM ICs. The ROM card may be configured into any quadrant of the processor's address space using jumper selection of the higher order bits. The ROM array is fully buffered from the microprocessor bus using low power buffer gates to assure minimum loading. The complete circuit diagram is given at Fig. 4.4. U1 and U2 are low power gates which isolate the capacitive loads of the ROM array from the system bus.  $A_0$  to  $A_9$  (the LSB address) are supplied directly to the 2708 address leads.  $A_{10}$ ,  $A_{11}$ ,  $A_{12}$  and  $A_{13}$  are buffered by U3 and U4 and used as inputs to a 74154 (one-of-16 decoder). This decoder generates the chip select signals to select one of the 2708's from the array. Address  $A_{14}$  and  $A_{15}$  are decoded to enable the data bus drivers U6 and U7. The state of  $A_{14}$  and  $A_{15}$  which enables the board is jumper selectable. The placement of these jumpers will determine where the ROM board appears in the processors memory map. Four jumpers are used to make the memory space selection. Only two of these jumpers are ever in place at any one time. Jumper insertion and the resulting memory map is shown below:

Memory locations occupied	Jumpers in place
C000 - FFFF <sub>16</sub>	J1, J4
8000 - BFFF <sub>16</sub>	J2, J3
4000 - 7FFF <sub>16</sub>	J2, J4
0000 - 3FFF <sub>16</sub>	J2, J3

#### 4.3.1.3 16K Dynamic RAM Module

This RAM module is a high density memory accessory for the CPU module. The complete circuit diagram is shown in Fig. 4.5. This RAM module uses 4096 dynamic RAM IC. This module accepts the multiplexed addresses and timing signals from the RAM REFRESHER Module through the refresh bus and communicates data thru system bus. Each 4096 byte bank of RAM has an associated TTL gate to supply the ROW Address Strobe (RAS) and Chip Select (CS) signals to the eight IC's comprising that bank. The RAS decoding is used to minimise the quiescent power dissipation. This is achieved by giving the RAS signal only to the particular RAM bank selected. During the refresh cycle the REF signal from the refresher module forces RAS to be applied to all the memory ICs. During the refresh cycle, processor does not receive  $\phi_2$ , hence does not generate  $VMA.\phi_2$ . This signal is gated through CS to the RAMs so that all RAMs are deselected during a refresh cycle. When RAM refresher module is used, the onboard clock should be disabled by removing U2 on CPU module since the clock is



now supplied by refresher module. Half of U<sub>4</sub> is used to detect a reference to the memory board. Pin 6 of this IC goes high when any of the four banks is to be read from or written into. The other half of U<sub>4</sub> and part of U<sub>7</sub> generate enable signals for a pair of Tri-state transceivers U<sub>5</sub> and U<sub>6</sub>, which have high input impedance to minimize the loading on memories and processor data bus. Only one half of these transceivers is enabled at any one time. The half that is to be enabled is determined by the state of the R/W line from the refresher module. This R/W signal is also combined with the WRITE pulse from the refresher module to apply the write signal to the RAM array at the proper time in the memory timing cycle. Most of the U<sub>3</sub> is used as a buffer to drive the capacitive load of the Column Address Stroke (CAS) pins on the RAM array where as U<sub>2</sub> is used as buffer for the multiplexed addresses for the RAM array. Typical wave forms of the timing signals are shown in Fig. 4.6. These signals are buffered by TTL gates to minimize loading on the signals. The configuration of the RAM module in the processor's memory space is jumper selectable. Each 4096 bite bank may be configured independently at sixteen locations. The jumper termination with its associated address is given in Fig. 4.7. All the supply voltages are derived from the Ram refresher module.



#### 4.3.1.4 Ram Refresher Module

This module is the link between the Dynamic RAM module and the CPU module. This provides the required timing and refreshing signals for dynamic RAM module and also buffers the address signals from CPU module. The complete circuit diagram is shown in Fig. 4.8.

IC1 comprises an 8 MHz crystal oscillator for the processor master clock which will be obtained by dividing the 8 MHz clock (pin 8 of IC1). When this module is to be used with CPU module the clock on CPU module should be disabled by removing the JK flip flop (IC2) on that module.

IC5 and IC6 (7495) form a divide-by-eight counter and memory clock generator. The signals shown in Fig. 4.9 with their waveforms are generated by this shift Register chain. The Row Address Strobe (  $\overline{RAS}$  ), Column Address Strobe (  $\overline{CAS}$  ) and  $\overline{WRITE}$  are the required timing signals for the dynamic RAM module (refer description of Dynamic RAM module); the processor clock  $\overline{\phi}_2$  is supplied to the system bus through a Nand Gate (IC7) and is also used to operate the memory address multiplexer consisting of IC10 and IC13. These ICs are tri-state low power schottky devices used for minimizing the bus loading. IC2, IC3 and half of IC4 form a 32  $\mu$ s timer which determines the refresh interval. When a refresh cycle is required, pin 12 of IC4 goes high; 125 ns into the next memory cycle pin 9 of IC4 goes high indicating that

the memory cycle is to be a refresh cycle. Refresh addresses from IC8, IC9 are supplied to the memory board through IC11 and IC12. The clock  $\overline{\phi}_2$  is suppressed during the refresh cycle. The REF signal is given to the memory card to signal it that a refresh cycle is in progress. The higher order bits of the address ( $A_{12}$ ,  $A_{13}$ ,  $A_{14}$ ,  $A_{15}$ ) are buffered by IC17 and are presented to a four-to-sixteen line decoder (IC14 74154). The output of this decoder is supplied to the RAM card where these will be used to select 4 K byte RAM banks. IC14 asserts RAMSEL when it decodes 'E' on the 4 highest address bits. The CPU module and interface modules use RAMSEL along with decoded address bits to generate chip select signals to activate the various PIAs, ACIAs etc. U15 asserts ROMEN2 when it decodes 'F' on the four highest address bits. ROMEN1 is the buffered version of R/W. Both ROMEN1 and ROMEN2 are used to enable the ROM on CPU module.

#### 4.3.1.5 8 K Static Ram Module

Although packing density is low, the advantage with static RAMs is that refreshing is not necessary for these memories. A 8 K static RAM module using Intel 2114 (1 K x 4 bit) static RAM is also designed and the complete circuit diagram is shown in Fig. 4.10. In this all the address lines are buffered using low power schottky devices (to minimize bus loading) IC3, IC4, IC5 (74LS365). R/W,  $\overline{VMA} \cdot \overline{\phi}_2$  are also buffered using these ICs. Data lines go to two

data bus transceivers (8833) that communicate with memory ICs. In this, there are two 4 K memory banks and the memory space allocation for these banks is jumper selectable. This is done using two 3-to-8 line decoders (74155) and two OR gates, and the outputs of these OR gates will form as chip select signal for a 1 K x 8 bit section in which two 2114s will be paralleled. The enabling of the data bus transceiver is done using the two bank select signals and R/W signal; R/W selects the mode of data bus transceiver i.e. transmit or receive. This module is also bus compatible following same tongue designation for the edge connector contacts.

#### 4.3.1.6 Console Module

The console I/O module provides an economic means of directly inputting / outputting information between operator and system bus. The complete circuit diagram is given at Fig. 4.11. The module has got two main parts, display and keyboard. It has got a real time clock which interrupts the processor at regular intervals. The display consists of fifteen digits of eight segment LED readouts and the display codes are under full software control for maximum versatility.

The refreshing feature of the display eliminates the need for latches and accomplishes this by turning on one digit at a time. The segments that are to be turned on will be determined by U1's "B side" bits. These are buffered by U5 and U6 which then drive the segments through current

limiting resistors  $R_1$  through  $R_8$ . Each common cathode of the readouts is driven by U3 and U4 . one-of-16 coder driven by the display refresher counter U7 (7493). U7 is cleared by  $CA_2$  of U1. No digit is on while U7 is clear. Then each successive digit is turned on, from left to right, by strobing U7's clock input by  $CB_2$  of U1. Control register B of U1 is therefore configured so that when a new set of data is written into the PIA,  $CB_2$  goes low in order to switch on the next column. The display can be turned off completely by control of  $CA_2$  of U2. A 'zero' turns on the segment.

The PIA (U1) A-side with its internal pull up resistors is connected directly to the key switch. The common row terminals of each switch are connected to  $PA_4$ - $PA_7$  of U1. The common-column terminals are connected to  $PA_0$ - $PA_3$  of U1. If the A side is configured as an input, the key switch may be inputted by reading the eight bit A-side data. U8 (CD4060) is a real time clock (CMOS oscillator / ripple counter) which gives interrupts to the CPU at a rate of 75, 150, 300 or 1200 interrupts/second depending upon jumper J3 connection. Normally IRQ interrupts are generated by the console module. However a simple jumper modification allows NMI type interrupt. The display refresh routine will be as follows. The routine receives interrupts from the module configured for an interrupt interval consists of two sections: Initialization code performed once at reset time

and interrupt driven code which at interrupt time gets the display code for the next digit and outputs it to the display drivers. The memory space occupied by the module is selected via jumpers J1 and J2.

#### 4.3.1.7 Cassette and RS 232 C Interface Module

This module provides the asynchronous communications to the CPU module through the use of a cassette deck or RS 232 console. The complete circuit diagram of this module is shown in Fig. 4.12. This module is 'not bus compatible' hence should be mounted separately, and uses the ACIA jumper assembly from CPU module.

**WRITE Operation:** During cassette write operations, the  $\overline{\text{RTS}}$  lead from ACIA is made low. This makes the IC14 as a divide-by-four or a divide-by-eight counter. The divide constants depends upon the state of the TXD lead from ACIA. The 4800 Hz clock (300 baud clock) from cassette clock and TTY interface board is divided to 2400 Hz for a 'one' from the ACIA or 1200 Hz for a 'zero'. For high speed operation the 2400 Hz output of IC5 is supplied to the ACIA operating in a divided by 'one' mode. Low speed operation is achieved by selecting the 4800 Hz clock while operating the ACIA in the divided by sixteen mode. The timing chart for write operation is shown in Fig. 4.13.

As it can be seen from the timing chart for the high speed operation, 'ONE' is recorded as a single cycle

of 2400 Hz while 'zero' is recorded as one half cycle of 1200 Hz. In the low speed operation 'one' is recorded as eight cycles of 2400 Hz while zero is recorded as four cycles of 1200 Hz. Cassette write operations inhibit the output to the RXD lead by allowing IC5 to be clocked set thus forcing RXD to the ACIA to be held marking. Output to the RS232 console is also inhibited by IC8.

READ Operation: IC2 and most of IC1 and IC3 comprise a limiter/edge detector which squares the tape audio data and generates short positive pulses at the output of IC3 (pin 11) which is also the reset signal to the baud rate clock. Hence these pulses are used to synchronize baud rate clock to the incoming data. The clock signal (300 baud) from baud rate clock is supplied to a missing pulse detector comprised of IC4. Missing pulses indicating 'zero' data force the output of IC9 (pin 11) high which causes the RXD lead low for each zero bit detected. Read clock is recovered from the data by IC5. Phasing ambiguity is removed when reception of the first zero occurs. The missing clock pulse allows a low to be loaded into IC4 (pin 9). IC5 pin 5 is constrained to become high in the next transition of the recovered clock so that the succeeding bits will be centre sampled by ACIA. Input from the RS232 console is locked out by the data multiplexer comprised of IC6 and IC9. Output to the console is inhibited by IC8. Read timing signals are shown in Fig. 4.14.

This cassette and RS232 interface module is also provided with a logic to changeover the connections between RS232 and TTY. Since TTY uses the same ACIA jumper assembly this logic is necessary which comprises of IC9, IC10, IC11, IC12, IC13 as shown in the diagram. The RS232 interface comprised of IC8, IC15 (MC1488 line driver) and a transistor  $Q_1$  (2N 2222) and  $D_3$ .

#### 4.3.1.8 Baud Rate Clock and TTY Interface (20mA Loop)

This module provides the necessary baud rate clock for asynchronous communications and also has got a TTY interface (20mA loop) circuitry. The circuit diagram is shown in Fig. 4.15 and this module also not bus compatible. Hence should be mounted separately.

**Baud Rate Clock:** This comprises of a crystal controlled 307.2 KHz clock derived by two inverters (IC5) and three delay type flip flops (IC1, IC2) which will be used by cassette interface module. This master clock is further divided by IC3, IC4 which form a counter and give standard terminal baud rates viz. 150, 300, 600, 1200, 2400, 4800 and 9600. These baud rates from 150 to 9600 baud are switch selectable using a DIP type switch. These switch selected rates are supplied to the ACIA via a clock multiplexer circuit comprised of IC6 and IC9 on cassette interface module.

TTY Interface (20 mA loop) : The necessary TXD, RXD signals for serial transmission of this TTY interface are derived from a simple switch over logic between RS232-TTY on cassette interface module. The baud rate will be fixed at 300 baud by connecting the on board baud rate clock on CPU module to the TXC, RXC clocks. This is also done by the switch over logic. The TXD signal is buffered by a NAND gate (IC6) and is coupled to a opto isolator (IC7) which in turn supplies the necessary current for the TTY loop. Similarly TTY output signals are coupled through a opto isolator (IC8) and a NAND gate (IC6) to the RXD terminal of ACIA. The TTY logic levels are converted to a current loop by the opto isolators.

#### 4.3.2 Microcomputer System Configuration and Software

The above described modules configure a complete microcomputer system with the input/output provisions for a cassette deck, RS 232 console or a Teletype and a console module with a Hex key board and fifteen eight segment LED display. The basic system memory map will be as follows:

##### a) CPU Module

Hex address	Component
0000 - 03FF	RAM
ED80 - EDF5	RAM (stack memory)
EE08	U9 ACIA control/status register
EE09	U9 Data Register



EE10	U8 (PIA-1) output register A
EE11	U8 output register B
EE12	U8 control register A
EE13	U8 control register B
EE20	U7 (PIA-2) output register A
EE21	U7 output register B
EE22	U7 control register A
EE23	U7 control register B
FC00 - FFFF	Read only memory

- b) Console module base address at EE80<sub>16</sub>
- c) 16K Dynamic Ram memory allocation from **5000 - 9FFF<sub>16</sub>**
- d) 8K Static Ram memory allocation from **2000 - 3FFF<sub>16</sub>**
- e) 16K ROM module memory allocation from -
- f) A/D converter PIA address **EE50<sub>16</sub>**

#### Software

The system software supports a ROM based 1K-byte loader/monitor/debugger programme for 6800. The monitor resides in 2708 ROM and is on CPU module. The monitor supports the following commands when entered from a teletype or video terminal.

Features of the monitor: The following are the monitor commands.

- M - Display/change memory
- I - Display/change instruction
- R - Display processor registers

CNTL-A - Display/change accumulator A  
CNTL-B - Display/change accumulator B  
CNTL-C - Display/change condition code register  
CNTL-P - Display/change program counter  
CNTL-X - Display/change index register  
G - Go to user program  
S - Single step user program  
D - Dump memory  
P - Punch loader compatible tape  
L - Load memory

The monitor also supports

- . free-format hexadecimal input
- . insertion and deletion of break-points
- . interrupt vectors

Free-format means the leading zeros can be omitted when entering hexadecimal address, data, OP codes, or the first or second byte of an operand. After the power-on condition and pushing the reset switch reverts system control to monitor. Then the monitor responds with a carriage return (CR), line feed (LF) and an asterisk (\*). The '\*' indicates that monitor is in the command mode and ready to accept any of the monitor commands. RESET should be used whenever power is first applied or system control to be returned to monitor.

## Interrupt Vectors

- a) Software Interrupt: If the processor encounters an SWI instruction, monitor responds by pushing the MPU registers onto the users stack and then vectors to memory address EDFA<sub>16</sub>. Memory addresses EDFA, EDFB and EDFC are reserved for the users SWI handler or a jump instruction to the SWI handler at another memory location.
- b) Interrupt Request: If the IRQ line is pulled low and the interrupt mask bit is not set, monitor responds by pushing the MPU registers onto the user stack and then vectors to memory address EDF7<sub>16</sub>. Memory locations EDF7, EDF8, and EDF9 are reserved for the user IRQ handler, or a jump instruction to the IRQ handler at another memory location.

### 4.3.3 The Specific Application Dependent Hardware

For the track profile measurement, since the signals are in analog form A/D converter is necessary for digitizing the input signals. Hence the following modules are used:

- a) A/D convertor module
- b) Analog multiplexer module

#### 4.3.3.1 A/D Converter Module

The complete circuit diagram of this module is shown in Fig. 4.16 which is configured using 8700 series A/D converter. In this, the eight bits of converted analog

data are presented to PIA peripheral bits PA7 to PA0. The most significant bit is PA7 and least significant bit is PA0. The A-side control lines give some freedom of control over the ADC. The ADC may 'free run' or convert only when required under program control. An interrupt can be specified at the end of the conversion cycle or programmed I/O techniques can be used. To sample a specific channel the following routine is adopted. The routine is in two parts: initialization routine called only once at the start of the program and a sampling routine called when a sample is to be taken.

The memory space occupied by the module is selected via jumpers J1 and J2. System gain may be adjusted using Pot P11 on A/D converter module. The adjustment of this Pot allows the ADC to accept and convert voltages from a 1 volt to 20 volt interval. Offset Pot P10 allows the ADC to accept either unipolar or bipolar signals. If bipolar signals are chosen the inherent coding is offset binary. If two's complement coding is needed, the conversion is done in the software.

#### 4.4 SYSTEM OPERATION

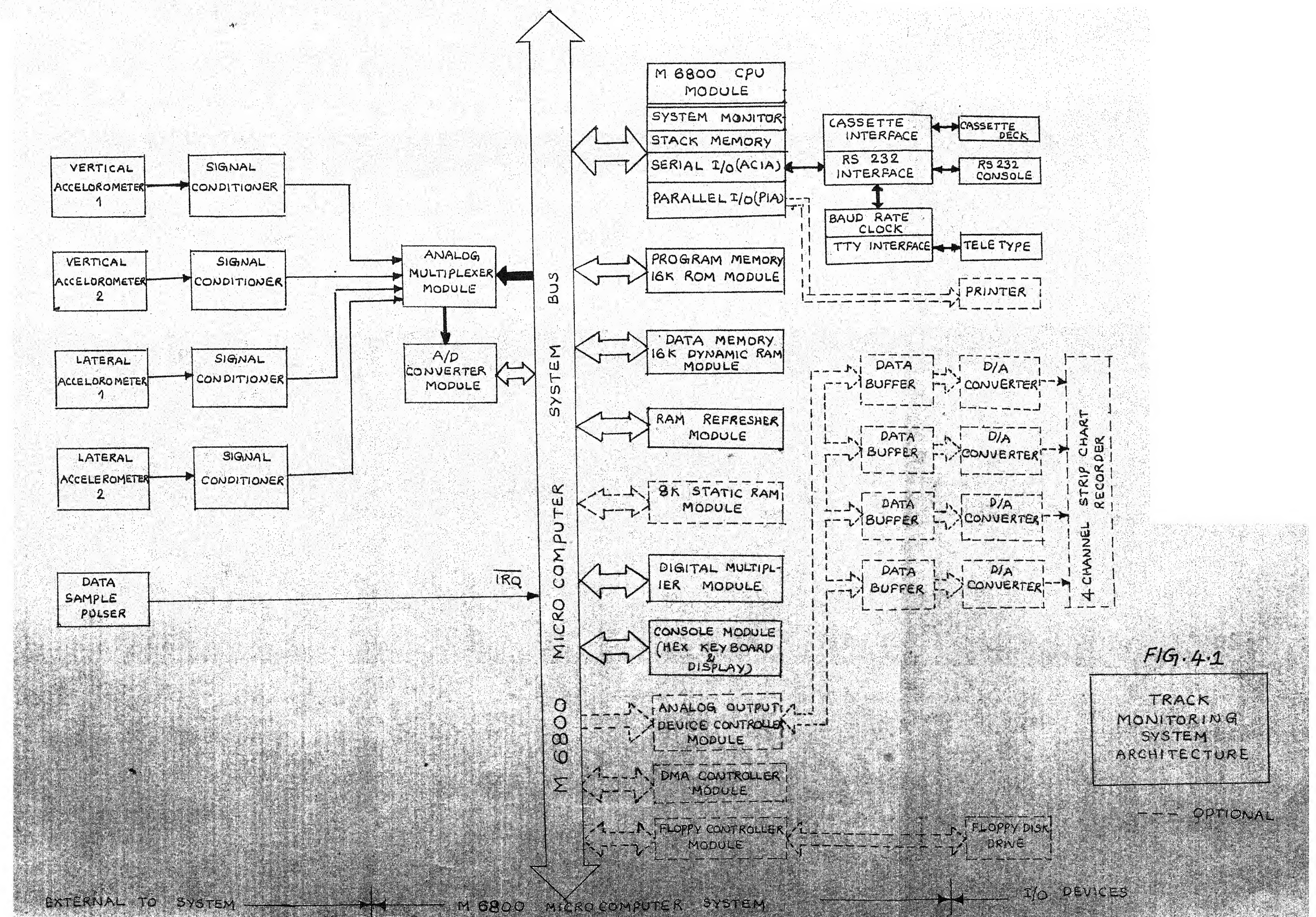
The signal processor for its operation, mainly uses the feature of interrupt vectors of the monitor. The console module works as a control panel with some keys marked as "RAT (Rail Track) monitor", "KM Scan", and "STOP". After the power on condition and system reset, the monitor takes over the control and waits for an input action. The console module, as described in the description of system hardware, gives regular interrupts. After the first interrupt is encountered, the monitor vectors to the one of interrupt vector address location. Since the console module is configured to NMI type interrupt the monitor vectors to the address location EDFD where EDFD, EDFE, EDFF are reserved for interrupt routine handler or a jump instruction to the IRQ handler. This routine tests the key pressed and if it is RAT monitor key, then the routine branches to the track monitoring routine, otherwise it waits until the key is depressed as mentioned in the operator-system operation interface flow diagram (Fig. 4.2). After the RAT monitor key is depressed, the track monitoring routine displays the word "FEED" on the console module LED display. Then the initial kilometer is entered and the routine performs the initialization of multiplexer and A/D modules. Data memory is divided into two buffer areas. When the data is collected, sampled and being stored at one buffer, the data processing on the other buffer is simultaneously performed. After 1 Km

track span data is evaluated, the results are buffered into the output data memory and cleared. Then next Km data is stored in this data buffer, processing of the data already stored in the other buffer is performed. Thus, the data buffers are alternatively used for data collection and processing.

The complete system operation is as follows. After the initialization of the multiplexer and A/D modules, the routine waits for the keyboard action, and checks whether Km Scan Key is depressed or not. This key is depressed at the start of the run, where the data is to be collected for the processing. If the Km Scan key is pressed, the routine increments the Km (present Km) and enables the data sample pulse generated by the rail wheel and its associated electronics. During the first Km of run, only data will be collected and stored in buffer 1 since no processing of the data is involved. In the next Km, data is stored in buffer 2 while the data in buffer 1 is processed for track evaluation purpose. The data processing scheme involves in finding the track profile of both left and right rails by filtering and double integrating the conditioned output of accelerometer. Then power spectral measurement of the track profile is done and the results are stored in the output data buffers, and after this the buffers will be cleared. In the third Km run, the data is stored in buffer 1 while the data in

buffer 2 is being processed. This alternate cycling between the data buffers is continued until the "Stop" key is depressed. After the depression of stop key, the routine disables the sample data pulse from the rail wheel, but continues processing of the data for the last Km. Then depending upon the status of the print key i.e. if Print Key is depressed or not the results will be printed on a printer and the control is taken over by the track monitoring routine for the next run. If the suspension of the activity of the processor is required at any moment, the system reset should be used for this purpose.







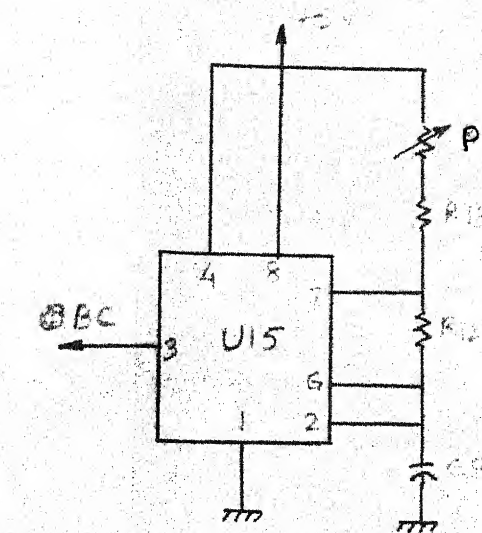




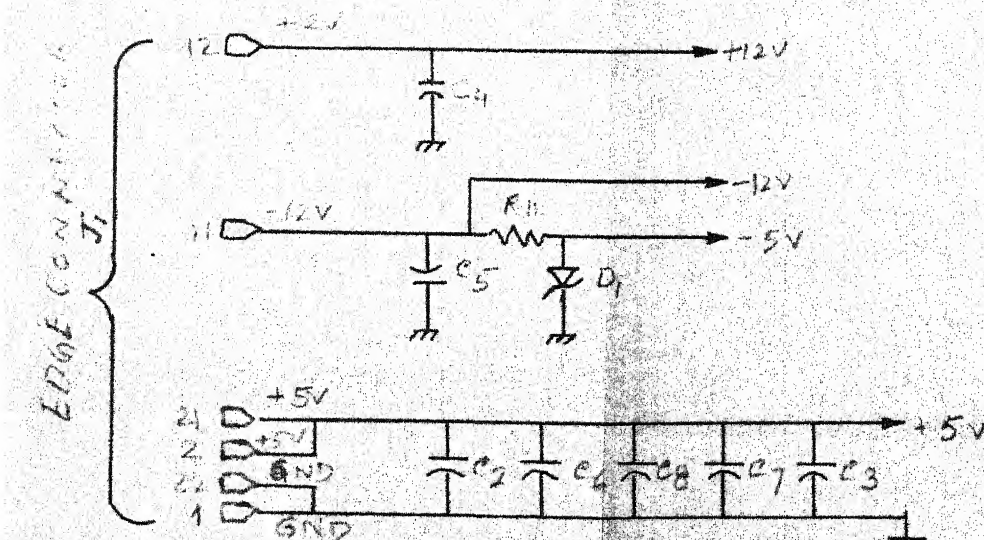


- R1 - 510Ω  
R2 - 220Ω  
R3 - 1.8KΩ  
R4 - 220Ω  
R5 - 4.7KΩ  
R6 - 4.7KΩ  
R7 - 15Ω  
R8 - 15Ω  
R9 - 1KΩ  
R11 - 150Ω 1/2W  
R12 - 1KΩ  
R13 - 1KΩ  
R14 - 4.7KΩ  
R15 - 4.7KΩ  
R16 - 4.7KΩ  
R17 - 4.7KΩ  
R20 - 510Ω  
R21 - 510Ω  
P1 - 50K Trimpot





ON BOARD BAUD RATE CLOCK



ON BOARD POWER DISTRIBUTION

- U1 - 7400
- U2 - 7473
- U3 - 7404
- U4 - 7410
- U5 - 7437
- U6 - 6800
- U7 - 6820
- U8 - 6820
- U9 - 6850
- U10 - 74LS05
- U11 - 74LS07
- U12 - 74LS05
- U13 - 2114
- U14 - 2708
- U15 - 555
- Q1, Q2 - 2N 2222
- Y1 - 4 MHz crystal

FIG. 4.3

M 6800 BASED SINGLE BOARD COMPUTER  
6800 SYSTEM / CPU





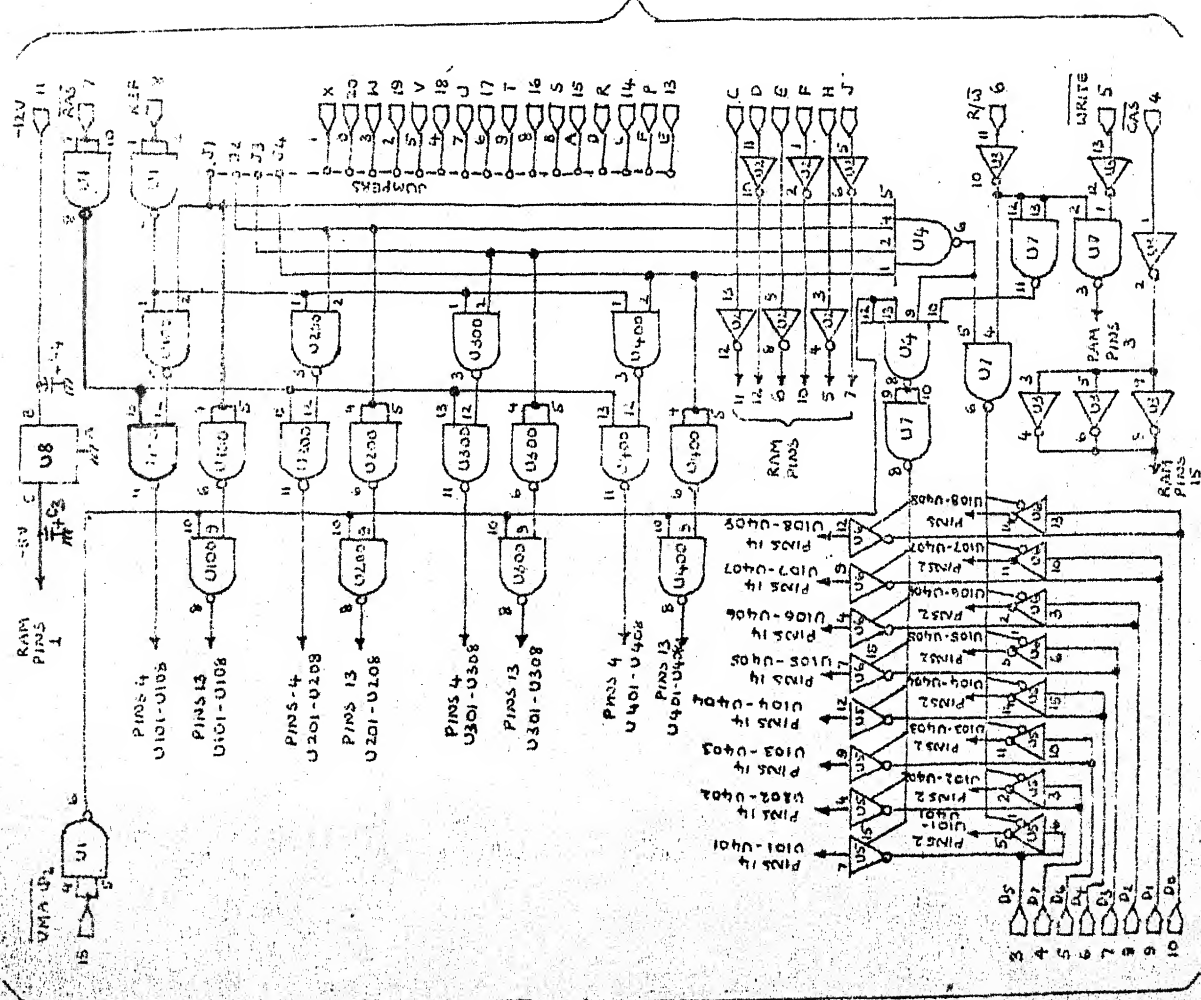
DYNAMIC RAM MODULE

FIG. 4.5

- U1 7400
- U2 7404
- U3 74HC+
- U4 7420
- U5 8T26
- U6 8T26
- U7 7400
- U8 79L05
- U100 7400
- U101-U108 4096
- U200 7400
- U201-U208 4096
- U300 7400
- U301-U308 4096
- U400 7400
- U401-U408 4096

EDGE (REFRESH BUS)

EDGE (WRITE BUS)



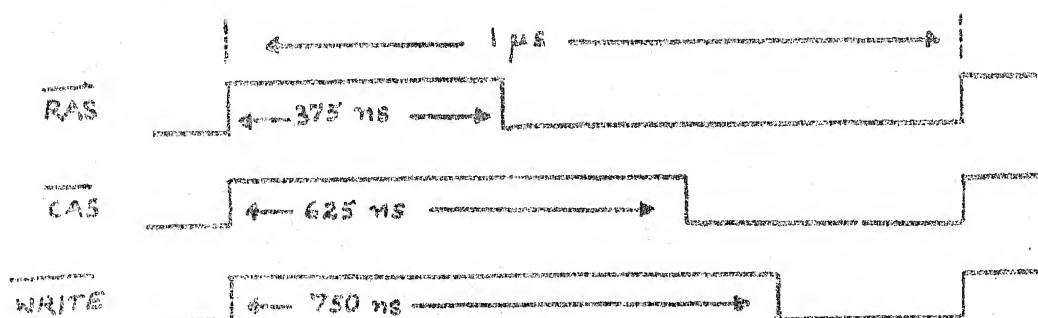


FIG. 4-6. TIMING SIGNALS FOR RAM MODULE

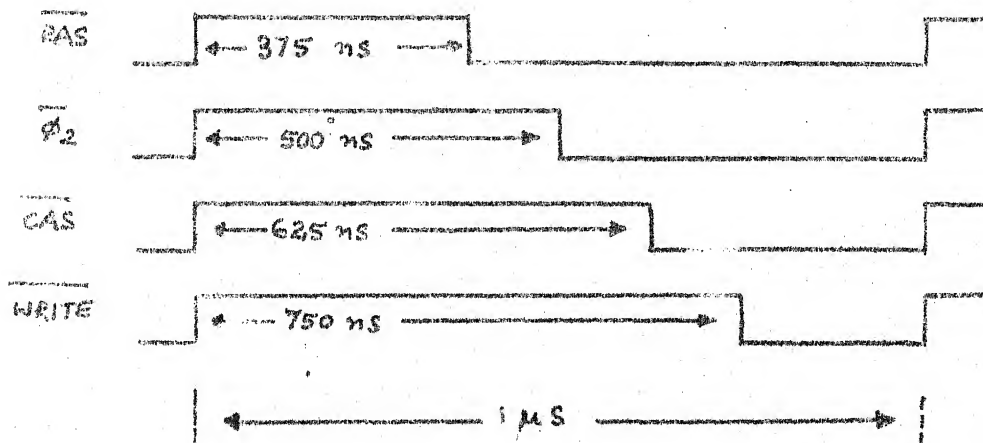


FIG. 4-9. TIMING SIGNALS OF RAM REFRESHER MODULE

Fig. 4.7 Jumper Termination and Associated  
Address for RAM Module

Jumper Termination	Memory Space
0	0000 - 0FFF
1	1000 - 1FFF
2	2000 - 3FFF
3	3000 - 3FFF
4	4000 - 4FFF
5	5000 - 5FFF
6	6000 - 6FFF
7	7000 - 7FFF
8	8000 - 8FFF
9	9000 - 9FFF
A	A000 - AFFF
B	B000 - BFFF
C	C000 - CFFF
D	D000 - DFFF
E	E000 - EFFF
F	F000 - FFFF



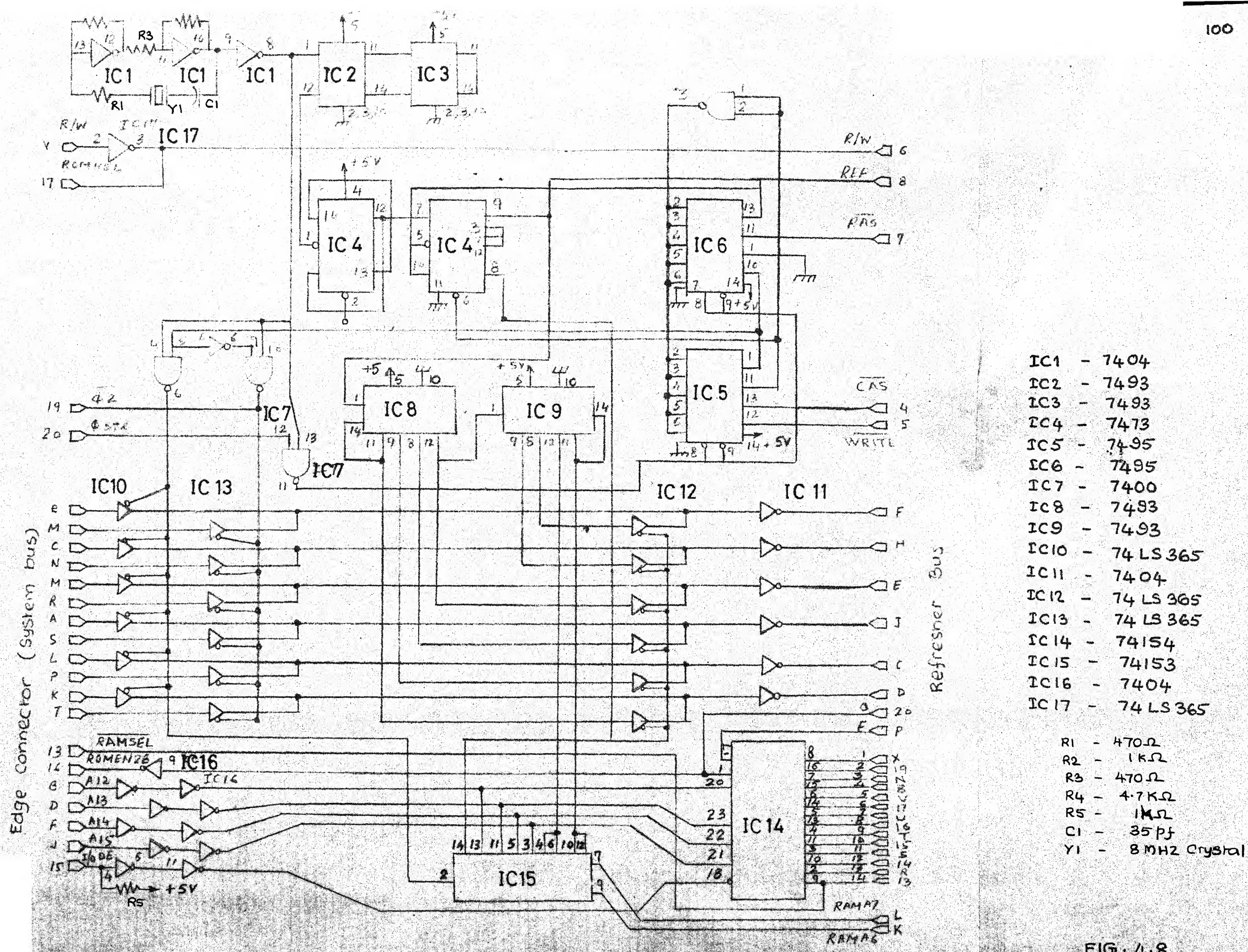


FIG. 4.8

RAM REFRESHER MODULE



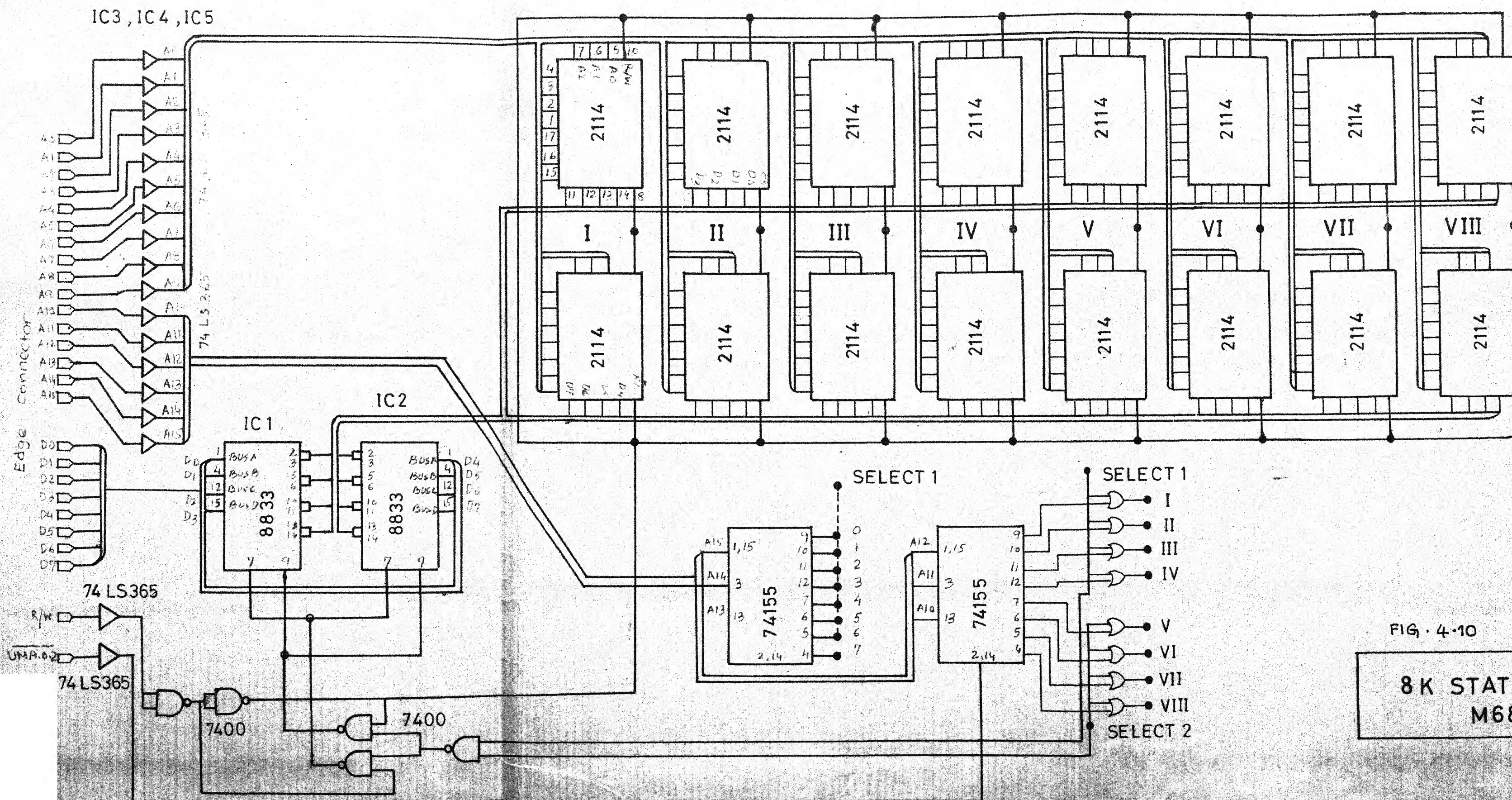
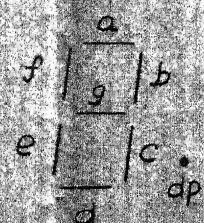


FIG. 4-10

8 K STATIC RAM MODULE  
M6800 / 8K RAM





R1-R9	470 $\Omega$
R10	1M $\Omega$
U1	6820
U2	7400
U3, U4	7445
U5, U6	7406
U7	7493
U8	CD 4060
U9-U11	5082 LED DISPLAY
KEYBOARD	Digitran KL Series
Y1	1.2288 MHZ

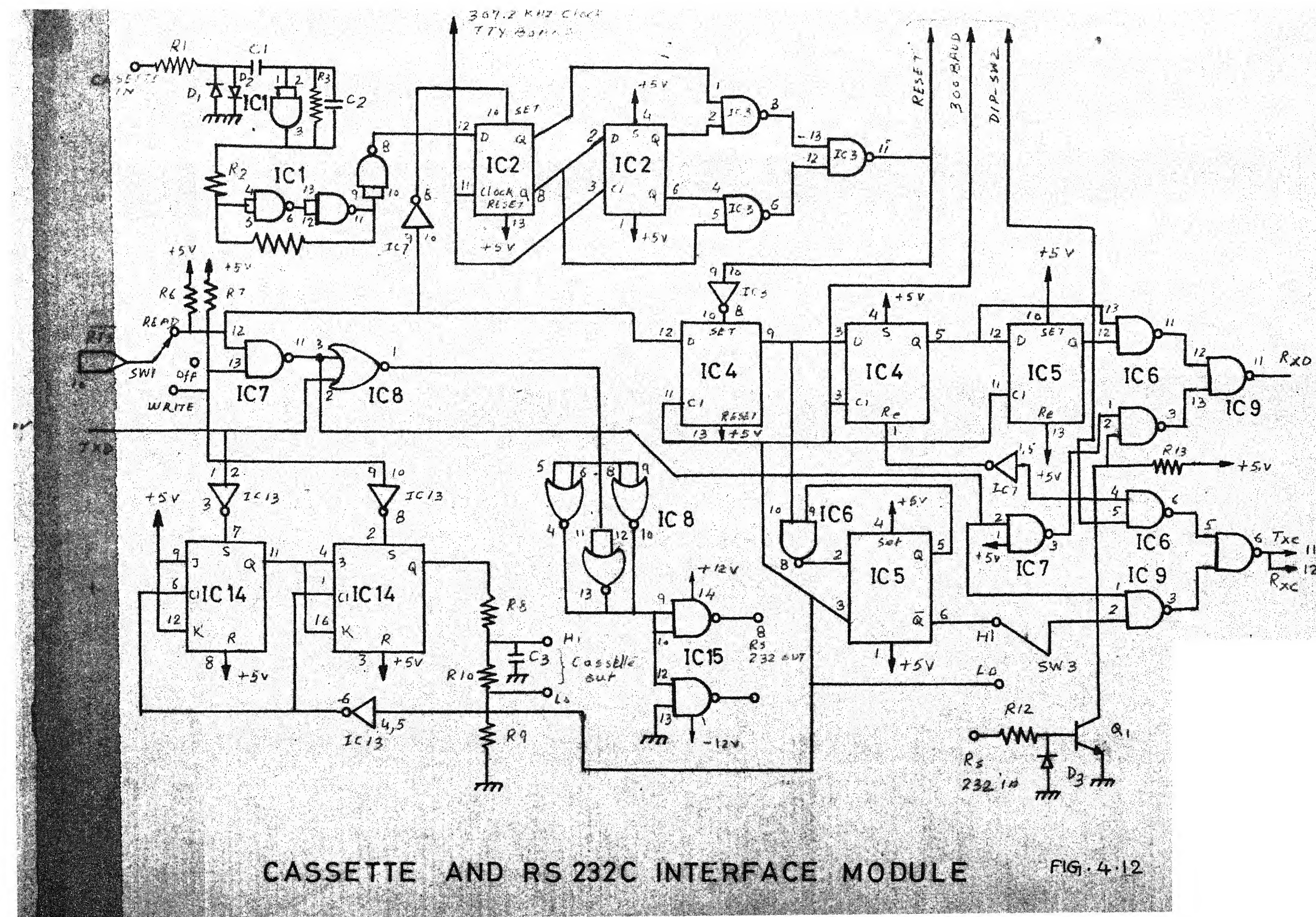
FIG. 4.11

CONSOLE MODULE









CASSETTE AND RS 232C INTERFACE MODULE

FIG. 4.12

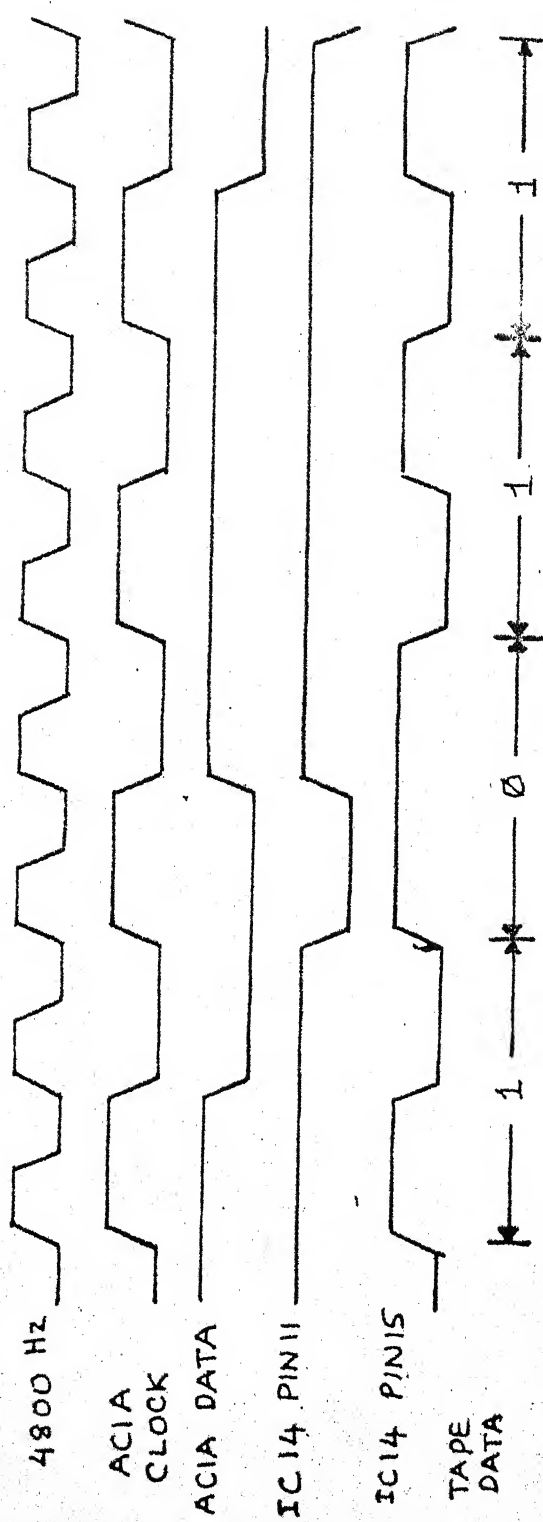


FIG. 4.13. TIMING CHART FOR WRITE OPERATION

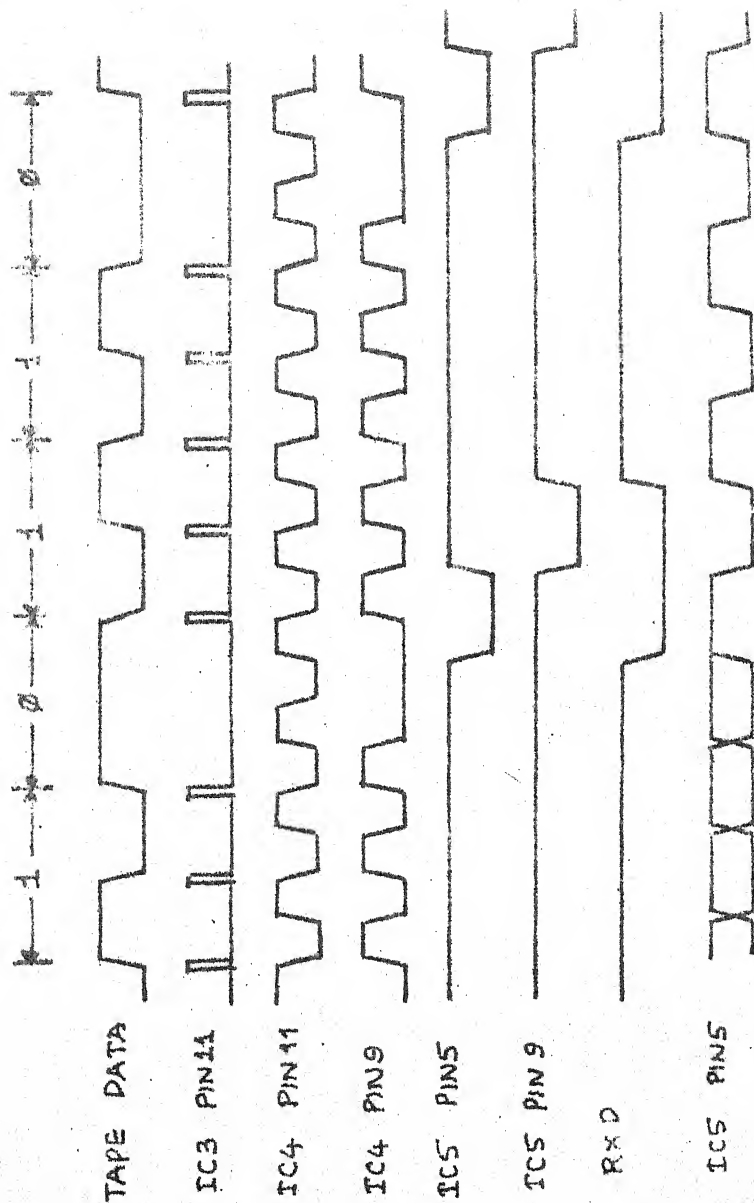
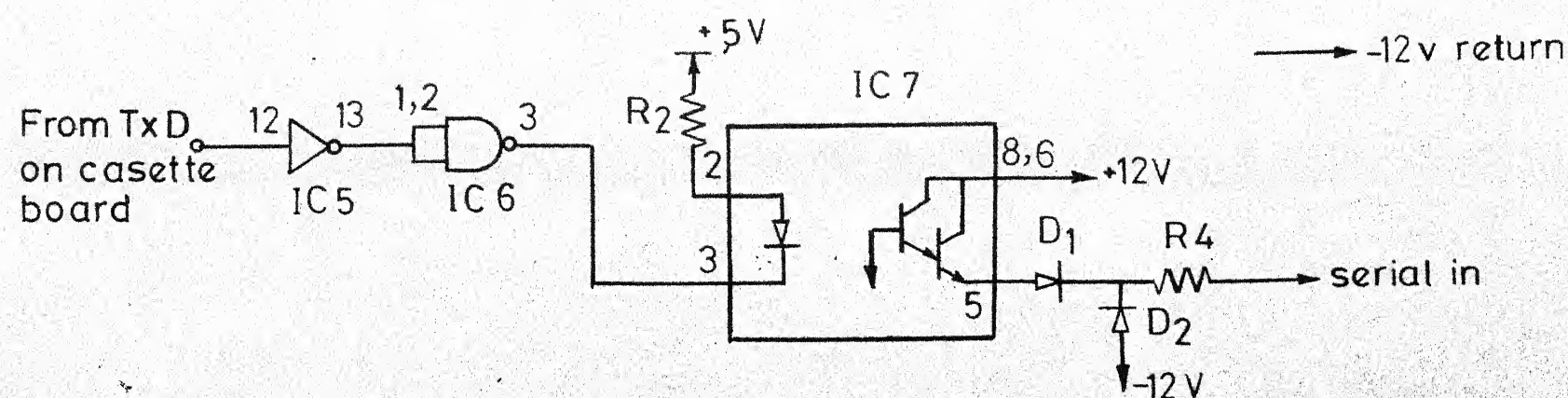
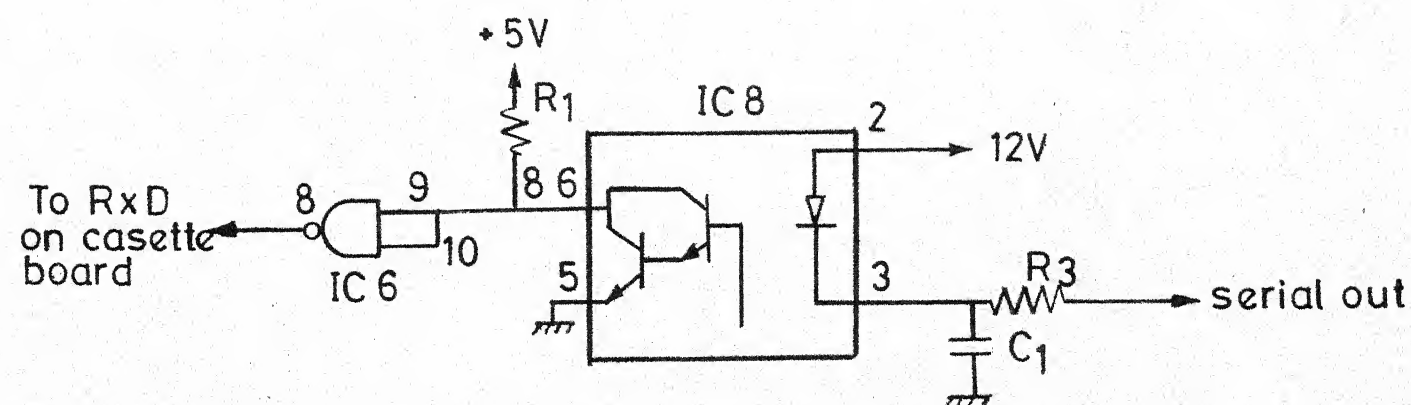
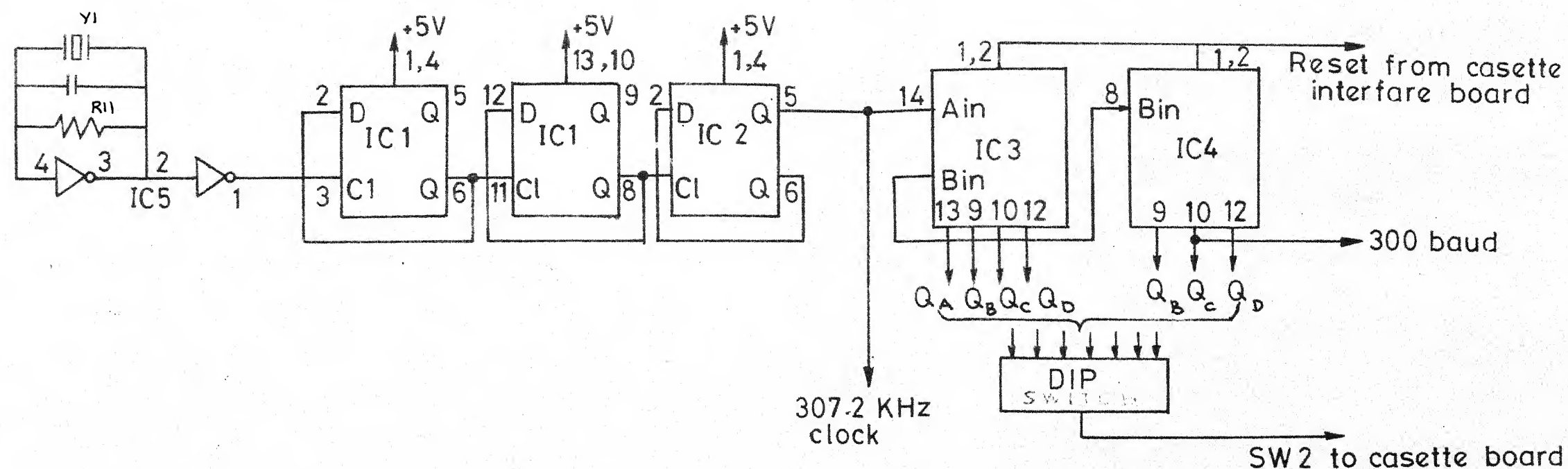


FIG. 4.14. TIMING CHART FOR READ OPERATION

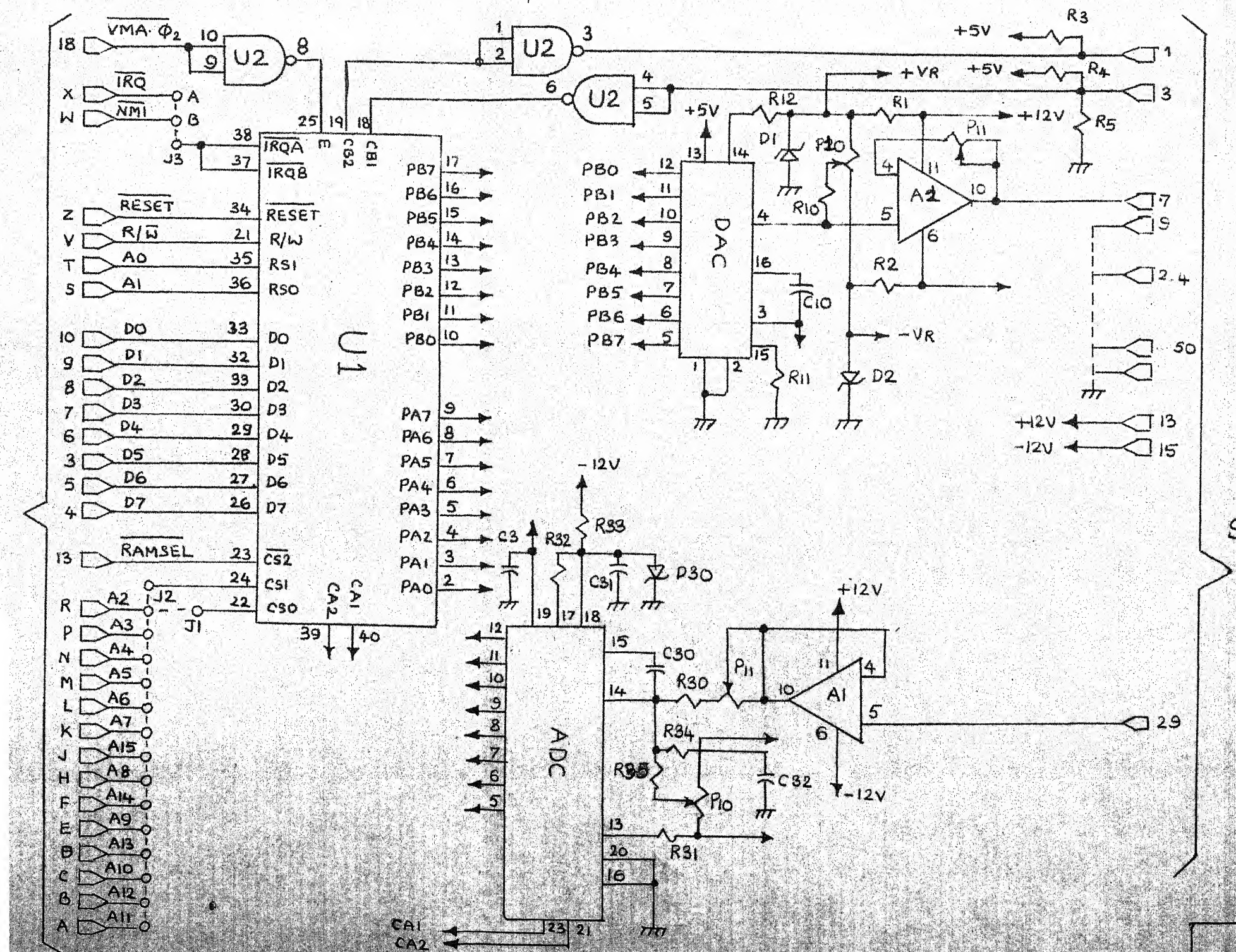




IC1	74C74
IC2	74C74
IC3	74C93
IC4	74C93
IC5	74C901
IC6	7400
IC7	6N139
IC8	6N139
R11	1MΩ
Y1	2.4576 MHz
R1	2KΩ
R2	1.2KΩ
R3	5.6KΩ, 1W
R4	1.2K, 1W
C1	0.01μ, 50V
D1, D2	1N4001

FIG. 4.15 CASSETTE CLOCK AND TTY INTERFACE





- |                                   |                     |
|-----------------------------------|---------------------|
| C <sub>1</sub> , C <sub>2</sub>   | 4.7M $\pm$ 10V      |
| C <sub>3</sub>                    | 0.1 $\mu$ 50V       |
| U <sub>1</sub>                    | 6820 PIA            |
| U <sub>2</sub>                    | 7400                |
| D <sub>1</sub> , D <sub>2</sub>   | 1N751               |
| R <sub>1</sub> , R <sub>2</sub>   | 150 $\Omega$ 1/2W   |
| R <sub>3</sub>                    | 4.7K                |
| R <sub>4</sub>                    | 220 $\Omega$        |
| R <sub>5</sub>                    | 330 $\Omega$        |
| FOR DAC                           |                     |
| R <sub>10</sub>                   | 4.75K 1%            |
| R <sub>11</sub>                   | 4.7K                |
| R <sub>12</sub>                   | 4.75K 1%            |
| P <sub>10</sub> , P <sub>11</sub> | 20K 10T cermet      |
| C <sub>10</sub>                   | 35 pF               |
| DAC                               | MC 1408L8           |
| A <sub>1</sub>                    | 741                 |
| FOR ADC                           |                     |
| R <sub>10</sub>                   | 499K 1%             |
| R <sub>30</sub>                   | 100K 1%             |
| R <sub>31</sub>                   | 249K 1%             |
| R <sub>32</sub>                   | 100K                |
| R <sub>33</sub>                   | 150 $\Omega$ 1/2W   |
| R <sub>34</sub>                   | 100 $\Omega$        |
| P <sub>10</sub>                   | 20K 10T cermet      |
| P <sub>11</sub>                   | 2M 10T cermet       |
| C <sub>30</sub>                   | 68 pF               |
| C <sub>31</sub>                   | 0.1 $\mu$ 50V       |
| C <sub>32</sub>                   | 270 pF              |
| A <sub>1</sub>                    | 741                 |
| D <sub>30</sub>                   | 1N751               |
| ADC                               | 8, 10 or 12 bit ADC |

FIG. 4-16

A/D CONVERTER MODULE



Table 4.1 Edge Connector Signal Summary

<u>Component Side</u>		<u>Wiring Side</u>	
<u>Tongue Designation</u>	<u>Signal</u>	<u>Tongue Designation</u>	<u>Signal</u>
1	Gnd	A	A11
2	+5V	B	A12
3	D5	C	A10
4	D7	D	A13
5	D6	E	A9
6	D4	F	A14
7	D3	H	A8
8	D2	J	A15
9	D1	K	A7
10	D0	L	A6
11	-12V	M	A5
12	+12V	N	A4
13	RAM SELECT	P	A3
14	-	R	A2
15	-	S	A1
16	ROM ENABLE 2	T	A0
17	ROM ENABLE 1	U	B.A
18	$\overline{\text{VMA}} \cdot \overline{\phi}_2$	V	R/ $\overline{\text{W}}$
19	$\overline{\text{BUS}} \cdot \overline{\phi}_2$	W	$\overline{\text{NMI}}$
20	$\overline{\phi}$ STRETCH	X	$\overline{\text{IRQ}}$
21	+5V	Y	$\overline{\text{HALT}}$
22	GND	Z	$\overline{\text{RESET}}$

TABLE 4.2 CPU Module Memory Mapping

<u>Hex Address</u>	<u>Component</u>
0000 - 03FF	RAM
ED80 - EDFF	RAM (Stack Memory)
EE08	U9 ACIA Control/Status Register
EE09	U9 Data Register
EE10	U8 (PIA-1) Output Register A
EE11	U8 Output Register B
EE12	U8 Control Register A
EE13	U8 Control Register B
EE20	U7 (PIA-2) Output Register A
EE21	U7 Output Register B
EE22	U7 Control Register A
EE23	U7 Control Register B
FC00 - FFFF	Read only Memory

Table 4.3 ACIA Serial Connector Signal Summary

<u>PIN Number</u>	<u>Signal</u>
1	+5V
2	On board Baud Clock
3	Gnd
4	Gnd
5	Gnd
6	+12V
7	-12V
8	<u>Data Carrier Detect</u>
9	Output Data
10	<u>Request to send</u>
11	Output clock
12	Input clock
13	Input data
14	<u>Clear to send</u>

## CHAPTER 5

### SOFTWARE IMPLEMENTATION, RESULTS AND DISCUSSIONS

#### 5.1 SOFTWARE IMPLEMENTATION

In this section, the implementation of composite highpass-integrating filter, Fast Fourier Transform and PSD measurement of track profile for 6800 microprocessor applications is described. A complete assembly program listing for these functions is given at Appencix 'A'. The memory requirement for the individual programs is given here. For higher flexibility the data memory locations for filter and PSD are considered separately for testing. To make up the complete track monitoring routine, these locations should be changed properly.

##### 5.1.1 High Pass filter and Integration

This program takes approximately 1K of the memory (1146 locations) and is implemented in 32 bit organization for higher accuracy. This is assembled from Memory address  $5000_{16}$  to  $5477_{16}$ . The data buffer consists of four sections and is assembled from  $2000_{16}$  to  $27FF_{16}$  (Buffer 1),  $2900_{16}$  to  $30FF_{16}$  (Buffer 2),  $3200_{16}$  to  $39FF_{16}$  (Buffer 3),  $4100_{16}$  to  $48FF_{16}$  (Buffer 4), each a 2K section of the memory. The data stored in the buffer 1 is first filtered, integrated and then stored in buffer 3 and again the data stored in buffer 3 (first high pass and integration) is again processed to get the double

integrated version of the original data and is stored in buffer 1. Then the control goes over to Buffer 2 for processing the next section of the data. Buffer 2, Buffer 4 are used for this. After double integration of the data in buffer 2, the control again goes back to buffer 1 and this repeats.

### 5.1.2 Fast Fourier Transform

The FFT routine takes approximately 4.5 K of memory (4580 locations) including the data locations for real and imaginary parts each a 1K section (for 512 points) and is assembled from 4000<sub>16</sub> to 51E4<sub>16</sub>. The data locations for real part start from 49CA<sub>16</sub> to 4DC9<sub>16</sub> and 4DCA<sub>16</sub> to 51C9<sub>16</sub> are for imaginary part. The data on which FFT analysis is to be done is first stored in these locations and after the run, the result is available at the same locations.

### 5.1.3 PSD Measurement

This routine takes 353 locations of the memory and uses the multiplication routine in the FFT program. This is assembled in two parts. One part is a high pass filter for detrending the data (removal of DC and very low frequencies) and the second part is for the PSD measurement. These are assembled from 5200<sub>16</sub> to 52C2<sub>16</sub> and 5500<sub>16</sub> to 559C<sub>16</sub>.

## 5.2 RESULTS

Since the accelerometer data is not available, the high pass filter and integrator algorithm is tested for DC superimposed sine wave and the various outputs are given at Fig. 5.1 for a section of the data. This program is tested for various frequencies of the input data and found to be satisfactory. However, the PSD measurement through FFT is tested using a typical track profile data, supplied by RDSO (Research, Development and Systems Organization, Lucknow) and the results are shown in Fig. 5.2. This is also tested using standard FFT Fortran subroutines on DEC-1090 computer and the results are found to be satisfactory. Due to the limited precision of signal processor which uses the 6800 micro-processor, the accuracy is somewhat affected. The run time of double integration algorithm is approximately 2 seconds, whereas for FFT subroutine and PSD routine the time is approximately 18 seconds. This is mainly due to the software multiply routine which takes an approximate time of 1.67 m sec for each 16 x 16 BIT multiplication. A hardware multiplier using one of the TRW multiplier chips reduces the multiplication time by approximately 1/5, since the worst case timing including all the instructions and returns from the subroutine will be about 250  $\mu$  sec.

### 5.3 CONCLUSIONS

In this thesis, a complete hardware system for routine track monitoring is described in detail. All the individual hardware modules are tested and packed in a 10" x 12" x 12" box. All the software routines are tested. However, the complete system performance is not evaluated due to the lack of the appropriate data. But it is expected that the system works satisfactorily in the real time environment due to its consistent performance while testing individual components.

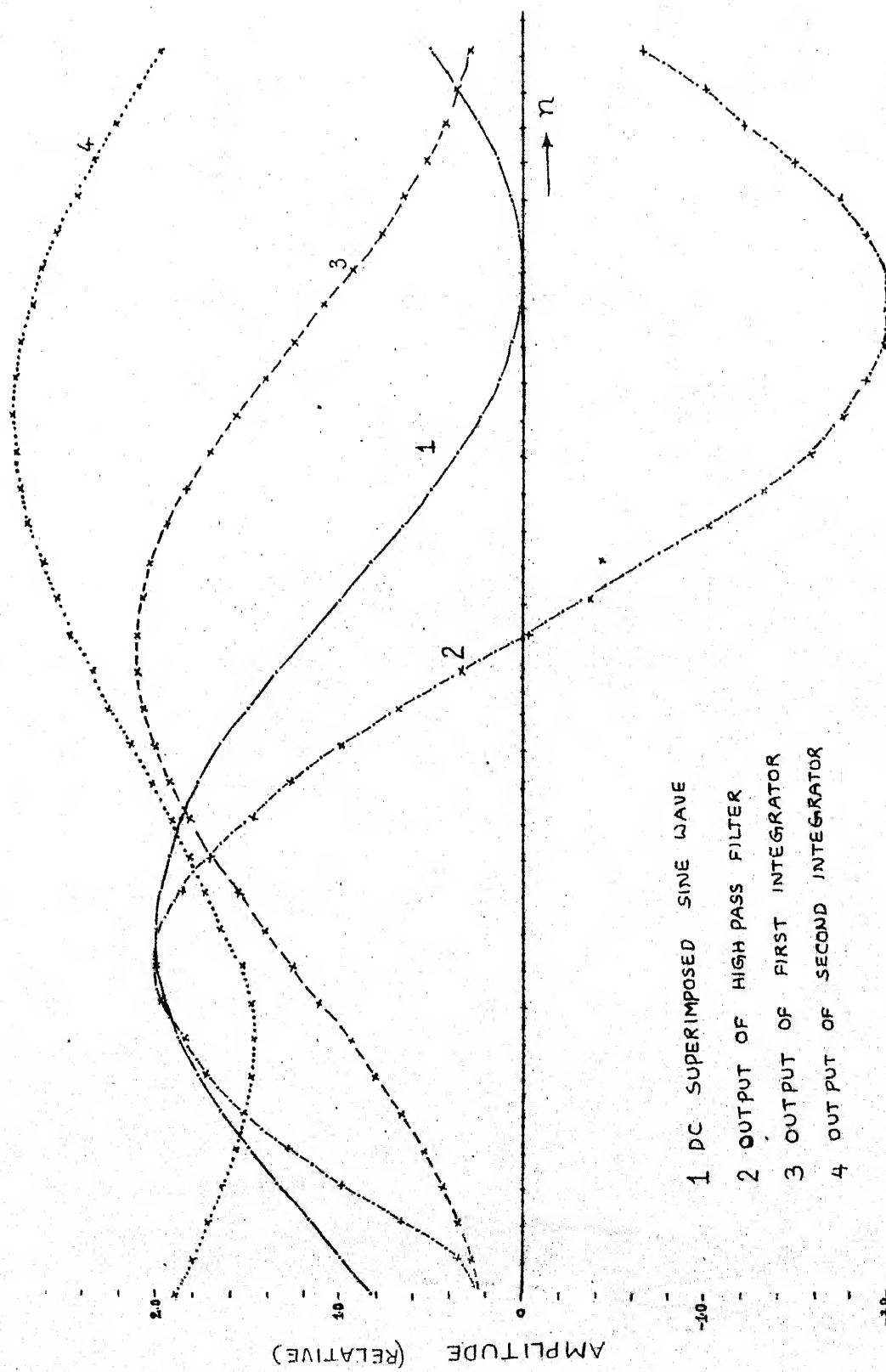
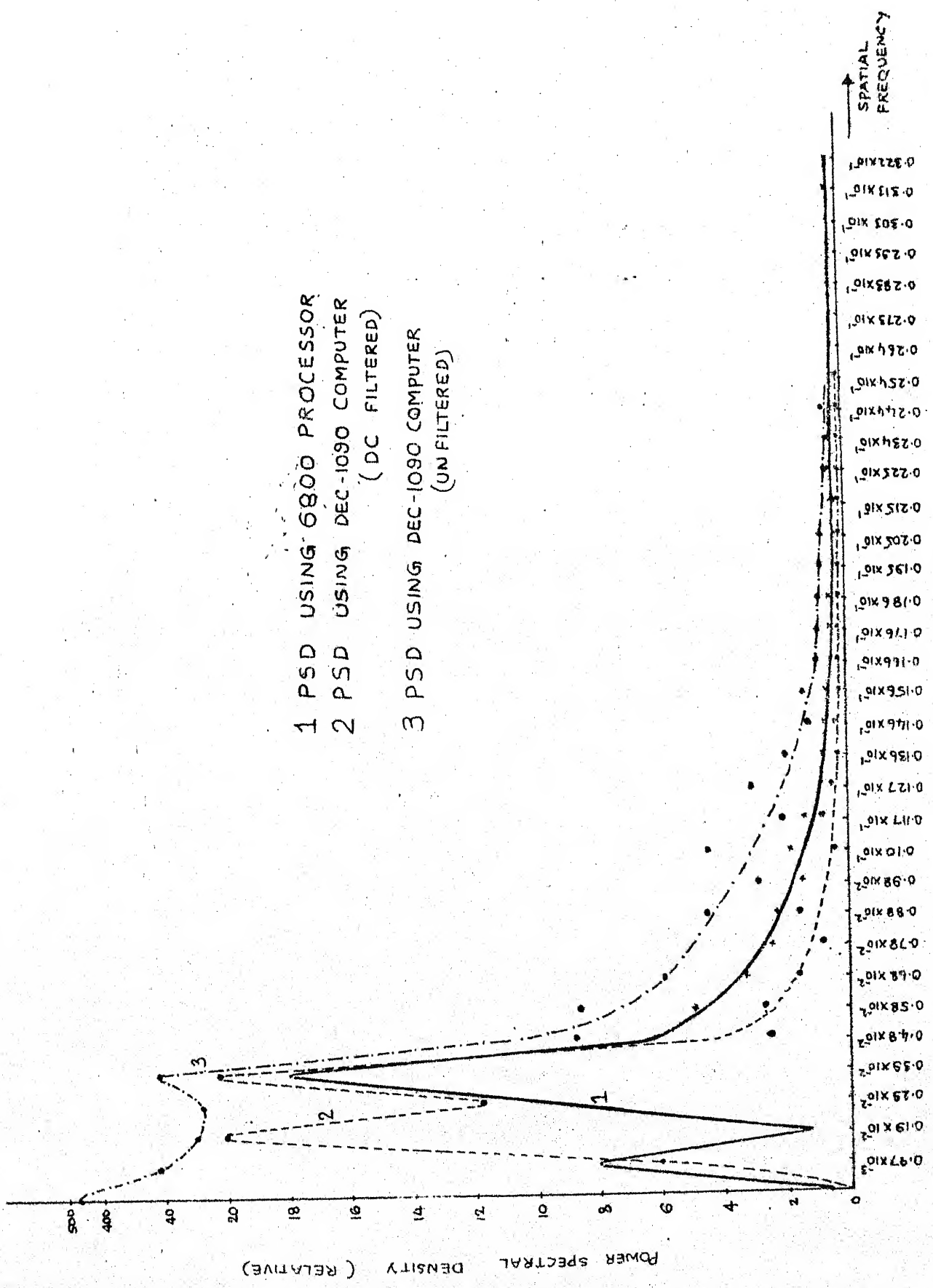


FIG. 5.1. TEST WAVEFORMS OF COMPOSITE FILTER





## LIST OF REFERENCES

1. L.R. Rabiner and B. Gold, "Theory and Application of Digital Signal Processing", Prentice Hall India Ltd., 1979.
2. A. Antoniou, "Digital Filters: Analysis and Design", Tata McGraw-Hill Publishing Company Ltd., New Delhi, 1980.
3. K. Nandakumar, "Digital Filtering of Low Frequency Signals by the Method of Incremental Computation", M.Tech. Thesis, Department of Electrical Engineering, I.I.T. Kanpur, Jan. 1981.
4. K.L. Chug, "A FFT Program for Microcomputer for Real Time Application", M.Tech. Thesis, Department of Electrical Engineering, I.I.T. Kanpur, August, 1978.
5. Mischa Schwartz, Leonard Shaw, "Signal Processing: Discrete Spectral Analysis, Detection and Estimation", McGraw Hill Kogakusha, 1975.

M 6800  
ASSEMBLY LISTING.

\* 6800 ASSEMBLY PROGRAM  
 \* FOR FIRST ORDER INCRE-  
 \* MENTAL FILTER AND  
 \* SIMPSON INTEGRATOR  
 \* FOLLOWING ARE WORKING  
 \* LOCATIONS FOR THE PROGRAM

1FFC	X1	EQU	\$1FFC
28FC	X2	EQU	\$28FC
31FC	Y1	EQU	\$31FC
40FC	Y2	EQU	\$40FC
4905	DELY	EQU	\$4905
4910	DELY0	EQU	\$4910
4915	DELY1	EQU	\$4915
4920	DELY2	EQU	\$4920
4925	DEL1	EQU	\$4925
4930	DEL2	EQU	\$4930
4935	INTER	EQU	\$4935
4940	INTER1	EQU	\$4940
4945	INTER2	EQU	\$4945
4950	TEMP	EQU	\$4950
4955	TEMP1	EQU	\$4955
4960	TEMP2	EQU	\$4960
4975	SHICOU	EQU	\$4975
4980	COUNT1	EQU	\$4980
4985	COUNT2	EQU	\$4985
4990	OUT0	EQU	\$4990
4995	OUT1	EQU	\$4995
49A0	OUT2	EQU	\$49A0

\* MAIN PROGRAM START

5000		ORG	\$5000
5000	7F 1F FC	CLR	X1
5003	7F 1F FD	CLR	X1+1
5006	7F 1F FE	CLR	X1+2
5009	7F 1F FF	CLR	X1+3
500C	7F 28 FC	CLR	X2
500F	7F 28 FD	CLR	X2+1
5012	7F 28 FE	CLR	X2+2
5015	7F 28 FF	CLR	X2+3
5018	7F 31 FC	CLR	Y1
501B	7F 31 FD	CLR	Y1+1
501E	7F 31 FE	CLR	Y1+2
5021	7F 31 FF	CLR	Y1+3
5024	7F 40 FC	CLR	Y2
5027	7F 40 FD	CLR	Y2+1
502A	7F 40 FE	CLR	Y2+2
502D	7F 40 FF	CLR	Y2+3
5030	7F 49 05	CLR	DELY
5033	7F 49 06	CLR	DELY+1
5036	7F 49 07	CLR	DELY+2
5039	7F 49 08	CLR	DELY+3
503C	7F 49 10	CLR	DELY0
503F	7F 49 11	CLR	DELY0+1
5042	7F 49 12	CLR	DELY0+2
5045	7F 49 13	CLR	DELY0+3
5048	7F 49 15	CLR	DELY1

504B	7F 49 16		CLR	DELY1+1
504E	7F 49 17		CLR	DELY1+2
5051	7F 49 18		CLR	DELY1+3
5054	7F 49 20		CLR	DELY2
5057	7F 49 21		CLR	DELY2+1
505A	7F 49 22		CLR	DELY2+2
505D	7F 49 23		CLR	DELY2+3
5060	7F 49 25		CLR	DEL1
5063	7F 49 26		CLR	DEL1+1
5066	7F 49 27		CLR	DEL1+2
5069	7F 49 28		CLR	DEL1+3
506C	7F 49 30		CLR	DEL2
506F	7F 49 31		CLR	DEL2+1
5072	7F 49 32		CLR	DEL2+2
5075	7F 49 33		CLR	DEL2+3
5078	7F 49 35		CLR	INTER
507B	7F 49 36		CLR	INTER+1
507E	7F 49 37		CLR	INTER+2
5081	7F 49 38		CLR	INTER+3
5084	7F 49 40		CLR	INTER1
5087	7F 49 41		CLR	INTER1+1
508A	7F 49 42		CLR	INTER1+2
508D	7F 49 43		CLR	INTER1+3
5090	7F 49 45		CLR	INTER2
5093	7F 49 46		CLR	INTER2+1
5096	7F 49 47		CLR	INTER2+2
5099	7F 49 48		CLR	INTER2+3
509C	7F 49 90		CLR	OUT0
509F	7F 49 91		CLR	OUT0+1
50A2	7F 49 92		CLR	OUT0+2
50A5	7F 49 93		CLR	OUT0+3
50A8	7F 49 95		CLR	OUT1
50AB	7F 49 96		CLR	OUT1+1
50AE	7F 49 97		CLR	OUT1+2
50B1	7F 49 98		CLR	OUT1+3
50B4	7F 49 A0		CLR	OUT2
50B7	7F 49 A1		CLR	OUT2+1
50BA	7F 49 A2		CLR	OUT2+2
50BD	7F 49 A3		CLR	OUT2+3
50C0	7F 49 50		CLR	TEMP
50C3	7F 49 55		CLR	TEMP1
50C6	7F 49 60		CLR	TEMP2
50C9	7F 49 75		CLR	SHICOU
50CC	CE 1F FF	OUTER	LDX	#\$1FFF
50CF	FF 49 80		STX	COUNT1
50D2	CE 32 03		LDX	#\$3203
50D5	FF 49 85		STX	COUNT2
			MAIN	LOOP OF FILTER PROGRAM
50D8	FE 49 80	* MAIN	LDX	COUNT1
50DB	8C 1F FF		CPX	#\$1FFF
50DE	27 12		BEQ	INNER1
50E0	8C 28 FF		CPX	#\$28FF
50E3	27 0D		BEQ	INNER1
50E5	8C 31 FF		CPX	#\$31FF
50E8	27 6B		BEQ	INNER2
50EA	8C 40 FF		CPX	#\$40FF

50ED 27 66  
50EF 7E 51 B5

\*  
\*

INNER1

50F2 B6 49 43  
50F5 B7 49 38  
50F8 E6 49 42  
50FB B7 49 37  
50FE B6 49 41  
5101 E7 49 36  
5104 B6 49 40  
5107 B7 49 35  
510A B6 49 18  
510D B7 49 08  
5110 B6 49 17  
5113 B7 49 07  
5116 E6 49 16  
5119 B7 49 06  
511C B6 49 15  
511F B7 49 05  
5122 B6 49 28  
5125 B7 49 13  
5128 B6 49 27  
512B B7 49 12  
512E B6 49 26  
5131 B7 49 11  
5134 B6 49 25  
5137 B7 49 10  
513A B6 49 98  
513D B7 49 93  
5140 B6 49 97  
5143 B7 49 92  
5146 B6 49 96  
5149 B7 49 91  
514C B6 49 95  
514F B7 49 90  
5152 7E 51 B5

\*  
\*

INNER2

5155 B6 49 48  
5158 B7 49 38  
515B B6 49 47  
515E B7 49 37  
5161 B6 49 46  
5164 B7 49 36  
5167 B6 49 45  
516A B7 49 35  
516D B6 49 23  
5170 B7 49 08  
5173 B6 49 22  
5176 B7 49 07  
5179 B6 49 21  
517C B7 49 06  
517F E6 49 20  
5182 B7 49 05  
5185 B6 49 33

BEG INNER2  
JMP INNER  
TAKING CARE OF DELAYED VALUES  
FOR THE FIRST LOOP  
LDA A INTER1+3  
STA A INTER+3  
LDA A INTER1+2  
STA A INTER+2  
LDA A INTER1+1  
STA A INTER+1  
LDA A INTER1  
STA A INTER  
LDA A DELY1+3  
STA A DELY+3  
LDA A DELY1+2  
STA A DELY+2  
LDA A DELY1+1  
STA A DELY+1  
LDA A DELY1  
STA A DELY  
LDA A DEL1+3  
STA A DELY0+3  
LDA A DEL1+2  
STA A DELY0+2  
LDA A DEL1+1  
STA A DELY0+1  
LDA A DEL1  
STA A DELY0  
LDA A OUT1+3  
STA A OUT0+3  
LDA A OUT1+2  
STA A OUT0+2  
LDA A OUT1+1  
STA A OUT0+1  
LDA A OUT1  
STA A OUT0  
JMP INNER  
TAKING CARE OF DELAYED VALUES  
FOR THE SECOND LOOP  
LDA A INTER2+3  
STA A INTER+3  
LDA A INTER2+2  
STA A INTER+2  
LDA A INTER2+1  
STA A INTER+1  
LDA A INTER2  
STA A INTER  
LDA A DELY2+3  
STA A DELY+3  
LDA A DELY2+2  
STA A DELY+2  
LDA A DELY2+1  
STA A DELY+1  
LDA A DELY2  
STA A IFLY  
LDA A DEL2+3

5188 B7 49 13  
 518B B6 49 32  
 518E B7 49 12  
 5191 B6 49 31  
 5194 B7 49 11  
 5197 B6 49 30  
 519A B7 49 10  
 519D B6 49 A3  
 51A0 B7 49 93  
 51A3 B6 49 A2  
 51A6 B7 49 92  
 51A9 B6 49 A1  
 51AC B7 49 91  
 51AF B6 49 A0  
 51B2 B7 49 90

51B5 B6 49 38  
 51B8 F6 49 37  
 51BE B0 49 08  
 51BE F2 49 07  
 51C1 B7 49 38  
 51C4 B7 49 53  
 51C7 F7 49 37  
 51CA F7 49 52  
 51CD B6 49 36  
 51D0 F6 49 35  
 51D3 B2 49 06  
 51D6 F2 49 05  
 51D9 B7 49 36  
 51DC B7 49 51  
 51DF F7 49 35  
 51E2 F7 49 50  
 51E5 86 05  
 51E7 B7 49 75  
 51EA 77 49 50  
 51ED 76 49 51  
 51F0 76 49 52  
 51F3 76 49 53  
 51F6 7A 49 75  
 51F9 7D 49 75  
 51FC 26 EC  
 51FE A6 04  
 5200 E6 03  
 5202 A0 00  
 5204 09  
 5205 E2 00  
 5207 B7 49 08  
 520A F7 49 07  
 520D 29  
 520E A6 04  
 5210 E6 03  
 5212 A2 00  
 5214 09  
 5215 E2 00  
 5217 08  
 5218 08

\*  
 INNER

LOOP

STA A DELY0+3  
 LDA A DEL2+2  
 STA A DELY0+2  
 LDA A DEL2+1  
 STA A DELY0+1  
 LDA A DEL2  
 STA A DELY0  
 LDA A OUT2+3  
 STA A OUT2+3  
 LDA A OUT2+2  
 STA A OUT2+2  
 LDA A OUT2+1  
 STA A OUT2+1  
 LDA A OUT2  
 STA A OUT0

INNER LOOP OF THE PROGRAM

LDA A INTER+3  
 LDA B INTER+2  
 SUB A DELY+3  
 SBC B DELY+2  
 STA A INTER+3  
 STA A TEMP+3  
 STA B INTER+2  
 STA B TEMP+2  
 LDA A INTER+1  
 LDA B INTER  
 SBC A DELY+1  
 SBC B DELY  
 STA A INTER+1  
 STA A TEMP+1  
 STA B INTER  
 STA B TEMP  
 LDA A #305  
 STA A SHICOU  
 ASR TEMP  
 ROR TEMP+1  
 ROR TEMP+2  
 ROR TEMP+3  
 DEC SHICOU  
 TST SHICOU  
 BNE LOOP  
 LDA A 4,X  
 LDA B 3,X  
 SUB A 0,X  
 DEX  
 SBC B 0,X  
 STA A DELY+3  
 STA B DELY+2  
 DEX  
 LDA A 4,X  
 LDA B 3,X  
 SBC A 0,X  
 LEX  
 SBC B 0,X  
 INX  
 INX

5219	08			INX	
521A	B7	49	06	STA A	DELY+1
521D	F7	49	05	STA B	DELY
5220	B6	49	08	LDA A	DELY+3
5223	F6	49	07	LDA B	DELY+2
5226	BB	49	53	ADD A	TEMP+3
5229	F9	49	52	ADC B	TEMP+2
522C	B7	49	08	STA A	DELY+3
522F	F7	49	07	STA B	DELY+2
5232	B6	49	06	LDA A	DELY+1
5235	F6	49	05	LDA B	DELY
5238	B9	49	51	ADC A	TEMP+1
523B	F9	49	50	ADC B	TEMP
523E	B7	49	06	STA A	DELY+1
5241	F7	49	05	STA B	DELY
5244	B6	49	08	LDA A	DELY+3
5247	F6	49	07	LDA B	DELY+2
524A	BB	49	13	ADD A	DELY0+3
524D	F9	49	12	ADC B	DELY0+2
5250	B7	49	13	STA A	DELY0+3
5253	B7	49	58	STA A	TEMP1+3
5256	F7	49	12	STA B	DELY0+2
5259	F7	49	57	STA B	TEMP1+2
525C	B6	49	06	LDA A	DELY+1
525F	F6	49	05	LDA B	DELY
5262	B9	49	11	ADC A	DELY0+1
5265	F9	49	10	ADC B	DELY0
5268	B7	49	11	STA A	DELY0+1
526B	B7	49	56	STA A	TEMP1+1
526E	F7	49	10	STA B	DELY0
5271	F7	49	55	STA B	TEMP1
5274	86	04		LDA A	#504
5276	B7	49	75	STA A	SHICOU
5279	77	49	55	ASR	TEMP1
527C	76	49	56	ROR	TEMP1+1
527F	76	49	57	ROR	TEMP1+2
5282	76	49	58	ROR	TEMP1+3
5285	7A	49	75	DEC	SHICOU
5288	7D	49	75	TST	SHICOU
528B	26	EC		BNE	LOOP1
528D	FF	49	60	STX	TEMP2
				* BRANCHING TO INTEGRATION ROUTINE	
5290	BD	54	46	JSR	INTEGR
5293	FE	49	85	LDX	COUNT2
5296	B6	49	58	LDA A	TEMP1+3
5299	A7	00		STA A	0,X
529B	09			DEX	
529C	B6	49	57	LDA A	TEMP1+2
529F	A7	00		STA A	0,X
52A1	09			DEX	
52A2	B6	49	56	LDA A	TEMP1+1
52A5	A7	00		STA A	0,X
52A7	09			DEX	
52A8	B6	49	55	LDA A	TEMP1
52AB	A7	00		STA A	0,X
52AD	FE	49	60	LDX	TEMP2



52B0 8C 27 FB  
 52B3 27 12  
 52B5 8C 30 FB  
 52B8 27 23  
 52BA 8C 39 FB  
 52BD 27 20  
 52BF 8C 48 FB  
 52C2 27 1D  
 52C4 7E 54 00

\*

\*

STORE1

52C7 A6 04  
 52C9 B7 28 FF  
 52CC A6 03  
 52CE B7 28 FE  
 52D1 A6 02  
 52D3 B7 28 FD  
 52D6 A6 01  
 52D8 B7 28 FC  
 52DB 20 06  
 52DD 20 71  
 52DF 20 6A  
 52E1 20 6A  
 52E3 B6 49 08  
 52E6 B7 49 18  
 52E9 B6 49 07  
 52EC B7 49 17  
 52EF B6 49 06  
 52F2 B7 49 16  
 52F5 B6 49 05  
 52F8 B7 49 15  
 52FB B6 49 38  
 52FE B7 49 43  
 5301 B6 49 37  
 5304 B7 49 42  
 5307 B6 49 36  
 530A B7 49 41  
 530D B6 49 35  
 5310 B7 49 40  
 5313 B6 49 13  
 5316 B7 49 28  
 5319 B6 49 12  
 531C B7 49 27  
 531F B6 49 11  
 5322 B7 49 26  
 5325 B6 49 10  
 5328 B7 49 25  
 532B B6 49 93  
 532E F6 49 92  
 5331 B7 49 98  
 5334 F7 49 97  
 5337 B6 49 91  
 533A F6 49 90  
 533D B7 49 96  
 5340 F7 49 95  
 5343 8C 20 FB

STORE2

STORE5

STORE6

PRST01

CPX #527FB  
 BEQ STORE1  
 CPX #530FB  
 BEQ STORE2  
 CPX #539FB  
 BEQ STORE5  
 CPX #548FB  
 BEQ STORE6  
 JMP NEXT

TAKING CARE OF LAST  
 LOCATION VALUES

LDA A 4,X  
 STA A X2+3  
 LDA A 3,X  
 STA A X2+2  
 LDA A 2,X  
 STA A X2+1  
 LDA A 1,X  
 STA A X2  
 BRA PRST01  
 BRA STORE2  
 BRA STORE5  
 BRA STORE6  
 LDA A DELY+3  
 STA A DELY1+3  
 LDA A DELY+2  
 STA A DELY1+2  
 LDA A DELY+1  
 STA A DELY1+1  
 LDA A DELY  
 STA A DELY1  
 LDA A INTER+3  
 STA A INTER1+3  
 LDA A INTER+2  
 STA A INTER1+2  
 LDA A INTER+1  
 STA A INTER1+1  
 LDA A INTER  
 STA A INTER1  
 LDA A DELY0+3  
 STA A DEL1+3  
 LDA A DELY0+2  
 STA A DEL1+2  
 LDA A DELY0+1  
 STA A DEL1+1  
 LDA A DELY0  
 STA A DEL1  
 LDA A OUT0+3  
 LDA B OUT0+2  
 STA A OUT1+3  
 STA B OUT1+2  
 LDA A OUT0+1  
 LDA B OUT0  
 STA A OUT1+1  
 STA B OUT1  
 CPX #530FB

5346	27 1F		BEO	FOLLO1
5348	7E 54 17		JMP	SECOND
534B	20 1D	STORE5	BRA	STORE3
534D	7E 53 E6	STORE6	JMP	STORE4
5350	A6 04	STORE2	LDA A	4,X
5352	B7 1F FF		STA A	X1+3
5355	A6 03		LDA A	3,X
5357	B7 1F FE		STA A	X1+2
535A	A6 02		LDA A	2,X
535C	B7 1F FD		STA A	X1+1
535F	A6 01		LDA A	1,X
5361	B7 1F FC		STA A	X1
5364	7E 52 E3		JMP	PRSTO1
5367	7E 54 26	FOLLO1	JMP	THIRD
536A	A6 04	STORE3	LDA A	4,X
536C	B7 40 FF		STA A	Y2+3
536F	A6 03		LDA A	3,X
5371	B7 40 FE		STA A	Y2+2
5374	A6 02		LDA A	2,X
5376	B7 40 FD		STA A	Y2+1
5379	A6 01		LDA A	1,X
537E	B7 40 FC		STA A	Y2
537E	B6 49 03	PRSTO2	LDA A	DELY+3
5381	B7 49 23		STA A	DELY2+3
5384	B6 49 07		LDA A	DELY+2
5387	B7 49 22		STA A	DELY2+2
538A	B6 49 06		LDA A	DELY+1
538D	B7 49 21		STA A	DELY2+1
5390	B6 49 05		LDA A	DELY
5393	B7 49 20		STA A	DELY2
5396	B6 49 38		LDA A	INTER+3
5399	B7 49 48		STA A	INTER2+3
539C	B6 49 37		LDA A	INTER+2
539F	B7 49 47		STA A	INTER2+2
53A2	B6 49 36		LDA A	INTER+1
53A5	B7 49 46		STA A	INTER2+1
53A8	B6 49 35		LDA A	INTER
53AB	B7 49 45		STA A	INTER2
53AE	B6 49 13		LDA A	DELY0+3
53B1	B7 49 33		STA A	DEL2+3
53B4	B6 49 12		LDA A	DELY0+2
53B7	B7 49 32		STA A	DEL2+2
53BA	B6 49 11		LDA A	DELY0+1
53BD	B7 49 31		STA A	DEL2+1
53C0	B6 49 10		LDA A	DELY0
53C3	B7 49 30		STA A	DEL2
53C6	B6 49 93		LDA A	OUT0+3
53C9	B7 49 A3		STA A	OUT2+3
53CC	B6 49 92		LDA A	OUT0+2
53CF	B7 49 A2		STA A	OUT2+2
53D2	B6 49 91		LDA A	OUT0+1
53D5	B7 49 A1		STA A	OUT2+1
53D8	B6 49 90		LDA A	OUT0
53DB	B7 49 A0		STA A	OUT2
53DE	8C 48 FB		CPX	#348FB
53E1	27 1A		BEO	FOLLO2

53E3	7E 54 35		JMP	FOURTH
53E6	A6 04	STOR14	LDA A	4,X
53E8	B7 31 FF		STA A	Y1+3
53EB	A6 03		LDA A	3,X
53ED	B7 31 FE		STA A	Y1+2
53F0	A6 02		LDA A	2,X
53F2	B7 31 FD		STA A	Y1+1
53F5	A6 01		LDA A	1,X
53F7	B7 31 FC		STA A	Y1
53FA	7E 53 7E		JMP	PRSTO2
53FD	7E 54 44	FOLLO2	JMP	OUT
5400	FE 49 80	NEXT	LDX	COUNT1
5403	08		INX	
5404	08		INX	
5405	08		INX	
5406	08		INX	
5407	FF 49 80		STX	COUNT1
540A	FE 49 85		LDX	COUNT2
540D	08		INX	
540E	08		INX	
540F	08		INX	
5410	08		INX	
5411	FF 49 85		STX	COUNT2
5414	7E 50 D8		JMP	MAIN
5417	CE 31 FF	SECOND	LDX	#531FF
541A	FF 49 80		STX	COUNT1
541D	CE 20 03		LDX	#52003
5420	FF 49 85		STX	COUNT2
5423	7E 50 D8		JMP	MAIN
5426	CE 40 FF	THIRD	LDX	#540FF
5429	FF 49 80		STX	COUNT1
542C	CE 29 03		LDX	#52903
542F	FF 49 85		STX	COUNT2
5432	7E 50 D8		JMP	MAIN
5435	CE 28 FF	FOURTH	LDX	#528FF
5438	FF 49 80		STX	COUNT1
543B	CE 41 03		LDX	#54103
543E	FF 49 85		STX	COUNT2
5441	7E 50 D8		JMP	MAIN
5444	0E	OUT	WAI	
5445	09		RES	
5446			SUBROUTINE FOR INTEGRATION	
5447		INTEGR	NOF	
5447	25 40 05		LDA A	TEMP1+0
5448	FE 49 87		LDA B	TEMP1+0
5449	0E 40 93		ADD A	OUT0+0
544A	79 40 92		ADD B	OUT0+2
544B	07 40 40		STA A	OUT0+3
544C	07 40 02		STA B	OUT0+2
544D	07 00 00		STA A	TEMP1+0
544E	07 40 07		STA A	TEMP1+2
544F	05 00 00		LDA A	TEMP1+1
5450	05 00 00		LDA B	TEMP1
5451	05 00 01		ADD A	OUT0+1
5452	05 00 00		ADD B	OUT0
5453	07 40 00		STA A	OUT0+1

546E F7 49 90  
5471 B7 49 56  
5474 F7 49 55  
5477 39  
5478

STA B OUT0  
STA A TEMP1+1  
STA B TEMP1  
RTS  
END

STATEMENTS =453

FREE BYTES =19460

NO ERRORS DETECTED

--

```

*      FFT IN PLACE PROGRAM
*      N IS NO.OF SAMPLES
*      N SHOULD BE POWER OF TWO
0080   ORG      $80

*
*      WORKING LOCATIONS FOR
*      MULTIPLICATION
*      USING BOOTH'S ALGORITHM
*
0080   Y        RMB      2
0082   XX       RMB      2
0084   U        RMB      4
0088   FF       RMB      1
4000   ORG      $4000
4000   01      FFTIN  NOP
4001   7E 43 74 JMP      FFT

*      257 VALUES OF SINE ARE
*      STORED FROM 0 TO PIE/2
*      INSTEPS OF 2PIE/1024
4004   00 00   SIN    FDB      $0000
4006   00 C9   FDB      $00C9
4008   01 92   FDB      $0192
400A   02 5B   FDB      $025B
400C   03 24   FDB      $0324
400E   03 FD   FDB      $03FD
4010   04 B6   FDB      $04B6
4012   05 7F   FDB      $057F
4014   06 48   FDB      $0648
4016   07 11   FDB      $0711
4018   07 D9   FDB      $07D9
401A   08 A2   FDB      $08A2
401C   09 6 B   FDB      $096B
401E   0A 33   FDB      $0A33
4020   0A FB   FDB      $0AFB
4022   0B C4   FDB      $0BC4
4024   0C 8C   FDB      $0C8C
4026   0D 54   FDB      $0D54
4028   0E 1C   FDB      $0E1C
402A   0E E4   FDB      $0EE4
402C   0F AB   FDB      $0FAB
402E   10 73   FDB      $1073
4030   11 3A   FDB      $113A
4032   12 01   FDB      $1201
4034   12 C8   FDB      $12C8
4036   13 8F   FDB      $138F
4038   14 55   FDB      $1455
403A   15 1C   FDB      $151C
403C   15 E2   FDB      $15E2
403E   16 A8   FDB      $16A8
4040   17 6E   FDB      $176E
4042   18 33   FDB      $1833
4044   18 F9   FDB      $18F9
4046   19 BE   FDB      $19BE
4048   1A 83   FDB      $1A83
404A   1B 47   FDB      $1B47
404C   1C C0   FDB      $1CC0

```

404E	1C	D0	FDB	\$1CD0
4050	1D	93	FDB	\$1D93
4052	1E	57	FDB	\$1E57
4054	1F	1A	FDB	\$1F1A
4056	1F	DD	FDB	\$1FDD
4058	20	9F	FDB	\$209F
405A	21	62	FDB	\$2162
405C	22	24	FDB	\$2224
405E	22	E5	FDB	\$22E5
4060	23	A7	FDB	\$23A7
4062	24	67	FDB	\$2467
4064	25	28	FDB	\$2528
4066	25	E8	FDB	\$25E8
4068	26	A8	FDB	\$26A8
406A	27	68	FDB	\$2768
406C	28	27	FDB	\$2827
406E	28	E5	FDB	\$28E5
4070	29	A4	FDB	\$29A4
4072	2A	62	FDB	\$2A62
4074	2B	1F	FDB	\$2B1F
4076	2B	DC	FDB	\$2BDC
4078	2C	99	FDB	\$2C99
407A	2D	55	FDB	\$2D55
407C	2E	11	FDB	\$2E11
407E	2E	CC	FDB	\$2ECC
4080	2F	87	FDB	\$2F87
4082	30	42	FDB	\$3042
4084	30	FC	FDB	\$30FC
4086	31	B5	FDB	\$31B5
4088	32	6E	FDB	\$326E
408A	33	27	FDB	\$3327
408C	33	DF	FDB	\$33DF
408E	34	97	FDB	\$3497
4090	35	4E	FDB	\$354E
4092	36	04	FDB	\$3604
4094	36	BA	FDB	\$36BA
4096	37	70	FDB	\$3770
4098	38	25	FDB	\$3825
409A	38	D9	FDB	\$38D9
409C	39	8D	FDB	\$398D
409E	3A	40	FDB	\$3A40
40A0	3A	F3	FDB	\$3AF3
40A2	3B	A5	FDB	\$3BA5
40A4	3C	57	FDB	\$3C57
40A6	3D	08	FDB	\$3D08
40A8	3D	B8	FDB	\$3DB8
40AA	3E	68	FDB	\$3E68
40AC	3F	17	FDB	\$3F17
40AE	3F	C6	FDB	\$3FC6
40B0	40	74	FDB	\$4074
40B2	41	21	FDB	\$4121
40B4	41	CE	FDB	\$41CE
40B6	42	7A	FDB	\$427A
40B8	43	26	FDB	\$4326
40BA	43	D1	FDB	\$43D1
40BC	44	7B	FDB	\$447B

40BE	45 24	FDB	\$4524
40C0	45 CD	FDB	\$45CD
40C2	46 75	FDB	\$4675
40C4	47 1D	FDB	\$471D
40C6	47 C4	FDE	\$47C4
40C8	48 6A	FDE	\$486A
40CA	49 0F	FDB	\$490F
40CC	49 B4	FDB	\$49B4
40CE	4A 58	FDB	\$4A58
40D0	4A F B	FDB	\$4AFB
40D2	4B 9E	FDB	\$4B9E
40D4	4C 40	FDB	\$4C40
40D6	4C E1	FDB	\$4CE1
40D8	4D 81	FDB	\$4D81
40DA	4E 21	FDB	\$4E21
40DC	4E C0	FDB	\$4EC0
40DE	4F 5E	FDB	\$4F5E
40E0	4F FB	FDB	\$4FFB
40E2	50 98	FDB	\$5098
40E4	51 34	FDB	\$5134
40E6	51 CF	FDB	\$51CF
40E8	52 69	FDB	\$5269
40EA	53 03	FDB	\$5303
40EC	53 9B	FDB	\$539B
40EE	54 33	FDB	\$5433
40F0	54 CA	FDB	\$54CA
40F2	55 60	FDB	\$5560
40F4	55 F6	FDB	\$55F6
40F6	56 8A	FDB	\$568A
40F8	57 1E	FDB	\$571E
40FA	57 B1	FDB	\$57B1
40FC	58 43	FDB	\$5843
40FE	58 D4	FDB	\$58D4
4100	59 64	FDB	\$5964
4102	59 F4	FDB	\$59F4
4104	5A 82	FDB	\$5A82
4106	5B 10	FDB	\$5B10
4108	5B 9D	FDB	\$5B9D
410A	5C 29	FDB	\$5C29
410C	5C B4	FDB	\$5CB4
410E	5D 3E	FDB	\$5D3E
4110	5D C8	FDB	\$5DC8
4112	5E 50	FDB	\$5E50
4114	5E D7	FDB	\$5ED7
4116	5F 5E	FDB	\$5F5E
4118	5F E4	FDB	\$5FE4
411A	60 68	FDB	\$6068
411C	60 EC	FDB	\$60EC
411E	61 6F	FDB	\$616F
4120	61 F1	FDB	\$61F1
4122	62 72	FDB	\$6272
4124	62 F2	FDB	\$62F2
4126	63 7 1	FDB	\$6371
4128	63 EF	FDB	\$63EF
412A	64 6C	FDB	\$646C
412C	64 E9	FDB	\$64E9



412E	65 6 4	FDB	\$6564
4130	65 DE	FDB	\$65DE
4132	66 57	FDB	\$6657
4134	66 D0	FDB	\$66D0
4136	67 47	FDB	\$6747
4138	67 BD	FDB	\$67BD
413A	68 32	FDB	\$6832
413C	68 A7	FDB	\$68A7
413E	69 1A	FDB	\$691A
4140	69 8C	FDB	\$698C
4142	69 FD	FDB	\$69FD
4144	6A 6E	FDB	\$6A6E
4146	6A DD	FDB	\$6ADD
4148	6B 4B	FDB	\$6B4B
414A	6B B8	FDB	\$6BB8
414C	6C 24	FDB	\$6C24
414E	6C 8F	FDB	\$6C8F
4150	6C F9	FDB	\$6CF9
4152	6D 62	FDB	\$6D62
4154	6D CA	FDB	\$6DCA
4156	6E 31	FDB	\$6E31
4158	6E 97	FDB	\$6E97
415A	6E FB	FDB	\$6EFB
415C	6F 5F	FDB	\$6F5F
415E	6F C2	FDB	\$6FC2
4160	70 23	FDB	\$7023
4162	70 83	FDB	\$7083
4164	70 E3	FDB	\$70E3
4166	71 41	FDB	\$7141
4168	71 9E	FDB	\$719E
416A	71 FA	FDB	\$71FA
416C	72 55	FDB	\$7255
416E	72 AF	FDB	\$72AF
4170	73 08	FDB	\$7308
4172	73 5F	<del>FDB</del>	<del>\$735F</del>
4174	73 B6	FDB	\$73B6
4176	74 0B	FDB	\$740B
4178	74 60	FDB	\$7460
417A	74 B3	FDB	\$74B3
417C	75 05	FDB	\$7505
417E	75 56	FDB	\$7556
4180	75 A6	FDB	\$75A6
4182	75 F 4	FDB	\$75F4
4184	76 42	FDB	\$7642
4186	76 8E	FDB	\$768E
4188	76 D9	FDB	\$76D9
418A	77 23	FDB	\$7723
418C	77 6C	FDB	\$776C
418E	77 B4	FDB	\$77B4
4190	77 FB	FDB	\$77FB
4192	78 40	FDB	\$7840
4194	78 85	FDB	\$7885
4196	78 C8	FDB	\$78C8
4198	79 0A	FDB	\$790A
419A	79 4A	FDB	\$794A
419C	79 8A	FDB	\$798A



420A	00 00	N	FDB	\$0000
		*	IA INITIAL VALUE IS N/2	
420C	00 00	IA	FDB	\$0000
		*	LL STORES LOG2N	
420E	00 00	LL	FDB	\$0000
4210	00 00	HH	FDB	\$0000 ;
		*	FOLLOWING PARAMETERS SET	
		*	OFFSETS FOR CALCULATING	
		*	SINE AND COSINE VALUES	
4212	02 00	CT512	FDB	\$0200
4214	00 00	S1024	FDB	\$0000
4216	04 00	C1024	FDB	\$0400
4218	00 00	SI512	FDB	\$0000
421A	00 00	SN512	FDB	\$0000
421C	FE 00	C512	FDB	\$FE00
		*	INNER LOOP PARAMETERS	
421E	00 01	IB	FDB	\$0001 ;
4220	00 00	IC	FDB	\$0000 ;
4222	00 00	ID	FDB	\$0000 ;
4224	00 00	I2D	FDB	\$0000 ;
4226	00 00	K	FDB	\$0000 ;
		*	SINE IS TEMPORARY	
		*	LOCATION TO SINE	
4228	00 00	SINE	FDB	\$0000 ;
		*	COSIN IS TEMPORARY	
		*	LOCATION TO COSINE	
422A	00 00	COSIN	FDB	\$0000 ;
422C	00	COUNT	FCB	\$00
		*	FLAGS FOR TESTING	
422D	00	FLAG1	FCB	\$00 ;
422E	00	FLAG2	FCB	\$00
422F	00	FLAG	FCB	\$00
4230	00 00	EL	FDB	\$0000
4232	00 00	EH	FDB	\$0000
4234	00 00	DL	FDB	\$0000
4236	00 00	DH	FDB	\$0000
		*	REAL PART CURRENT	
		*	ADDRESS STORE	
4238	00 00	MIR	FDB	\$0000 ;
		*	IMAG.PART CURENT	
		*	ADDRESS STORE	
423A	00 00	MII	FDB	\$0000 ;
423C	00 00	NMR	FDB	\$0000
423E	00 00	NMI	FDB	\$0000
		*	CURRENT REAL PART STORE	
4240	00 00	XYRMI	FDB	\$0000 ;
		*	CURRENT IMAG.PART STORE	
4242	00 00	XYIMI	FDB	\$0000 ;
		*	WORKING LOCATIONS TO	
		*	STORE REAL&IMAG.PARTS	
4244	00 00	AREAL	FDB	\$0000 ;
4246	00 00	AIMAG	FDB	\$0000 ;
4248	00 00	REAL1	FDB	\$0000
424A	00 00	BREAL	FDB	\$0000
424C	00 00	IMAG1	FDB	\$0000
424E	00 00	BIMAG	FDB	\$0000

420A	00 00	N	FDB	\$0000
		*	IA INITIAL VALUE IS N/2	
420C	00 00	IA	FDB	\$0000
		*	LL STORES LOG2N	
420E	00 00	LL	FDB	\$0000
4210	00 00	HH	FDB	\$0000 ;
		*	FOLLOWING PARAMETERS SET	
		*	OFFSETS FOR CALCULATING	
		*	SINE AND COSINE VALUES	
4212	02 00	CT512	FDB	\$0200
4214	00 00	S1024	FDB	\$0000
4216	04 00	C1024	FDB	\$0400
4218	00 00	SI512	FDB	\$0000
421A	00 00	SN512	FDB	\$0000
421C	FE 00	C512	FDB	\$FE00
		*	INNER LOOP PARAMETERS	
421E	00 01	IB	FDB	\$0001 ;
4220	00 00	IC	FDB	\$0000 ;
4222	00 00	ID	FDB	\$0000 ;
4224	00 00	I2D	FDB	\$0000 ;
4226	00 00	K	FDB	\$0000 ;
		*	SINE IS TEMPORARY	
		*	LOCATION TO SINE	
4228	00 00	SINE	FDB	\$0000 ;
		*	COSIN IS TEMPORARY	
		*	LOCATION TO COSINE	
422A	00 00	COSIN	FDB	\$0000 ;
422C	00	COUNT	FCB	\$00
		*	FLAGS FOR TESTING	
422D	00	FLAG1	FCB	\$00 ;
422E	00	FLAG2	FCB	\$00
422F	00	FLAG	FCB	\$00
4230	00 00	EL	FDB	\$0000
4232	00 00	EH	FDB	\$0000
4234	00 00	DL	FDB	\$0000
4236	00 00	DH	FDB	\$0000
		*	REAL PART CURRENT	
		*	ADDRESS STORE	
4238	00 00	MIR	FDB	\$0000 ;
		*	IMAG.PART CURENT	
		*	ADDRESS STORE	
423A	00 00	MII	FDB	\$0000 ;
423C	00 00	NMR	FDB	\$0000
423E	00 00	NMI	FDB	\$0000
		*	CURRENT REAL PART STORE	
4240	00 00	XYRMI	FDB	\$0000 ;
		*	CURRENT IMAG.PART STORE	
4242	00 00	XYIMI	FDB	\$0000 ;
		*	WORKING LOCATIONS TO	
		*	STORE REAL&IMAG.PARTS	
4244	00 00	AREAL	FDB	\$0000 ;
4246	00 00	AIMAG	FDB	\$0000 ;
4248	00 00	REAL1	FDB	\$0000
424A	00 00	BREAL	FDB	\$0000
424C	00 00	IMAG1	FDB	\$0000
424E	00 00	BIMAG	FDB	\$0000

4250	00	FLAG4	FCB	\$00	
4251	00	BFLAG	FCB	\$00	
4252	00	LL8	FCB	\$00	
		*	TEMP ADDRESS LOCATIONS		
		*	OF BIT REVERSAL ROUTINE		
4253	00 00	TREAL	FDB	\$0000	;
4255	00 00	TIMAG	FDB	\$0000	;
		*	BITRN STORES BIT REVERSED#		
4257	00 00	BITRN	FDB	\$0000	;
		*	MAJOR WORK LOCATIONS		
		*	OF FFT PROGRAM		
4259	00	H	FCB	\$00	;
425A	00	L	FCB	\$00	;
425B	00	D	FCB	\$00	;
425C	00	E	FCB	\$00	;
425D	00	B1	FCB	\$00	;
425E	00	C	FCB	\$00	;
		*	DPMUL IS A SUBROUTINE TO		
		*	MULTIPLY TWO'S COMPLIMENT		
		*	NO. USING BOOTH'S ALGORITHM		
		*	MULTIPLIER AND MULTIPLICAND		
		*	SHOULD BE STORED AT DE,HL		
		*	WORK LOCATIONS AND THE		
		*	RESULT WILL BE AT HL		
425F	01	DPMUL	NOP		
4260	FE 42 5B		LDX	D	
4263	DF 80		STX	Y	
4265	FE 42 59		LDX	H	
4268	DF 82		STX	XX	
426A	CE 00 05		LDX	#5	
426D	4F		CLR A		
426E	A7 83	LP1	STA A	U-1,X	
4270	09		DEX		
4271	26 F B		BNE	LP1	
4273	CE 00 10		LDX	#16	
4276	96 81	LP2	LDA A	Y+1	
4278	84 01		AND A	#1	
427A	16		TAB		
427B	98 88		EOR A	FF	
427D	27 1D		BEQ	SHIFT	
427F	5D		TST B		
4280	27 0E		BEQ	ADD	
4282	96 85		LDA A	U+1	
4284	D6 84		LDA B	U	
4286	90 83		SUB A	XX+1	
4288	D2 82		SBC B	XX	
428A	97 85		STA A	U+1	
428C	D7 84		STA B	U	
428E	20 0C		BRA	SHIFT	
4290	96 85	ADD	LDA A	U+1	
4292	D6 84		LDA B	U	
4294	9B 83		ADD A	XX+1	
4296	D9 82		ADC B	XX	
4298	97 85		STA A	U+1	
429A	D7 8 4		STA B	U	
429C	7F 00 88	SHIFT	CLR	FF	

429F 76 00 80  
 42A2 76 00 81  
 42A5 79 00 88  
 42A8 77 00 84  
 42AB 76 00 85  
 42AE 76 00 86  
 42B1 76 00 87  
 42B4 09  
 42B5 26 BF  
 42B7 78 00 86  
 42BA 79 00 85  
 42BD 79 00 84  
 42C0 96 84  
 42C2 D6 85  
 42C4 B7 42 59  
 42C7 F7 42 5A  
 42CA 39

ROR Y  
 ROR Y+1  
 ROL FF  
 ASR U  
 ROR U+1  
 ROR U+2  
 ROR U+3  
 DEX  
 BNE LP2  
 ASL U+2  
 ROL U+1  
 ROL U  
 LDA A U  
 LDA B U+1  
 STA A H  
 STA B L  
 RTS

\* SUBROUTINE COMPL FINDS  
 \* TWO'S COMPLIMENT OF 16  
 \* BIT NUMBER STORED AT HL  
 \* RESULT AT HL

42CB 01  
 42CC 4F  
 42CD B6 42 5A  
 42D0 F6 42 59  
 42D3 53  
 42D4 43  
 42D5 8B 01  
 42D7 C9 00  
 42D9 B7 42 5A  
 42DC F7 42 59  
 42DF 39

COMPL NOP  
 CLR A  
 LDA A L  
 LDA B H  
 COM B  
 COM A  
 ADD A #\$01  
 ADC B #\$00  
 STA A L  
 STA B H  
 RTS

\* SUBROUTINE OFL DIVIDES  
 \* 16 BIT NUMBER STORED  
 \* AT HL BY 2; RESULT AT HL

42E0 01  
 42E1 86 00  
 42E3 B7 42 50  
 42E6 B6 42 59  
 42E9 84 80  
 42EB 27 08  
 42ED 86 01  
 42EF B7 42 50  
 42F2 BD 42 CB  
 42F5 01  
 42F6 0C  
 42F7 76 42 59  
 42FA 76 42 5A  
 42FD B6 42 50  
 4300 81 01  
 4302 2B 03  
 4304 BD 42 CB  
 4307 39

OFL NOP  
 LDA A #\$00  
 STA A FLAG4  
 LDA A H  
 AND A #\$80  
 BEQ DIVIDE  
 LDA A #\$01  
 STA A FLAG4  
 JSR COMPL  
 DIVIDE NOP  
 CLC  
 ROR H  
 ROR L  
 LDA A FLAG4  
 CMP A #\$01  
 BMI OVER  
 JSR COMPL  
 OVER RTS

\* SUBROUTINE BITR FINDS  
 \* BIT REVERSED NO. OF A  
 \*

\* NO. STORED AT HL  
\* RESULT AT HL

4308	01	BITR	NOP	
4309	FE 42 59		LDX	H
430C	FF 42 5B		STX	D
430F	B6 42 51		LDA A	BFLAG
4312	81 01		CMP A	#\$01
4314	2B 3A		BMI	LLLE8
4316	B6 42 5C	LLGT8	LDA A	E
4319	C6 08		LDA B	#\$08
431B	CE 00 00		LDX	#\$00
431E	FF 42 59		STX	H
4321	0C	BRLP3	CLC	
4322	79 42 5A		ROL	L
4325	79 42 59		ROL	H
4328	46		ROR A	
4329	24 07		BCC	BRLP4
432B	FE 42 59		LDX	H
432E	08		INX	
432F	FF 42 59		STX	H
4332	5A	BRLP4	DEC B	
4333	26 EC		BNE	BRLP3
4335	F6 42 52		LDA B	LL8
4338	B6 42 5B		LDA A	D
433B	0C	BRLP5	CLC	
433C	79 42 5A		ROL	L
433F	79 42 59		ROL	H
4342	46		ROR A	
4343	24 07		BCC	BRLP6
4345	FE 42 59		LDX	H
4348	08		INX	
4349	FF 42 59		STX	H
434C	5A	BRLP6	DEC B	
434D	26 EC		BNE	BRLP5
434F	39		RTS	
4350	01	LLLE8	NOP	
4351	CE 42 0E		LDX	#LL
4354	B6 42 5C		LDA A	E
4357	E6 00		LDA B	,X
4359	CE 00 00		LDX	#\$00
435C	FF 42 59		STX	H
435F	0C	BRLP1	CLC	
4360	79 42 5A		ROL	L
4363	79 42 59		ROL	H
4366	46		ROR A	
4367	24 07		BCC	BRLP2
4369	FE 42 59		LDX	H
436C	08		INX	
436D	FF 42 59		STX	H
4370	5A	BRLP2	DEC B	
4371	26 EC		BNE	BRLP1
4373	39		RTS	

\*  
\* MAIN FFT PROGRAM STARTS  
\* N HAS #OF SAMPLE POINTS

4374	FE 42 0A	FFT	LDX	N	;
4377	7F 42 59		CLR	H	
<del>437A</del>	<del>7F 42 5A</del>		<del>CLR</del>	L	
437D	7F 42 5B		CLR	D	
4380	7F 42 5C		CLR	E	
4383	7F 42 5E		CLR	C	
4386	7F 42 5D		CLR	B1	
4389	FF 42 59		STX	H	
		*	TO CALCULATE LOG2N		
438C	BD 51 CC		JSR	LOG2N	;
438F	0C		CLC		
4390	76 42 59		ROR	H	
4393	76 42 5A		ROR	L	
4396	FE 42 59		LDX	H	
4399	FF 42 0C		STX	IA	
439C	FF 42 06		STX	NI2	
439F	F6 42 5E		LDA B	C	
43A2	86 08		LDA A	#\$08	
43A4	11		CBA		
		*	CHECKING LOG2N>8 OR <8		
43A5	2B 06		BMI	GT8	;
43A7	4F		CLR A		
43A8	B7 42 51		STA A	BFLAG	
43AB	20 0B		BRA	LT8	
43AD	86 01	GT8	LDA A	#\$01	
43AF	B7 42 51		STA A	BFLAG	
43B2	17		TBA		
43B3	80 08		SUB A	#\$08	
43B5	B7 42 52		STA A	LL8	
43B8	17	LT8	TBA		
43B9	B7 42 0E		STA A	LL	
43BC	80 02		SUB A	#\$02	
43BE	16		TAB		
43BF	0C		CLC		
43C0	86 01		LDA A	#\$01	
43C2	46		ROR A		
43C3	46	LOOP	ROR A		
43C4	5A		DEC B		
<del>43C5</del>	<del>20 0C</del>		<del>BIE</del>	LOOP	
43C7	B7 42 10		STA A	HH	
		*	CALCULATION OF DIFFERENT		
		*	OFFSETS TO GENERATE		
		*	SINE AND COSINE VALUES		
43CA	CE 40 04		LDX	#\$IN	;
43CD	FF 42 5B		STX	D	;
43D0	B6 42 16		LDA A	C1024	;
43D3	F6 42 17		LDA B	C1024+1	
43D6	FB 42 5C		ADD B	E	
43D9	B9 42 5B		ADC A	D	
43DC	B7 42 14		STA A	S1024	
43DF	F7 42 15		STA B	S1024+1	
43E2	CE 40 04		LDX	#\$IN	
43E5	FF 42 5B		STX	D	
43E8	B6 42 1D		LDA A	C512+1	
43EB	F6 42 1C		LDA B	C512	
43EE	BB 42 5C		ADD A	E	

43F1	F9 42 5B	ADC B	D
43F4	B7 42 19	STA A	SI512+1
43F7	F7 42 18	STA B	SI512
43FA	CE 40 04	LDX	#SIN
43FD	FF 42 5B	STX	D
4400	B6 42 13	LDA A	CT512+1
4403	F6 42 12	LDA B	CT512
4406	BB 42 5C	ADD A	E
4409	F9 42 5B	ADC B	D
440C	B7 42 1B	STA A	SN512+1
440F	F7 42 1A	STA B	SN512
4412	4F	CLR A	
4413	B7 42 08	STA A	I
4416	CE 00 01	LDX	#\$0001
4419	FF 42 1E	STX	IB
	*	OUTER LOOP	
	*	PARAMETERS SETTING	
441C	CE 00 00	LDX	#\$0000 ;
441F	FF 42 20	STX	IC ;
4422	FF 42 26	STX	K
4425	FE 42 0C	LDX	IA
4428	FF 42 59	STX	H
442B	FF 42 22	STX	ID
442E	0C	CLC	
442F	79 42 5A	ROL	L
4432	79 42 59	ROL	H
4435	FE 42 59	LDX	H
4438	FF 42 24	STX	I2D
	*	INNER LOOP PARAMETERS	
	*	SETTING	
443B	FE 42 0C	LDX	IA ;
443E	FF 42 5B	STX	D ;
4441	FE 42 20	LDX	IC
4444	FF 42 59	STX	H
	*	POWER OF W CALCULATED	
4447	01	NOP	
4448	0C	CLC	
4449	76 42 5B	ROR	D
444C	76 42 5C	ROR	E
444F	25 08	BCS	OICIA
4451	76 42 59	ROR	H
4454	76 42 5A	ROR	L
4457	20 EE	BRA	ICIA
4459	01	NOP	
445A	BD 43 08	JSR	BITR
445D	4F	CLR A	
445E	B6 42 10	LDA A	HH
4461	46	ROR A	
4462	81 00	CMP A	#\$00
4464	27 08	BEQ	FINIS
4466	78 42 5A	ASL	L
4469	79 42 59	ROL	H
446C	20 F 3	BRA	ICLP
446E	01	NOP	
	FINIS		
	- *	CHECK POWER OF W>256	
	*	OR <=256	

446F	01	GL256	NOP	
4470	B6 42 59		LDA A	H
4473	81 01		CMP A	#\$01
4475	25 3A		BCS	NLT257
4477	81 01		CMP A	#\$01
4479	26 07		BNE	GT256
447B	F6 42 5A	ACHEC	LDA B	L
447E	C1 01		CMP B	#\$01
4480	25 2F		BCS	NLT257
		*	VALUES OF SINE AND COSIN	
		*	FOR W>256	
4482	01	GT256	NOP	
4483	78 42 5A		ASL	L
4486	79 42 59		ROL	H
4489	FE 42 59		LDX	H
448C	FF 42 5B		STX	D
448F	4F		CLR A	
4490	B6 42 15		LDA A	S1024+1
4493	F6 42 14		LDA B	S1024
4496	B0 42 5C		SUB A	E
4499	F2 42 5B		SBC B	D
449C	B7 42 5A		STA A	L
449F	F7 42 59		STA B	H
44A2	FE 42 59		LDX	H
44A5	A6 00		LDA A	,X
44A7	08		INX	
44A8	E6 00		LDA B	,X
44AA	CE 42 28		LDX	#SINE
44AD	A7 00		STA A	,X
44AF	20 02		BRA	NEXT
44B1	20 2F	NLT257	BRA	LT257
44B3	08	NEXT	INX	
44B4	E7 00		STA B	,X
44B6	B6 42 19		LDA A	S1512+1
44B9	F6 42 18		LDA B	S1512
44BC	BB 42 5C		ADD A	E
44BF	F9 42 5B		ADC B	D
44C2	B7 42 5A		STA A	L
44C5	F7 42 59		STA B	H
44C8	4F		CLR A	
44C9	FE 42 59		LDX	H
44CC	A6 00		LDA A	,X
44CE	08		INX	
44CF	E6 0 0		LDA B	,X
44D1	CE 42 2B		LDX	#COSIN+1
44D4	43		COM A	
44D5	53		COM B	
44D6	CB 01		ADD B	#\$01
44D8	89 00		ADC A	#\$00
44DA	E7 00		STA B	,X
44DC	09		DEX	
44DD	A7 00		STA A	,X
44DF	7E 45 40		JMP	IN1
		*	VALUES OF SINE AND COSIN	
		*	FOR W<=256	
44E2	01	LT257	NOP	



44E3	78	42	5A	ASL	L
44E6	79	42	59	ROL	H
44E9	FE	42	59	LDX	H
44EC	FF	42	5B	STX	D
44EF	CE	40	04	LDX	#SIN
44F2	FF	42	59	STX	H
44F5	B6	42	5A	LDA A	L
44F8	F6	42	59	LDA B	H
44FB	BB	42	5C	ADD A	E
44FE	F9	42	5B	ADC B	D
4501	B7	42	5A	STA A	L
4504	F7	42	59	STA B	H
4507	FE	42	59	LDX	H
450A	A6	00		LDA A	,X
450C	08			INX	
450D	E6	00		LDA B	,X
450F	FF	42	59	STX	H
4512	CE	42	28	LDX	#SINE
4515	A7	00		STA A	,X
4517	08			INX	
4518	E7	00		STA B	,X
451A	4F			CLR A	
451B	B6	42	1B	LDA A	SN512+1
451E	F6	42	1A	LDA B	SN512
4521	B0	42	5C	SUB A	E
4524	F2	42	5B	SBC B	D
4527	B7	42	5A	STA A	L
452A	F7	42	59	STA B	H
452D	FE	42	59	LDX	H
4530	A6	00		LDA A	,X
4532	08			INX	
4533	E6	00		LDA B	,X
4535	FF	42	59	STX	H
4538	CE	42	2A	LDX	#COSIN
453B	A7	00		STA A	,X
453D	08			INX	
453E	E7	00		STA B	,X
4540	01		INI	NOP	
4541	FE	42	0C	LDX	IA
4544	FF	42	59	STX	H
4547	78	42	5A	ASL	L
454A	79	42	59	ROL	H
454D	FE	42	59	LDX	H
4550	FF	42	5B	STX	D
4553	CE	49	CA	LDX	#XREAL
4556	FF	42	59	STX	H
4559	B6	42	5A	LDA A	L
455C	F6	42	59	LDA B	H
455F	BB	42	5C	ADD A	E
4562	F9	42	5B	ADC B	D
4565	B7	42	39	STA A	MIR+1
4568	F7	42	38	STA B	MIR
456B	CE	4D	CA	LDX	#XIMAG
456E	FF	42	59	STX	H
4571	B6	42	5A	LDA A	L
4574	F6	42	59	LDA B	H

4577	BB 42 5C	ADD A	E
457A	F9 42 5B	ADC B	D
457D	B7 42 3B	STA A	MII+1
4580	F7 42 3A	STA B	MII
4583	FE 42 20	LDX	IC
4586	FF 42 59	STX	H
4589	78 42 5A	ASL	L
458C	79 42 59	ROL	H
458F	B6 42 5A	LDA A	L
4592	F6 42 59	LDA B	H
4595	B7 42 5E	STA A	C
4598	F7 42 5D	STA B	B1
* INNER MOST LOOP			
459B	01	IMOST	NOP
459C	B6 42 5E	LDA A	C
459F	F6 42 5D	LDA B	B1
45A2	36	PSH A	
45A3	37	PSH B	
45A4	BB 42 39	ADD A	MIR+1
45A7	F9 42 38	ADC B	MIR
45AA	B7 42 5A	STA A	L
45AD	F7 42 59	STA B	H
45B0	FE 42 59	LDX	H
45B3	A6 00	LDA A	,X
45B5	08	INX	
45B6	E6 00	LDA B	,X
45B8	FF 42 5B	STX	D
45BB	B7 42 59	STA A	H
45BE	F7 42 5A	STA B	L
45C1	BD 42 E0	JSR	OFL
45C4	FE 42 59	LDX	H
45C7	FF 42 40	STX	XYRMI
45CA	FF 42 5B	STX	D
45CD	FE 42 2A	LDX	COSIN
45D0	FF 42 59	STX	H
45D3	BD 42 5F	JSR	DPMUL
45D6	FE 42 59	LDX	H
45D9	FF 42 48	STX	REAL1
45DC	33	PUL B	
45DD	32	PUL A	
45DE	BB 42 3B	ADD A	MII+1
45E1	F9 42 3A	ADC B	MII
45E4	B7 42 5A	STA A	L
45E7	F7 42 59	STA B	H
45EA	FE 42 59	LDX	H
45ED	A6 00	LDA A	,X
45EF	08	INX	
45F0	E6 00	LDA B	,X
45F2	FF 42 5B	STX	D
45F5	B7 42 59	STA A	H
45F8	F7 42 5A	STA B	L
45FB	BD 42 E0	JSR	OFL
45FE	FE 42 59	LDX	H
4601	FF 42 42	STX	XYIMI
4604	FF 42 5B	STX	D
4607	FE 42 28	LDX	SINE

460A	FF	42 59	STX	H
460D	B6	42 5E	LDA A	C
4610	F6	42 5D	LDA B	B1
4613	36		PSH A	
4614	37		PSH B	
4615	BD	42 5F	JSR	DPMUL
4618	FE	42 59	LDX	H
461B	FF	42 5B	STX	D
461E	B6	42 49	LDA A	REAL1+1
4621	F6	42 48	LDA B	REAL1
4624	BB	42 5C	ADD A	E
4627	F9	42 5B	ADC B	D
462A	B7	42 4B	STA A	BREAL+1
462D	F7	42 4A	STA B	BREAL
4630	FE	42 42	LDX	XYIMI
4633	FF	42 5B	STX	D
4636	FE	42 2A	LDX	COSIN
4639	FF	42 59	STX	H
463C	BD	42 5F	JSR	DPMUL
463F	FE	42 59	LDX	H
4642	FF	42 4C	STX	IMAG1
4645	FE	42 40	LDX	XYRMI
4648	F F	42 5B	STX	D
464B	FE	42 28	LDX	SINE
464E	FF	42 59	STX	H
4651	BD	42 5F	JSR	DPMUL
4654	FE	42 59	LDX	H
4657	BD	42 CB	JSR	COMPL
465A	B6	42 5A	LDA A	L
465D	F6	42 59	LDA B	H
4660	BB	42 4D	ADD A	IMAG1+1
4663	F9	42 4C	ADC B	IMAG1
4666	B7	42 5A	STA A	L
4669	F7	42 59	STA B	H
466C	FE	42 59	LDX	H
466F	FF	42 4E	STX	BIMAG
4672	33		PUL B	
4673	32		PUL A	
4674	B7	42 5E	STA A	C
4677	F7	42 5D	STA B	B1
467A	CE	49 CA	LDX	#XREAL
467D	FF	42 59	STX	H
4680	BB	42 5A	ADD A	L
4683	F9	42 59	ADC B	H
4686	B7	42 5A	STA A	L
4689	F7	42 59	STA B	H
468C	FE	42 59	LDX	H
468F	A6	0 0	LDA A	,X
4691	08		INX	
4692	E6	00	LDA B	,X
4694	B7	42 59	STA A	H
4697	F7	42 5A	STA B	L
469A	BD	42 E0	JSR	OFL
469D	FE	42 59	LDX	H
46A0	FF	42 44	STX	AREAL
46A3	CE	4D CA	LDX	#XIMAG

46A6	FF	42 59	STX	H
46A9	B6	42 5E	LDA A	C
46AC	F6	42 5D	LDA B	B1
46AF	BB	42 5A	ADD A	L
46B2	F9	42 59	ADC B	H
46B5	B7	42 5A	STA A	L
46B8	F7	42 59	STA B	H
46BB	FE	42 59	LDX	H
46BE	A6	00	LDA A	,X
46C0	08		INX	
46C1	E6	00	LDA B	,X
46C3	B7	42 59	STA A	H
46C6	F7	42 5A	STA B	L
46C9	BD	42 E0	JSR	OFL
46CC	FE	42 59	LDX	H
46CF	FF	42 46	STX	AIMAG
46D2	B6	42 4B	LDA A	BREAL+1
46D5	F6	42 4A	LDA B	BREAL
46D8	BB	42 45	ADD A	AREAL+1
46DB	F9	42 44	ADC B	AREAL
46DE	B7	42 5C	STA A	E
46E1	F7	42 5B	STA B	D
46E4	CE	49 CA	LDX	#XREAL
46E7	FF	42 59	STX	H
46EA	B6	42 5A	LDA A	L
46ED	F6	42 59	LDA B	H
46F0	BB	42 5E	ADD A	C
46F3	F9	42 5D	ADC B	B1
46F6	B7	42 5A	STA A	L
46F9	F7	42 59	STA B	H
46FC	FE	42 59	LDX	H
46FF	B6	42 5B	LDA A	D
4702	F6	42 5C	LDA B	E
4705	A7	00	STA A	,X
4707	08		INX	
4708	E7	00	STA B	,X
			* A REAL-B REAL CALCULATED	
470A	FE	42 4A	LDX	BREAL
470D	FF	42 59	STX	H
4710	BD	42 CB	JSR	COMPL
4713	B6	42 5A	LDA A	L
4716	F6	42 59	LDA B	H
4719	BB	42 45	ADD A	AREAL+1
471C	F9	42 44	ADC B	AREAL
471F	B7	42 5C	STA A	E
4722	F7	42 5B	STA B	D
4725	B6	42 5E	LDA A	C
4728	F6	42 5D	LDA B	B1
472B	BB	42 39	ADD A	MIR+1
472E	F9	42 38	ADC B	MIR
4731	B7	42 5A	STA A	L
4734	F7	42 59	STA B	H
4737	FE	42 59	LDX	H
473A	B6	42 5B	LDA A	D
473D	A7	00	STA A	,X
473F	08		INX	

4740	F6	42 5C	LDA B	E
4743	E7	00	STA B	,X
		*	AIMAG+BIMAG	CALCULATED
4745	B6	42 4F	LDA A	BIMAG+1
4748	F6	42 4E	LDA B	BIMAG
474B	BB	42 47	ADD A	AIMAG+1
474E	F9	42 46	ADC B	AIMAG
4751	B7	42 5C	STA A	E
4754	F7	42 5B	STA B	D
4757	CE	4D CA	LDX	#XIMAG
475A	FF	42 59	STX	H
475D	B6	42 5A	LDA A	L
4760	F6	42 59	LDA B	H
4763	BB	42 5E	ADD A	C
4766	F9	42 5D	ADC B	B1
4769	B7	42 5A	STA A	L
476C	F7	42 59	STA B	H
476F	FE	42 59	LDX	H
4772	B6	42 5B	LDA A	D
4775	A7	00	STA A	,X
4777	08		INX	
4778	F6	42 5C	LDA B	E
477B	E7	00	STA B	,X
477D	FE	42 4E	LDX	BIMAG
4780	FF	42 59	STX	H
4783	BD	42 CB	JSR	COMPL
4786	FE	42 59	LDX	H
4789	FF	42 5B	STX	D
478C	B6	42 47	LDA A	AIMAG+1
478F	F6	42 46	LDA B	AIMAG
4792	BB	42 5C	ADD A	E
4795	F9	42 5B	ADC B	D
4798	B7	42 5C	STA A	E
479B	F7	42 5B	STA B	D
479E	B6	42 3B	LDA A	MII+1
47A1	F6	42 3A	LDA B	MII
47A4	BB	42 5E	ADD A	C
47A7	F9	42 5D	ADC B	B1
47AA	B7	42 5A	STA A	L
47AD	F7	42 59	STA B	H
47B0	FE	42 59	LDX	H
47B3	B6	42 5B	LDA A	D
47B6	A7	00	STA A	,X
47B8	08		INX	
47B9	F6	42 5C	LDA B	E
47BC	E7	00	STA B	,X
47BE	FE	42 5D	LDX	B1
47C1	08		INX	
47C2	08		INX	
47C3	FF	42 5D	STX	B1
47C6	B6	42 5E	LDA A	C
47C9	CE	42 25	LDX	#I2D+1
47CC	A1	00	CMP A	,X
47CE	26	02	BNE	IMOST1
47D0	20	03	BRA	NEXT3
			NEXT ITERATION OF	

47D2	7E 45 9B	* IMOST1	INNER MOST LOOP	
47D5	09	NEXT3	JMP IMOST	;
47D6	B6 42 5D		DEX	;
47D9	A1 00		LDA A B1	;
47DB	26 02		CMP A ,X	
47DD	20 03		BNE IMOST2	
47DF	7E 45 9B	IMOST2	BRA NEXT4	
			JMP IMOST	
		*	NEXT ITERATION OF	
		*	INNER LOOP	
47E2	FE 42 0C	NEXT4	LDX IA	;
47E5	FF 42 59		STX H	;
47E8	78 42 5A		ASL L	;
47EB	79 42 59		ROL H	
47EE	FE 42 59		LDX H	
47F1	FF 42 5B		STX D	
47F4	B6 42 21		LDA A IC+1	
47F7	F6 42 20		LDA B IC	
47FA	BB 42 5C		ADD A E	
47FD	F9 42 5B		ADC B D	
4800	B7 42 21		STA A IC+1	
4803	F7 42 20		STA B IC	
4806	B6 42 23		LDA A ID+1	
4809	F6 42 22		LDA B ID	
480C	BB 42 5C		ADD A E	
480F	F9 42 5B		ADC B D	
4812	B7 42 23		STA A ID+1	
4815	F7 42 22		STA B ID	
4818	48		ASL A	
4819	59		ROL B	
481A	B7 42 25		STA A I2D+1	
481D	F7 42 24		STA B I2D	
4820	FE 42 26		LDX K	
4823	08		INX	
4824	FF 42 26		STX K	
4827	FF 42 5B		STX D	
482A	CE 42 1F		LDX #IB+1	
482D	B6 42 5C		LDA A E	
4830	A1 00		CMP A ,X	
4832	26 02		BNE INNER1	
4834	20 03		BRA NEXT5	
4836	7E 44 3B	INNER1	JMP INNER	
4839	09	NEXT5	DEX	
483A	B6 42 5B		LDA A D	
483D	A1 00		CMP A ,X	
483F	26 02		BNE INNER2	
4841	20 03		BRA NEXT6	
4843	7E 44 3B	INNER2	JMP INNER	
		*	NEXT ITERATION OF	
		*	OUTER LOOP	
4846	4F	NEXT6	CLR A	
4847	B6 42 1F		LDA A IB+1	
484A	F6 42 1E		LDA B IB	
484D	49		ROL A	
484E	59		ROL B	
484F	B7 42 1F		STA A IB+1	

4852	F7 42 1E		STA B	IB
4855	4F		CLR A	
4856	B6 42 0D		LDA A	IA+1
4859	F6 42 0C		LDA B	IA
485C	56		ROR B	
485D	46		ROR A	
485E	B7 42 0D		STA A	IA+1
4861	F7 42 0C		STA B	IA
4864	7C 42 08		INC	I
4867	B6 42 08		LDA A	I
486A	CE 42 0E		LDX	#LL
486D	A1 00		CMP A	,X
486F	26 02		BNE	OUTER1
4871	20 03		BRA	NEXTE
4873	7E 44 1C	OUTER1	JMP	OUTER
		*	UNSCRAMBLING OF OUTPUT	
4876	CE 00 00	NEXTE	LDX	#\$0000
4879	FF 42 5D		STX	B1
487C	B6 42 5E	XLP1	LDA A	C
487F	F6 42 5D		LDA B	B1
4882	B7 42 5A		STA A	L
4885	F7 42 59		STA B	H
4888	36		PSH A	
4889	37		PSH B	
488A	BD 43 08		JSR	BITR
488D	B6 42 59		LDA A	H
4890	B1 42 5D		CMP A	B1
4893	2B 04		BMI	NLPCON
4895	27 05		BEQ	NCHECA
4897	20 06		BRA	EXCHG
4899	7E 49 9E	NLPCON	JMP	LPCON
489C	7E 49 91	NCHECA	JMP	CHECA
489F	01	EXCHG	NOP	
48A0	78 42 5A		ASL	L
48A3	79 42 59		ROL	H
48A6	FE 42 59		LDX	H
48A9	FF 42 57		STX	BITRN
48AC	FF 42 5B		STX	D
48AF	78 42 5E		ASL	C
48B2	79 42 5D		ROL	B1
48B5	CE 49 CA		LDX	#XREAL
48B8	FF 42 59		STX	H
48BB	B6 42 5A		LDA A	L
48BE	F6 42 59		LDA B	H
48C1	BB 42 5C		ADD A	E
48C4	F9 42 5B		ADC B	D
48C7	B7 42 5A		STA A	L
48CA	F7 42 59		STA B	H
48CD	FE 42 59		LDX	H
48D0	A6 00		LDA A	,X
48D2	08		INX	
48D3	E6 00		LDA B	,X
48D5	09		DEX	
48D6	FF 42 5B		STX	D
48D9	B7 42 54		STA A	TREAL+1
48DC	F7 42 53		STA B	TREAL

48DF	CE 49 CA	LDX	#XREAL
48E2	FF 42 59	STX	H
48E5	B6 42 5A	LDA A	L
48E8	F6 42 59	LDA B	H
48EB	BB 42 5E	ADD A	C
48EE	F9 42 5D	ADC B	B1
48F1	B7 42 5A	STA A	L
48F4	F7 42 59	STA B	H
48F7	FE 42 59	LDX	H
48FA	A6 00	LDA A	,X
48FC	08	INX	
48FD	E6 00	LDA B	,X
48FF	09	DEX	
4900	FF 51 CA	STX	TEMP
4903	FE 42 5B	LDX	D
4906	A7 00	STA A	,X
4908	08	INX	
4909	E7 00	STA B	,X
490B	FE 42 53	LDX	TREAL
490E	FF 42 59	STX	H
4911	FE 51 CA	LDX	TEMP
4914	B6 42 5A	LDA A	L
4917	A7 00	STA A	,X
4919	08	INX	
491A	B6 42 59	LDA A	H
491D	A7 00	STA A	,X
491F	FE 42 57	LDX	BITRN
4922	FF 42 5B	STX	D
4925	CE 4D CA	LDX	#XIMAG
4928	FF 42 59	STX	H
492B	B6 42 5A	LDA A	L
492E	F6 42 59	LDA B	H
4931	BB 42 5C	ADD A	E
4934	F9 42 5B	ADC B	D
4937	B7 42 5A	STA A	L
493A	F7 42 59	STA B	H
493D	FE 42 59	LDX	H
4940	A6 00	LDA A	,X
4942	08	INX	
4943	E6 00	LDA B	,X
4945	09	DEX	
4946	FF 42 5B	STX	D
4949	B7 42 56	STA A	TIMAG+1
494C	F7 42 55	STA B	TIMAG
494F	CE 4D CA	LDX	#XIMAG
4952	FF 42 59	STX	H
4955	B6 42 5E	LDA A	C
4958	F6 42 5D	LDA B	B1
495B	BB 42 5A	ADD A	L
495E	F9 42 59	ADC B	H
4961	B7 42 5A	STA A	L
4964	F7 42 59	STA B	H
4967	FE 42 59	LDX	H
496A	A6 00	LDA A	,X
496C	08	INX	
496D	E6 00	LDA B	,X



496F	09		DEX	
4970	FF 51	CA	STX	TEMP
4973	FE 42	5B	LDX	D
4976	A7 00		STA A	,X
4978	08		INX	
4979	E7 00		STA B	,X
497B	FE 42	55	LDX	TIMAG
497E	FF 42	59	STX	H
4981	FE 51	CA	LDX	TEMP
4984	B6 42	5A	LDA A	L
4987	A7 00		STA A	,X
4989	B6 42	59	LDA A	H
498C	08		INX	
498D	A7 00		STA A	,X
498F	20 0D		BRA	LPCON
4991	B6 42	5A	LDA A	L
4994	B1 42	5E	CMP A	C
4997	27 05		BEQ	LPCON
4999	2B 03		BMI	LPCON
499B	7E 48	9F	JMP	EXCHG
499E	33		PUL B	
499F	32		PUL A	
49A0	8B 01		ADD A	#101
49A2	25 02		BCS	NEXT8
49A4	20 01		BRA	NEXT7
49A6	5C		INC B	
49A7	B7 42	5E	STA A	C
49AA	F7 42	5D	STA B	B1
49AD	FE 42	0A	LDX	N
49B0	FF 42	59	STX	H
49B3	B6 42	59	LDA A	H
49B6	B1 42	5D	CMP A	B1
49B9	27 03		BEQ	SCHEC
49BB	7E 48	7C	JMP	XLPI
49BE	B6 42	5A	LDA A	L
49C1	B1 42	5E	CMP A	C
49C4	27 03		BEQ	XEND
49C6	7E 48	7C	JMP	XLPI
			* END OF FFT SUBROUTINE	
49C9	39		XEND	RTS ;
			* XREAL STORES 512 REAL VALUES	
49CA			XREAL	RMB 1024 ;
			* XIMAG STORES 512 IMAG.VALUES	
4DCA			XIMAG	RMB 1024 ;
			* TEMP WORK LOCATIONS	
51CA	00		TEMP	FCB 00 ;
51CB	00		TEMP1	FCB 00
			* LOG2N SUBROUTINE FINDS LOG.OF N	
			* LOG2N	
51CC	C6 08		LDA B	#\$08
51CE	B6 42	5A	LDA A	L
51D1	0C		CLC	
51D2	46		ROR A	
51D3	25 0D		BCS	OUT
51D5	7C 42	5E	INC	C

51D8	5A		DEC B
51D9	26 F7		BNE POWER
51DB	C6 08		LDA B #08
51DD	B6 42 59		LDA A H
51E0	20 F 0		BRA POWER
51E2	01	OUT	NOP
51E3	39		RTS
51E4			END

STATEMENTS =1184

FREE BYTES =11986

NO ERRORS DETECTED

--

```

*
*
*   ASSEMBLY ROUTINE FOR
*   PSD MEASUREMENT
*

```

```

49CA      XREAL      EQU      $49CA
4DCA      XIMAG      EQU      $4DCA
4BCA      XREAL1     EQU      $4BCA
4FCA      XIMAG1     EQU      $4FCA
5600      XRESUL     EQU      $5600
425F      DPMUL      EQU      $425F
4259      H          EQU      $4259
425A      L          EQU      $425A
425B      D          EQU      $425B
425C      E          EQU      $425C

```

```

*
*   SUBROUTINE OVERFLOW
*

```

```

5400      ORG          $5400
5400      01          OFL      NOP
5401      78 42 5A    ASL      L
5404      79 42 59    ROL      H
5407      78 42 5A    ASL      L
540A      79 42 59    ROL      H
540D      78 42 5A    ASL      L
5410      79 42 59    ROL      H
5413      78 42 5A    ASL      L
5416      79 42 59    ROL      H
5419      39          RTS

```

```

*
*   MAIN PSD ROUTINE STARTS
*

```

```

5500      ORG          $5500
5500      00 00      TEMP    FDB      $0000
5502      00 00      TEMP1   FDB      $0000
5504      00 00      TEMP2   FDB      $0000
5506      00 00      TEMP3   FDB      $0000
5508      00 00      TEMP4   FDB      $0000
550A      CE 4B CA    LDX      #XREAL1
550D      FF 55 00    STX      TEMP
5510      CE 4F CA    LDX      #XIMAG1
5513      FF 55 02    STX      TEMP1
5516      CE 56 00    LDX      #XRESUL
5519      FF 55 08    STX      TEMP4
551C      FE 55 00    INNER   LDX      TEMP
551F      A6 00      START    LDA      A,X
5521      08          INX
5522      E6 00      LDA      B,X
5524      08          INX
5525      FF 55 00    STX      TEMP
5528      B7 42 59    STA      A,H
552B      F7 42 5A    STA      B,L
552E      BD 54 00    JSR      OFL
5531      FE 42 59    LDX      H
5534      FF 42 5B    STX      D

```

```

*
*   DPMUL IS 16BIT MULTIPLY

```

